2024

Scaffold Hopping for the Lead Optimization of the Orally Active Antileishmanial Pyrrolo-Quinazoline Alkaloid Natural Product Peganine

Sunitha Jada
South Dakota State University, sunitha.j90@gmail.com

SCAFFOLD HOPPING FOR THE LEAD OPTIMIZATION OF THE ORALLY ACTIVE ANTILEISHMANIAL PYRROLO-QUINAZOLINE ALKALOID NATURAL PRODUCT PEGANINE

BY

SUNITHA JADA

A thesis submitted in partial fulfillment of the requirements for the

Master of Science

Major in Pharmaceutical Sciences

South Dakota State University

2024

THESIS ACCEPTANCE PAGE
Sunitha Jada

This thesis is approved as a creditable and independent investigation by a candidate for the master's degree and is acceptable for meeting the thesis requirements for this degree. Acceptance of this does not imply that the conclusions reached by the candidate are necessarily the conclusions of the major department.

Tanvir Khaliq
Advisor Date

Dr. Hemachand Tummala
Department Head Date

Nicole Lounsbery, PhD
Director, Graduate School Date

THIS THESIS IS DEDICATED TO MY PARENTS AND FAMILY

ACKNOWLEDGEMENTS

I am overwhelmed with gratitude towards the many individuals who have supported, guided, and encouraged me throughout my academic and research journey at South Dakota State University (SDSU). I extend my heartfelt appreciation to each and every one of them.

I must begin by expressing my sincere thanks to my advisor, Dr. Tanvir Khaliq, for his unwavering mentorship, invaluable advice, and continuous support throughout my graduate research and education. I consider it an honor to have had the opportunity to work under his guidance and within his laboratory.

I would also like to extend my heartfelt gratitude to my master's advisory committee members, Dr. Jayarama Bhat Gunaje and Dr. Melanie Caffe, for their continuous support, feedback, and motivation, which have been crucial to my academic growth and success.

I am grateful to the Department of Pharmaceutical Sciences at SDSU for their constant support and assistance, which has significantly contributed to my academic and research endeavors.

I would also like to thank the Department of Biology and Microbiology and the Department of Chemistry and Biochemistry for providing me with the opportunity to serve as a teaching assistant, which has been an incredibly enriching experience.

I want to give a huge shoutout to Dr. Matthew Miller and Dr. Jewell Melody for always having my back and guiding me along the way. Their support and advice have

truly helped me grow professionally. Also, big thanks to the awesome people at the Department of Chemistry and Biochemistry NMR facility for backing my research efforts.

I can't forget to mention the amazing team in my lab - Veerpal Kaur, Hyunjun Cho, and Lainee Marie Mentzer. Their dedication and support have made my research experience incredibly rewarding. I'm truly thankful for each one of them.

I am profoundly grateful to my family for their unconditional love, unwavering support, and encouragement throughout this journey. I extend my heartfelt gratitude to my parents, Mr. Ananda Rao Jada, and Mrs. Jamuna Jada, for their unconditional love and encouragement. I am grateful to my husband, Mr. Pradeep Kumar Merum, and my children, Monvee Merum and Sanvik Merum, for their unwavering support and understanding. I also extend my thanks to my sisters, Santhoshi Jada, and Sowjanya Jada, for their continuous support and encouragement. Their unwavering support has been a constant source of strength and inspiration, for which I am truly grateful.

Sunitha Jada

CONTENTS

ABBREVIATIONS

CL	Cutaneous Leishmaniasis
COX2	Cyclooxygenase 2
CYP450	Cytochrome P450
CYP2D6	Cytochrome P450 2D6
DMF	Dimethyl Formamide
DCM	Dichloromethane
DMM	Dimethyl Malonate
DMC	Dimethyl Carbonate
DMSO	Dimethyl Sulfoxide
DCC	N, N'-Dicyclohexylcarbodiimide
DMAP	4-Dimethylaminopyridine
DIEA	N, N-Diisopropylethylamine
DBU	1,8-Diazabicyclo(5.4.0)undec-7-ene
DME	1,2-Dimethoxyethane
DIAD	Diisopropyl Azodicarboxylate
EDC	1-Ethyl-3-(3-dimethylaminopropyl) Carbodiimide
EC_{50}	Half maximal Effective Concentration
HIV	Human Immunodeficiency Virus
HOBT	Hydroxy Benzotriazole
IUPAC	International Union of Pure and Applied Chemistry
KBr	Potassium Bromide
$KHCO_3$	Potassium Bicarbonate

K_2CO_3	Potassium Carbonate
LAH	Lithium Aluminium Hydride
LiOH	Lithium Hydroxide
L-AmB	Liposomal Amphotericin B
MCL	Mucocutaneous Leishmaniasis
MeOH	Methanol
MeI	Methyl Iodide
MS	Mass Spectrometry
MAP	Mitogen Ativated Protein
MK2	Mitogen Activated Protein (MAP) Kinase-Activated Protein Kinase 2
$NaBH_4$	Sodium Borohydride
NMR	Nuclear Magnetic Resonance
PPh_3	Triphenylphosphine
PKDL	Post Kala-azar Dermal Leishmaniasis
SI	Selectivity Index
$SOCl_2$	Thionyl Chloride
TLC	Thin Layer Chromatography
THF	Tetrahydrofuran
VL	Visceral Leishmaniasis

LIST OF FIGURES

LIST OF TABLES

ABSTRACT

SCAFFOLD HOPPING FOR THE LEAD OPTIMIZATION OF THE ORALLY ACTIVE ANTILEISHMANIAL PYRROLO-QUINAZOLINE ALKALOID NATURAL PRODUCT PEGANINE

SUNITHA JADA

2024

Leishmaniasis is a protozoan parasitic disease caused by the species *Leishmania* that affects millions of people around the world. It is a serious public health concern in the developing world with about 1 million cases and 70,000 fatalities occurring each year. It has several forms with visceral, and cutaneous leishmaniasis being the most common forms of the disease. Visceral leishmaniasis, caused by the *Leishmania donovani* occurs mainly in Brazil, Eastern Africa, and India, and is fatal if left untreated. The current treatments for leishmaniasis such as pentavalent antimonials, amphotericin B, miltefosine, paromomycin, pentamidine, and some azoles suffer from serious drawbacks. Examples are parasitic resistance, toxicity, reduced efficacy, cost, longer duration, and except for miltefosine, have routes of administration incompatible with the settings where the disease is endemic. Therefore, new, safe, short, and orally acting drugs are urgently needed to effectively treat leishmaniasis.

We have identified a pyrroloquinazoline alkaloid natural product lead peganine from *Peganum harmala* that shows promising activity against visceral leishmaniasis. It selectively inhibits the growth of the intracellular *L. donovani* parasites, amastigotes without significant toxicity to the host macrophages. Preliminary studies have shown that

peganine inhibits *L. donovani* topoisomerase 1 with a unique mechanism of action different from the known DNA-topoisomerase 1 inhibitor, camptothecin. Most importantly, it significantly reduces the parasitic burden in hamsters infected with visceral leishmaniasis infection following oral administration. However, peganine shows *in vivo* efficacy at a relatively high dose, therefore, structural modification of the lead molecule is necessary to optimize its antileishmanial activity.

Our laboratory is focused on the design, synthesis, and evaluation of biological activity of novel analogs of peganine to explore their structure-activity relationships (SARs) and identify novel analogs with improved antileishmanial activity. We have used scaffold hopping drug design strategy to design a novel scaffold of peganine for synthesis and evaluation of its antileishmanial activity. We have replaced the core benzenoid ring of peganine with a pyridine ring to enhance the hydrogen bonding interactions with the target enzyme and improve the antileishmanial activity of the new scaffold. The total synthesis of the analog was accomplished up to the penultimate step in moderate to excellent yields. The intermediaries were characterized by mass spectrometry and Nuclear Magnetic Resonance (NMR). The synthesis of the final step is being carried out to obtain the target molecule.

CHAPTER 1

DRUG DISCOVERY FOR LEISHMANIASIS AND SCAFFOLD HOPPING FOR PROTOZOAN PARASITIC DISEASES

1 Introduction:

1.1 Leishmaniasis:

Leishmaniasis is a neglected tropical disease caused by the protozoan parasite *Leishmania* that primarily affects underprivileged communities in both developing and underdeveloped nations worldwide [1]. This highlights the importance of targeted interventions and support in these vulnerable areas and the disproportionate burden of the disease on populations facing economic challenges [1, 2]. The genus *Leishmania* was named in honor of the British pathologist Sir William Boog Leishman, who first described it in 1900 [2].

1.2 Statistics of Leishmaniasis:

Leishmaniasis stands prominently among the top 10 neglected tropical diseases on the global scale, impacting over 12 million people [3, 4]. This parasitic disease has cast its influence over 100 countries spanning Europe, Africa, Asia, and the Americas [4, 5]. Despite its widespread occurrence, the alarming fact is that more than 90% of new cases emerge within a specific set of 13 nations facing a high burden of leishmaniasis [2, 4]. These countries, including Afghanistan, Algeria, Bangladesh, Bolivia, Brazil, Colombia, Ethiopia, India, Iran, Peru, South Sudan, Sudan, and Syria, grapple with the significant challenges posed by this disease [1, 4].

1.3 Leishmaniasis in the United States:

In general, Leishmaniasis is a zoonotic disease transmitted by vectors and is distinguished by a complex cycle of transmission involving a variety of parasite species,

reservoirs, and vectors [6, 7]. Protozoa from the genus *Leishmania* causes the disease, which spreads to humans and animals through bites from *Psychodidae* family of insects [3]. Leishmaniasis is a disease that affects more people in the United States than is generally recognized. It can result from both imported and locally acquired infections [6, 8].

A significant rise in cutaneous leishmaniasis (CL) cases has been linked to the significant deployment of millions of military to Iraq and Afghanistan [7-9]. But the greater worry stems from the potential that a considerable proportion of people may be suffering from undiagnosed asymptomatic visceral leishmaniasis (VL) [7, 9]. Due to its lack of obvious symptoms, this form of the disease can be difficult to identify, which emphasizes the importance of raising awareness and conducting surveillance among affected populations [8].

1.4 Types of Leishmaniasis:

Leishmaniasis manifests in three forms, each distinguished by clinical signs and symptoms: cutaneous leishmaniasis (CL), visceral leishmaniasis (VL), and mucocutaneous leishmaniasis (MCL) [1, 5, 10].

1.4.1 Cutaneous Leishmaniasis (CL):

Cutaneous Leishmaniasis, caused by *Leishmania* the most prevalent form, typically results in skin ulcers on exposed body parts such as the face, arms, and legs. In severe cases, it can lead to a substantial number of lesions, causing significant disability and permanent scarring described in Table 1.1 [5, 10, 11].

Table 1.1: *Leishmania* species correlated with human infections and their associated leishmaniasis syndromes [12, 13].

Clinical Presentation	Species	Symptoms
Visceral Leishmaniasis (VL)	*L.donovani* *L.infantum*	Prolonged fever, spleno-megaly, hepatomegaly, pancytopenia, progressive anemia, and weight loss
Cutaneous Leishmaniasis (CL)	*L. braziliensis, L. panamensis, L. guyanensis, L. tropica, L. major and L. aethiopica, L. amazonensis, L. mexicana and L. peruviana*	An erythematous papule eventually leaves severe scarring at the site of the sand fly bite.
Mucocutaneous Leishmaniasis (MCL)	*L. braziliensis, L. aethiopica, L. panamensis,*	Damaging and deformative lesions of the mucosal membranes, along with the Oro-nasopharyngeal mucosa's destruction

1.4.2 Mucocutaneous Leishmaniasis (MCL):

The most incapacitating type of leishmaniasis, mucocutaneous leishmaniasis (MCL), is potentially fatal, especially in those with weakened immune systems. The oronasal junction is the main site of ulceration in MCL [10, 11]. This type may eventual-

ly result in nasal collapse due to the destruction of the nasal septum and cartilage, described in Table 1.1 [14]. The seriousness of MCL emphasizes how crucial early detection and intervention are, particularly in groups with weakened immune systems [1, 3, 14].

1.4.3 Visceral Leishmaniasis:

1.4.3.1 Epidemiology:

The Irish physician Charles Donovan first identified the causative organism of visceral leishmaniasis in 1903 after finding the parasite in the spleen of a soldier who died to the illness [2, 15]. Charles Donovan is credited with the modern-day discovery that *Leishmania* parasites are the cause of leishmaniasis [15].

The parasites *Leishmania donovani* and *Leishmania infantum* are the main causes of visceral leishmaniasis (VL) [16]. In South America, VL can be referred to as *Leishmania chagasi* [17]. The role of female sandflies as vectors in the spread of Leishmania parasites is crucial [18]. More specifically, *Leishmania donovani* and *Leishmania infantum* have different transmission dynamics [18]. About 13,000 cases of visceral leishmaniasis were reported globally in 2020, making it a serious global health concern even today [19]. Around 200 million people worldwide are at risk from VL, which is endemic in more than 70 countries [20]. Over 90% of cases are concentrated in countries like: Brazil, India, and Eastern Africa [16].

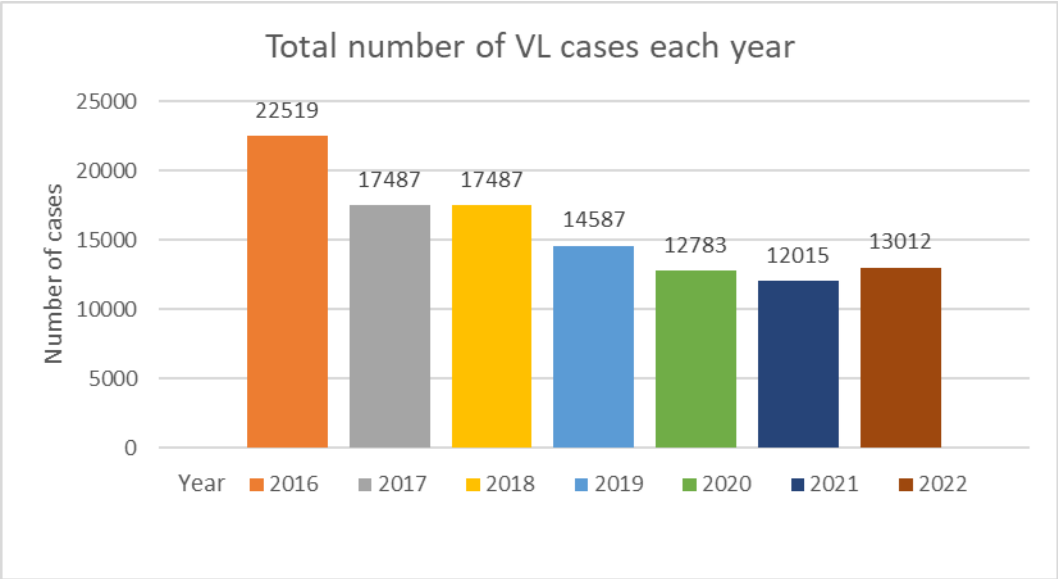

Figure 1.1: The total number of VL cases from the year 2016 to 2022[1]

Over the years, the trend of VL infection has varied (figure 1.1), it indicates that the number of cases from 2016 to 2022, and the number fluctuating, which indicates the severeness of the disease.

When it comes to endemic regions, between 2016 and 2017, the Indian subcontinent had a declining trend in VL cases, whereas Eastern Africa experienced an increase in cases[21, 22]. In 2016 and 2017, Brazil's VL caseload remained steady. Though less frequently, VL cases have also been reported in Europe and the Eastern Mediterranean[21]. With evidence of sub-national outbreaks in Italy, Greece, Spain, and Romania, concerns regarding the emergence of VL in nations like Armenia, Azerbaijan, France, Greece, and Libya are growing[21].

1.4.3.2 Transmission:

Although 95% of VL infections also known as kala-azar are fatal if left untreated, the majority are sub-clinical or asymptomatic [23]. Hepatomegaly, splenomegaly, fever, weight loss, exhaustion, anorexia, anemia, and finally death is among the clinical symptoms [24]. Poor rural communities are primarily affected by VL, which is spread by female sandflies. Mass migrations to endemic areas or alterations to sandfly habitats, like deforestation, can trigger outbreaks [25]. The number of people with HIV who are immunosuppressed is rising in some areas, which contributes to the increase in VL cases. For the purpose of creating efficient preventative and control measures against this disease associated with poverty, it is essential to comprehend the immune response and the dynamics of VL transmission [17].

Visceral leishmaniasis transmission depends on a number of important factors. The main vectors for the spread of *Leishmania* parasites are female sandflies [26]. During blood meals from infected hosts, these insects pick up the parasite. They then serve as reservoirs, passing the parasite to other hosts during subsequent feedings. Various *Leishmania* species have distinct reservoir hosts [24]. For instance, humans are the main reservoirs in areas where *L. donovani* is endemic, whereas dogs and other wild mammals are the main carriers of *L. infantum* in regions such as the Mediterranean and Latin America. These reservoir hosts are essential to the parasite's survival in the environment and help spread it to sandflies [7, 10, 27].

1.5 *Leishmania*:

The genus *Leishmania*, belonging to the family *Trypanosomatidae* (order *Kinetoplastida*), encompasses two main groups: old world species found in Europe, Africa, and Asia, and new world species prevalent in America [28]. Among the 53 described species of *Leishmania*, 31 affect mammals, with 20 posing a pathogenic risk to humans [7]. The transmission dynamics of *Leishmania* species vary, with some exhibiting zoonotic transmission involving complex reservoir hosts and others relying on human-to-human transmission facilitated by the vector [11]. *Leishmania donovani*, traditionally considered zoonotic, has been found in animals and humans in India and East Africa. Each *Leishmania* species's global distribution dictates the type of disease prevalent in an area, with *L. donovani* causing visceral leishmaniasis in South Asia and Africa, *L. infantum* in the Mediterranean, Middle East, Latin America, and parts of Asia, and others like *L. major* and *L. tropica* causing cutaneous leishmaniasis in various regions [7, 10, 11, 28].

1.5.1 Life cycle of *Leishmania* Parasite:

Leishmania species exhibit a heteroxenous life cycle involving two main morphological forms: amastigotes within the mammalian host's macrophages and promastigotes in the gut of sand fly vectors [29]. The cycle begins when an infected female sand fly injects metacyclic promastigotes into the human body during a blood meal [30]. These promastigotes are phagocytosed by host macrophages, where they transform into amastigotes, proliferate, and subsequently lyse the macrophages to infect other phagocytes [31].

The sand fly vector acquires *Leishmania* parasites from infected mammalian hosts during blood meals, primarily targeting the skin where amastigotes are present [32]. The parasites undergo further development within the sand fly, ultimately leading to the production of metacyclic promastigotes that are deposited into the skin of a new mammalian host during subsequent blood meals, thereby perpetuating the transmission cycle of the disease [33-35].

1.6 Current treatments for leishmaniasis:

Various pharmacological interventions are used in current leishmaniasis treatments, depending on the kind and severity of the infection [36]. Historically, the cornerstone of treatment has been antimony-containing substances like sodium stibogluconate (**1**) and meglumine antimoniate (**2**); however, resistance to these medications has emerged in some regions [37]. Other drugs such as amphotericin B (**3**), miltefosine (**4**), and paromomycin (**5**) are also good choices; in particular, miltefosine has been approved for oral use under certain circumstances [38].

For cutaneous manifestations, topical treatments may be used; combination therapies and supportive care measures improve patient management and treatment effectiveness even more. In order to address new issues and enhance outcomes for afflicted individuals, leishmaniasis treatment: strategies are dynamic. This is highlighted by ongoing research into novel drug candidates and immunotherapeutic approaches [39].

Currently available pharmacological agents for the treatment of visceral leishmaniasis (VL) include pentavalent antimonials (Figure 1.2, **1** and **2**), amphotericin B (Figure 1.2, **3**) in different forms, miltefosine (Figure 1.2, **4**), paromomycin (Figure 1.2, **5**), and

pentamidine (Figure 1.2, **6**). Interestingly, some of these medications are also used to treat mucocutaneous leishmaniasis (MCL), post-kala-azar dermal leishmaniasis (PKDL), and cutaneous leishmaniasis (CL) because of their broad-spectrum activity. As a result, they can be used to treat a variety of leishmaniasis syndromes in addition to VL. This adaptability highlights how these drugs are multidimensional in their approach to treating various disease manifestations [24, 40-42].

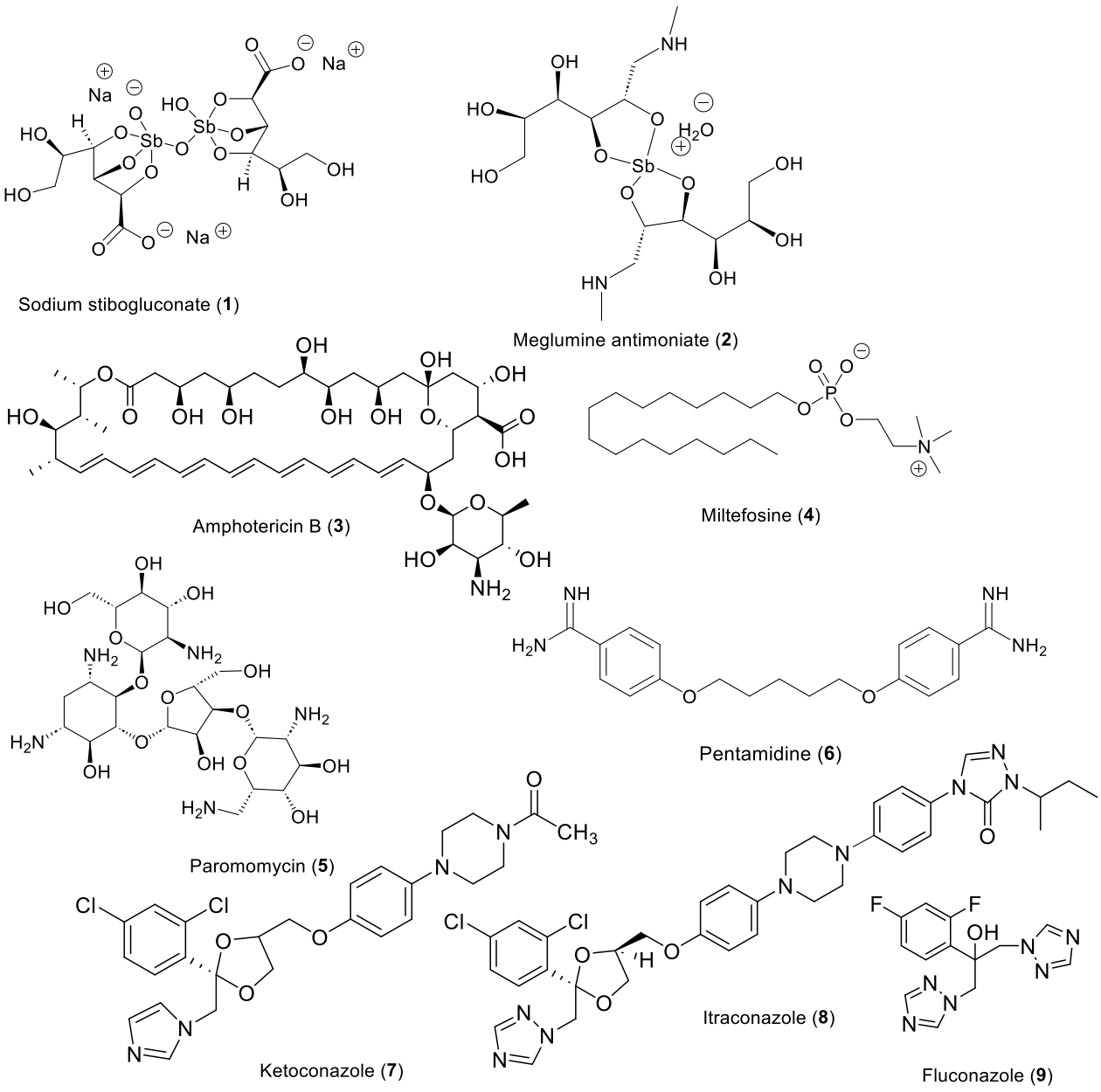

Figure 1.2: Current drugs used to treat leishmaniasis

1.6.1 Pentavalent Antimonials:

Pentavalent antimonials, (Table 1.2) including sodium stibogluconate (Figure 1.2, **1**) and meglumine antimoniate (Figure 1.2, **2**), have been the mainstay of leishmaniasis treatment for several decades. These drugs have significant efficacy in treating cuta-

neous and visceral leishmaniasis, but their toxicity and potential resistance have limited their use in some regions [43-45].

Pentavalent antimonial work by inhibiting the enzymes involved in the metabolism of glucose, which is essential for the survival of *Leishmania* parasites. The drugs are generally administered intravenously or intramuscularly, and the treatment course can last up to 28 days, depending on the severity of the disease [45, 46].

However, the use of pentavalent antimonial is associated with several side effects, including nausea, vomiting, diarrhea, pancreatitis, and cardiac toxicity [45]. The toxicity of these drugs is dose-dependent, and this can lead to serious complications in some patients. The most severe side effect of antimonial is cardiotoxicity, which can lead to electrocardiogram abnormalities, arrhythmias, and heart failure [47].

Furthermore, the emergence of resistant strains of *Leishmania* has made antimonial less effective in some regions. In some parts of the world, up to 60% of *Leishmania* parasites have been reported to be resistant to antimonial. This has led to the development of alternative treatments, such as amphotericin B, miltefosine, and paromomycin [43, 45].

Despite their limitations, pentavalent antimonials remain an important treatment option for leishmaniasis. They are widely available and relatively inexpensive compared to other treatments. Furthermore, their efficacy in treating leishmaniasis is high, especially in regions where resistance to antimonials is low [44, 45].

Pentavalent antimonials are an important treatment for leishmaniasis, but their use is limited due to their toxicity and parasitic resistance. The use of antimonials should

be carefully monitored to avoid serious complications, and alternative treatments should be considered in regions where resistance is high [48].

1.6.2 Amphotericin B:

Amphotericin B (Table 1.2) (Figure 1.2, **3**) is a polyene macrolide antibiotic that has been used for over 50 years to treat leishmaniasis. The drug is highly effective against all forms of leishmaniasis, including cutaneous, visceral, and mucocutaneous leishmaniasis. However, its toxicity limits its use and makes it a second-line treatment option [49].

Amphotericin B works by binding it to ergosterol, which is a component of the cell membrane of *Leishmania* parasites. This binding leads to the formation of pores in the cell membrane, which causes the cell to leak and eventually die. The drug is usually administered intravenously, and the treatment course can last up to 28 days, depending on the severity of the disease [50, 51].

Unfortunately, the use of amphotericin B is associated with several side effects, including fever, chills, nausea, vomiting, and renal toxicity. The most serious side effect of the drug is nephrotoxicity, which can lead to acute kidney injury and electrolyte imbalances. This toxicity is dose-dependent and can be reduced by the use of liposomal formulations of the drug [50, 52].

The cost of amphotericin B is also a limiting factor, making it difficult to access in resource-poor settings, where the disease burden is often the highest. In such settings, alternative treatments such as pentavalent antimonials, paromomycin, and miltefosine are often used [51, 53].

Despite its limitations, amphotericin B remains an important treatment option for leishmaniasis, especially in severe cases where other treatments have failed or where resistance to other treatments is high. The drug has been used successfully in combination therapy with other drugs, such as azole antifungals and pentavalent antimonial, to reduce the risk of toxicity and improve efficacy [54].

Amphotericin B is a highly effective treatment for leishmaniasis, but its toxicity and cost limit its use [41]. The use of the drug should be carefully monitored and reserved for severe cases where other treatments have failed, or where resistance to other treatments is high [55]. Alternative treatments should be considered in resource-poor settings, where the cost of the drug is a significant barrier to access [54, 55].

1.6.3: Miltefosine:

Miltefosine (Table 1.2) (Figure 1.2, **4**) is an oral drug that is used to treat leishmaniasis, a parasitic disease caused by the Leishmania species. Miltefosine is the first oral drug approved for the treatment of leishmaniasis, and it is effective against all forms of the disease, including cutaneous, mucocutaneous, and visceral leishmaniasis. Miltefosine was originally developed as an anticancer drug, but it was later found to be effective against leishmaniasis [56, 57].

Miltefosine works by inhibiting the synthesis of cell membrane phospholipids in *Leishmania* parasites. Following oral administration, it is rapidly absorbed from the gastrointestinal tract. Miltefosine is distributed throughout the body, including the skin, liver, spleen, and bone marrow. The drug is metabolized in the liver and excreted in the feces and urine [58, 59].

Miltefosine has several advantages over other drugs used to treat leishmaniasis. First, it is an oral drug, which makes it more convenient for patients. Second, it is effective against all forms of leishmaniasis, including drug-resistant strains of the parasite. Third, it has a low toxicity profile compared to other drugs used to treat leishmaniasis [57, 60].

Miltefosine is associated with several side effects, including gastrointestinal symptoms, such as nausea, vomiting, and diarrhea. These side effects are usually mild and self-limiting and can be managed with supportive care [56]. Miltefosine can also cause liver toxicity, and it is contraindicated in patients with liver disease. In addition, miltefosine is teratogenic and is contraindicated in pregnant women [61]. Miltefosine is currently approved for the treatment of leishmaniasis in several countries, including India, Brazil, and Germany. The drug is also being studied for the treatment of other parasitic diseases, such as Chagas disease and sleeping sickness [62].

Miltefosine is an effective and well-tolerated oral drug for the treatment of leishmaniasis. The drug has several advantages over other drugs used to treat leishmaniasis, including its oral administration, broad-spectrum activity, and low toxicity profile [63]. However, miltefosine is associated with several side effects, and its use should be carefully monitored in patients with liver disease or during pregnancy [64].

1.6.4 Paromomycin:

Paromomycin (Table 1.2) (Figure 1.2, **5**) is an aminoglycoside antibiotic that is used to treat leishmaniasis. Paromomycin works by binding to the ribosome of *Leishmania* parasites, inhibiting protein synthesis, and ultimately leading to the death of the par-

asites [65]. Paromomycin is effective against all forms of leishmaniasis, including cutaneous, mucocutaneous, and visceral leishmaniasis [66, 67].

Paromomycin is administered intravenously or intramuscularly, and the treatment course can last up to 21 days. Paromomycin is generally well-tolerated, but it can cause renal toxicity and ototoxicity [65]. Renal toxicity is the most common side effect of paromomycin, and it can lead to electrolyte imbalances, such as hypokalemia and hypomagnesemia. Ototoxicity is less common but can lead to tinnitus, hearing loss, and vertigo [68].

Paromomycin is distributed throughout the body, including the liver, spleen, and bone marrow. The drug is excreted unchanged in the urine, and it is not metabolized in the body. Paromomycin has a low toxicity profile compared to other drugs used to treat leishmaniasis, such as pentavalent antimonial and amphotericin B [69, 70].

Paromomycin is currently approved for the treatment of leishmaniasis in several countries, including India, Ethiopia, and Sudan. The drug is also being studied for the treatment of other parasitic diseases, such as cryptosporidiosis and giardiasis [71].

Paromomycin is an effective and well-tolerated drug for the treatment of leishmaniasis. The drug has a low toxicity profile compared to other drugs used to treat leishmaniasis, and it is effective against all forms of the disease [72]. However, paromomycin is associated with renal toxicity and ototoxicity, and its use should be carefully monitored in patients with renal or ear disorders [65].

1.6.5 Pentamidine

Pentamidine (Table 1.2) (Figure 1.2, **6**) is the aromatic diamidine compound which has been repurposed to treat leishmaniasis, a parasitic disease spread by the bites of infected sandflies and caused by Leishmania parasites. The original purpose of this medication was to treat another parasitic illness called trypanosomiasis as an antiprotozoal agent. By interfering with the parasites' ability to synthesize DNA, pentamidine prevents leishmaniasis by killing the disease-causing agent. Depending on the kind and severity of the leishmaniasis infection, it can be given via a variety of methods, such as aerosolized formulations, intravenous injections, or muscle injections [73].

Pentamidine is an effective medication, but side effects include nausea, vomiting, abdominal pain, and injection site reactions are possible. But it still plays a crucial role in the treatment arsenal against leishmaniasis, especially in areas where the disease is endemic and there are few other options for treating it because of resource limitations or drug resistance. Pentamidine formulation optimization and novel drug delivery strategies are the subjects of ongoing research aimed at enhancing the drug's efficacy and safety profile in the treatment of leishmaniasis [74].

Table 1.2: Summary of current drugs for visceral leishmaniasis [13]

Drugs	Efficacy	Advantages	Limitations
Pentavalent Antimonial – Sodium stibogluconate and Meglumine antimoniate	35-95%	Low cost	Drug resistance
Amphotericin B	>95%	Effective against antimonial resistance	Nephrotoxicity, hypokalemia, and myocarditis
Miltefosine	94-97%	Highly potent	Teratogenicity, occasional hepato- and nephrotoxicity
Paromomycin	95%	Low cost	Reversible ototoxicity
Pentamidine	70-80%	Low dosage with combination of other drugs	Hypoglycemia, hypotension, fever, myocarditis, and renal toxicity
Azoles – Ketoconazole, Fluconazole, Itraconazole	59-89%	Consistently efficacious, mild side effects	Limited studies

1.6.6 Azoles

Ketoconazole (Table 1.2) (Figure 1.2, **7**), itraconazole (Figure 1.2, **8**) and fluconazole (Figure 1.2, **9**) are antifungal medications that have shown efficacy against Leishmania parasites, contributing to their potential as treatments for leishmaniasis.

Ketoconazole (Figure 1.2, **7**) is a broad-spectrum antifungal agent that inhibits the synthesis of ergosterol, an essential component of fungal cell membranes. Studies have indicated its potential in treating various forms of leishmaniasis, although its use may be limited due to concerns about side effects and drug interactions [75, 76].

Similar to ketoconazole, itraconazole (Figure 1.2, **8**) is an azole antifungal agent that disrupts the integrity of fungal cell membranes by inhibiting the synthesis of ergosterol. It has shown efficacy against *Leishmania* parasites in addition to its antifungal characteristics. Clinical trials on itraconazole have shown encouraging results in treating various forms of leishmaniasis; however, there is a chance that it will cause side effects or interact with other medications [77].

Another azole antifungal drug that interferes with ergosterol synthesis is fluconazole (Figure 1.2, **9**) which works by blocking the enzyme lanosterol 14α-demethylase (CYP 51), which is dependent on fungal cytochrome P450. Fluconazole is mainly used to treat systemic candidiasis and superficial fungal infections, but it has also been investigated as a possible treatment for leishmaniasis. Its effectiveness against *Leishmania* parasites, however, might be less than that of ketoconazole and itraconazole [75, 77]. All three azoles have similar mechanism of action; they inhibit the 14α-demethylase or CYP 51.

More antifungal drugs show promise as treatments for leishmaniasis; however, more studies are required to maximize their application, establish suitable dosages, and evaluate their efficacy and safety in clinical settings.

1.7 Drug discovery for leishmaniasis:

1.7.1 Natural products:

Natural products isolated from plants and animals have been at the forefront of discovering novel antileishmanial agents. This is mainly attributed to their unique and diverse chemical architecture and pharmacophores and often possessing drug-like properties. The majority of new small molecules derived from or inspired by natural products have been discovered for the treatment of infectious diseases since mid-1980s **[**78**]**. Although natural products possess good lead properties for a drug discovery program, their structural complexity poses synthetic challenges which prevents further optimization of their biological activity and pharmacokinetic properties. Natural products also have great potential in the identification of novel targets leading to a targeted drug discovery approach. Natural products derived from plants and marine organisms that possess antileishmanial activity has been extensively reviewed [79, 80]**.**

Various natural products have been derived from plants and fungi and have proven to be valuable lead molecules for anti-infective drug discovery programs. Specifically, diverse natural products (Figure 1.3) have shown promising activity in various *in vitro* and *in vivo* models of leishmaniasis [81]**.**

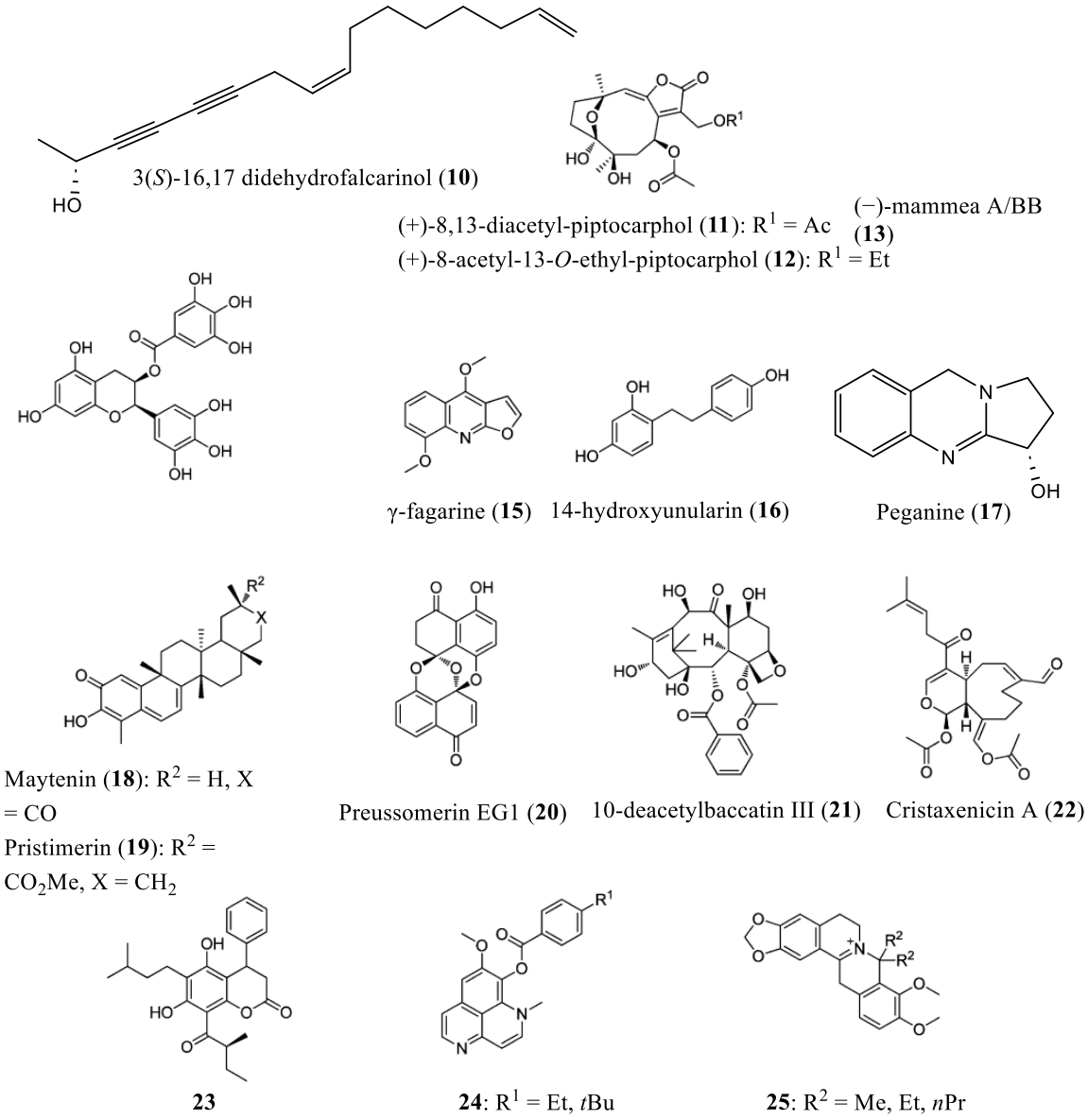

Figure 1.3: Natural products and their semisynthetic derivaives showing acticity against leishmanaisis

3(*S*)-16,17 didehydrofalcarinol (Figure 1.3, **10**) was discovered from the plants *Sarcococca hookeriana* and *Tridax procumbens* for cutaneous leishmaniasis by the axenic bioassay-guided fractionation of the plant [82]. Parthenolide exhibited antileishmanial activity in an axenic *L. amazonensis* parasite assay [83]. Two potent sesquiterpene lactones (+)-8,13-diacetyl-piptocarphol (Figure 1.3, **11**) and (+)-8-acetyl-13-*O*-

ethyl-piptocarphol (Figure 1.3, **12**), were isolated from the extract of the *Pseudelephantopus spicatus [84]*. A potent coumarin natural product (−)-mammea A/BB (Figure 1.3, **13**) was isolated from *Calophyllum brasiliens [85]***,** showing an EC_{50} of 0.88 µg/mL against *L. amazonensis* axenic amastigotes and showed significant reduction of lesion size with no toxicity following intramuscular administration for 30 days. The most abundant flavanol of green tea (−)-epigallocatechin 3-*O*-gallate (Figure 1.3, **14**), showed substantial reduction in lesion size against *L. amazonensis* following oral administration to mice at the dose of 30 mg/kg/d, 5 d/wk. over 52 days [86]. The γ-fagarine (Figure 1.3, **15**) isolated from *Helietta apiculata* showed 97% reduction in parasite burden following oral administration to mice infected with *L. amazonensis* at the dose of 10 mg/kg for 14 days. 14-hydroxyunularin (Figure 1.3, **16**) isolated from a bryophyte exhibited 93% reduction in lesion parasite burden following subcutaneous administration to mice infected with *L. amazonensis* at a dose of 10 mg/kg for 15 days [87]. A pyrrolloquinazoline alkaloid, peganine (Figure 1.3, **17**) was isolated from *Peganum harmala* and exhibited promising activity (Peganine hydrochloride dihydrate an orally active antileishmanial agent against *Leishmania donovani*, the causative species for the more lethal visceral leishmaniasis. Peganine showed significant (80%) reduction in parasite burden following oral administration to hamsters infected with visceral leishmaniasis without any toxicity to the host macrophages. Thus, peganine has emerged as a promising lead compound for further development against leishmaniasis [88].

Several natural products extracted from various plants like *Septoria pistaciarum [89]*, *Abrus schimperi*, *Prosopis glandulosa var. glandulosa [90]*, *Clerodendrum eriophyllum*, and *Uvaria grandiflora [91]* have also shown antileishmanial activity *in*

vitro against *L. donovani* The protoberberine palmatine exhibited activity against *L. infantum [92],* and the quinonemethides maytenin (Figure 1.3, **18**) and pristimerin (Figure 1.3, **19**) showed activity against *L. chagasi [93]*.

Preussomerin EG1 (Figure 1.3, **20**) has shown potent antileishmanial activity in the axenic amastigotes-based assay [94]. The taxoid 10-deacetylbaccatin III (Figure 1.3, **21**), isolated from *Taxus baccata* showed potent antileishmanial activity *in vitro* against the intracellular amastigote of *L. donovani* with an EC_{50} value of 0.07 µM and an SI value of > 10, compared to Taxol, which is cytotoxic at nanomolar concentrations [95].

Many marine invertebrates or associated bacteria have also contributed to the drug discovery pipeline for leishmaniasis (Figure 1.3). Cristaxenicin A (Figure 1.3, **22**) showed promising activity *in vitro* against *L. amazonensis* promastigotes, (EC_{50} = 0.09 µM) [96]. The crude extract of the sponge *Plakortis angulospiculatus* yielded plakortide P, which showed activity *in vitro* against *L.* The venom of the scorpion *Tityus discrepans [97]* and the crude venom from the snake *Bungarus caeruleus* have also been reported to be active against *L. mexicana* promastigotes [98].

1.7.2. Structure-activity relationships (SARs) of natural product leads:

Compounds were also obtained through optimization of antileishmanial activity of the natural product leads isolated from plant and animal sources. Systematic exploration of their structure-activity relationships either via semi-synthesis or total synthesis has led to more potent and new molecules for further development. However, this process is often hampered by the lack of a sufficient number of natural products obtained and their structural complexity. The natural product coumarin (−)-mammea A/BB (#)

(EC_{50} = 3.0 µg/mL) isolated from *C. Brasiliense* upon reduction of the terminal isobutene moiety afforded a more potent semisynthetic derivative **23** (Figure 1.3), with an EC_{50} of 0.37 µg/mL against *L. amazonensis* promastigotes [99]. The active phenolic marine natural product isoaaptamine (EC_{50} = 0.7 µg/mL), from the sponge *Aaptos* sp., upon esterification resulted in two analogs (Figure 1.3, **24**) that showed more potent activity (EC_{50} values (0.4 µg/mL and 0.1 µg/mL) compared to the parent against *L. donovani* [100]. Although 8,8-dialkyldihydroberberine derivatives (Figure 1.3, **25**) showed potent activity *in vitro* against the intracellular *L. donovani* amastigotes, no *in vivo* efficacy was observed following intraperitoneal (i.p.) administration to mice for 5 days presumably due to poor pharmacokinetic properties [101].

1.8. Quinazoline Alkaloids:

Many marketed drugs are based on quinazoline and quinazolinone scaffolds, which are important nitrogen heterocyclic compounds with a variety of biological activities [102]. Quinazoline, also called 1,3-diazanaphthalene, is a light yellow crystalline solid made up of one pyrimidine and one benzene ring [103]. These substances are used in many different therapeutic applications and show a wide range of biological activities [104]. Quinazoline is a crucial compound in medicinal chemistry. It has a benzo fused ring system with nitrogen atoms at the first and third positions [105]. Paal and Bush proposed the quinazoline ring structure numbering scheme two years later, in 1889 [106].

Quinazolinone, a quinazoline ketonic form with a carbonyl group at position four, is typically synthesized by chemical reactions or derived from natural sources [107].

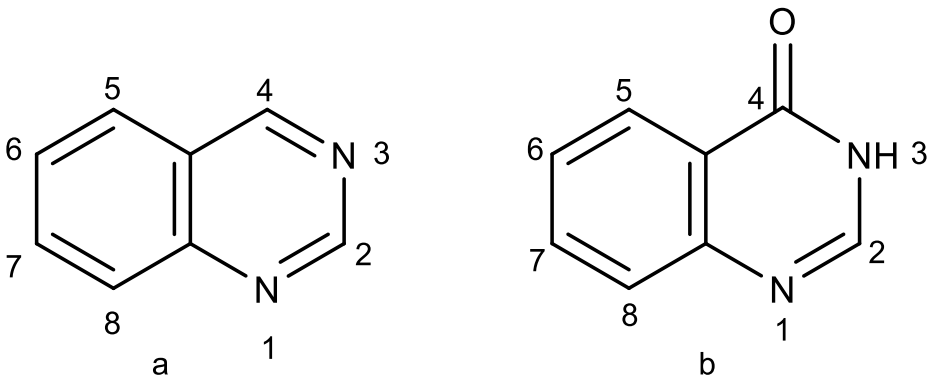

Figure 1.4: Quinazoline and Quinazolinone structure and numbering following IUPAC nomenclature.

1.8.1 History of Development:

Quinazolines are the fundamental constituents of more than 200 naturally occurring alkaloids that are present in microbes, plants, and animals [108]. As a "privileged structure" in pharmaceutical research and development, the quinazoline moiety is ubiquitous in various clinically used drugs including anti-infective agents [109]. After identifying its isomeric relationship to substances such as cinnoline and quinoxaline, Widdege suggested the term "quinazoline" in 1887 [109]. Other names for this heterocyclic system include benzo-1,3-diazine, benzylene amidine, phenmiazine, 5,6-benzopyrimidine, and 1,3-diazanaphthalene [110].The first quinazoline alkaloid (figure 1.5) to be isolated from *Adhatoda vasica* was vasicine (±) (peganine), which was known for its strong bronchodilator properties and was discovered in 1888 [107, 111]. In 1895, August Bischler and Lang reported its synthesis by decarboxylating the 2-carboxy derivative. Other techniques include the Niementowski synthesis, which yields 4-oxo-3,4-dihydroquinazolines by reacting amide and anthranilic acid [112]. Among its isomers are phthalizine, cinnoline, and quinoaxoline [112]. Similar in activity to quinazoline, quinazolinone is fur-

ther divided into 2-quinazolinone and 4-quinazolinone according to patterns of substitution [106].

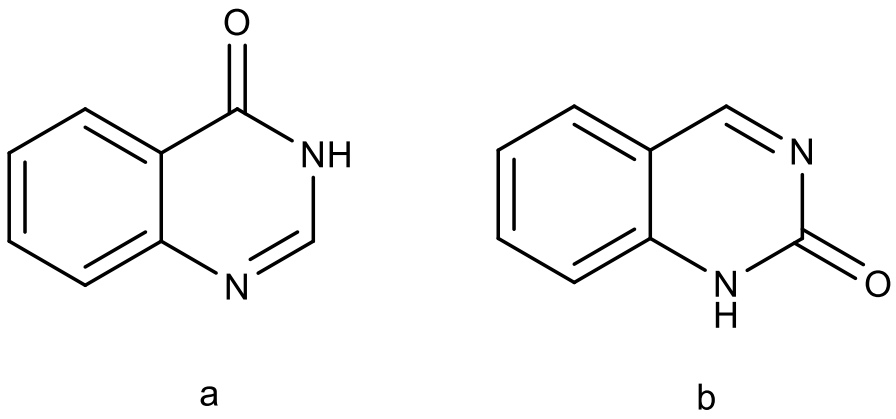

Figure 1.5: 4-quinazolinone(a) and 2-quinazolinone(b).

Quinazoline is an important compound in pharmaceutical chemistry that is used in many medications, clinical candidates, and bioactive compounds [109]. With their diverse array of privileged structures, quinazolines offer effective targeting of various receptors [113]. In medicinal applications, quinazoline exhibits a plethora of activities spanning antimalarial, antimicrobial, antitubercular, anticonvulsant, anticancer, antihypertensive, antidiabetic, anti-inflammatory, anti-cholinesterase, cellular phosphorylation inhibition, dihydrofolate reductase inhibition, kinase inhibition, tubulin polymerization inhibition, diuretic, antipsychotic, dopamine agonist, and anti-HIV properties [105, 108] as shown in figure1.5.

Quinazoline derivatives show a broad spectrum of potential biological activities, supporting the development of antitumor, antimicrobial, antimalarial, antiviral, and antidiabetic therapies, among other treatments for different conditions [114]. As a result, quinazoline compounds are important tools for scientists working on the development,

synthesis, and improvement of medications that will one day be used to treat a variety of illnesses [111]. Their diverse pharmacological characteristics render them auspicious contenders for the creation of innovative treatments aimed at addressing numerous health issues in various medical domains [111].

The polarization of the 3,4-double bond appears in quinazoline reactions, and the two nitrogen atoms in the pyrimidine ring are non-equivalent [115]. The nature and location of the substituents, whether they are on the pyrimidine or benzene ring, as well as the degree of conjugation on the pyrimidine ring, are the main determinants of the properties of substituted quinazolines [102].

Numerous alkaloids exhibit a wide range of biological activities, such as fumi quinazolines, rutaecarpine, vasicine, and luotonin A [107]. *Peganum harmala* seeds provide vasicine, which has cardiac depressant, uterine stimulant, and mucolytic effects [103]. Deoxyvasicine, on the other hand, has potential as an Alzheimer's disease treatment [107]. Traditional Chinese medicine's tryptanthrin exhibits insecticidal properties and promotes neuronal differentiation [116]. *Evodia rutaecarpa* yields rutaecarpine, which has antitumor, anti-inflammatory, and cardioprotective properties [114]. Isolated from Aspergillus fumigatus, fumiquinazolines exhibit strong topo-II inhibition and cytotoxic activity [114]. Plant families contain both pyrrole-quinazolinones and indole-quinazolinones, which have different biological effects [104]. Luotonin A functions as a human topoisomerase-I poison and is derived from *Peganum nigellastrum* [104]. Furthermore, quinazolinones that have been isolated from microbes have additional therapeutic potential [111]. All things considered; these alkaloids are a wealth of bioactive substances with potential medical uses [107].

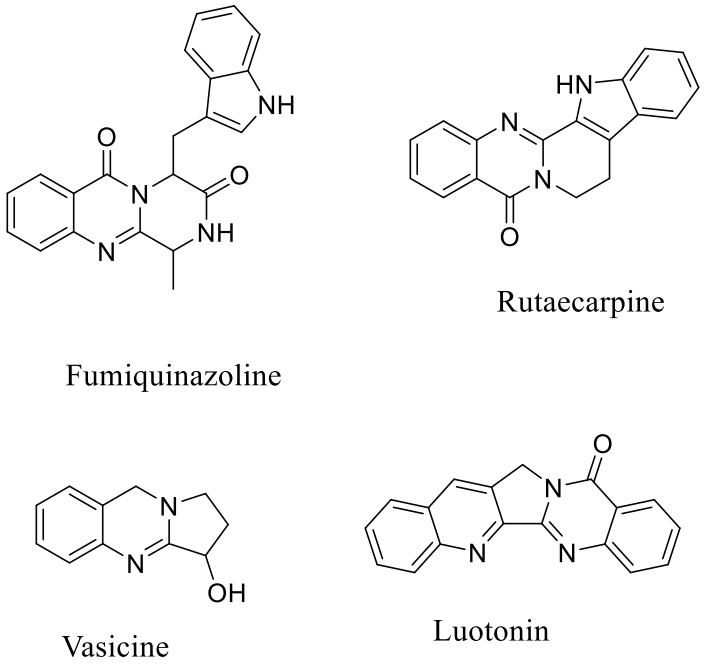

Figure 1.6: Structures of fumi quinazolines, rutaecarpine, vasicine, and luotonin

1.8.2 Antiprotozoal activity of quinazoline alkaloids:

1.8.2.1 Antimalarial activity:

Malaria continues to be a major global health concern, accounting for millions of cases and hundreds of thousands of deaths each year [117]. Significant risks are associated with Plasmodium falciparum and *Plasmodium vivax*, particularly for children and expectant mothers [22]. Parasite resistance has spurred a search for new treatments, concentrating on natural sources like medicinal plants, despite the effectiveness of medications like quinine and artemisinin derivatives [118]. Research on alkaloids derived from medicinal plants must go on to combat malaria and overcome drug resistance [119].

Febrifugine (Figure 1.7, **26**) an alkaloid from *Dichroa febrifuga*, has a history of use against malaria in China. However, its clinical use has been limited due to associated

adverse effects [22]. Studies have explored modifications and synthetic derivatives to enhance safety and efficacy [104]. Febrifugine, along with Isofebrifugine (Figure 1.7, **27**) showed significant antimalarial effects, with Febrifugine demonstrating superior potency against Plasmodium falciparum compared to Chloroquine (Figure 1.7, **28**) [104].

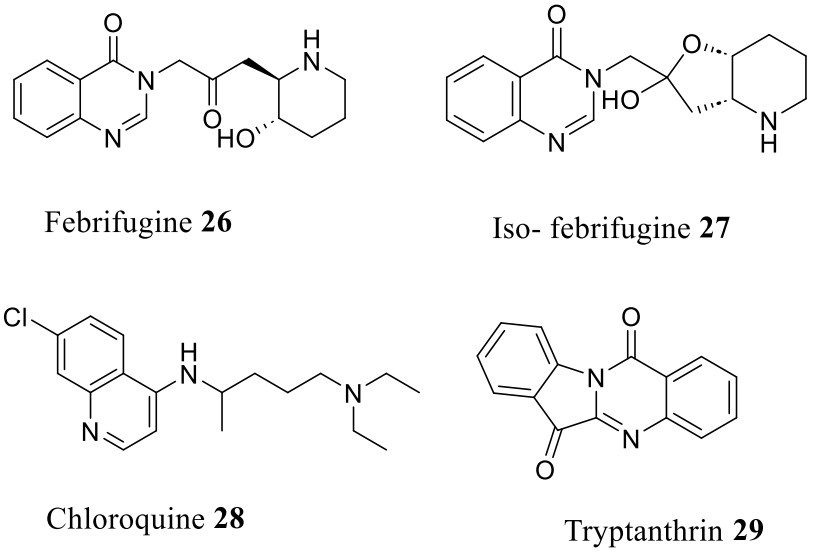

Figure 1.7: Quinazoline Alkaloids showing Anti-malarial activity

Further studies on quinazoline derivatives, such as tryptanthrin (Figure 1.7, **29**) revealed promising antimalarial activity [104, 116]. Additionally, efforts to design 2,3-substituted quinazolin-4(3H)-one derivatives inspired by febrifugine aimed at developing simpler and cost-effective antimalarial drugs [120]. Despite the challenges associated with febrifugine, ongoing research strives to leverage its structural features while addressing safety concerns, offering potential for more effective and safer antimalarial treatments [121].

1.8.2.2 Anti-trypanosomal activity of quinazoline alkaloids:

Quinazoline alkaloids (figure 1.8) also exhibit a wide range of biological activities, including anti-trypanosomal activity [104]. These alkaloids are found in a variety of plant species, including *Peganum harmala, Peganum nigellastrum,* and *Zanthoxylum chiloperone*. The quinazoline alkaloids that have been identified as anti-trypanosomal agents include peganine, harmaline, harmine, and vasicinone [104, 122].

Peganine (Figure 1.8, **31**) is a quinazoline alkaloid that is found in the seeds of *Peganum harmala*. Peganine has been shown to exhibit potent anti-trypanosomal activity against *Trypanosoma brucei*, the causative agent of African sleeping sickness. Peganine works by inhibiting the activity of the trypanosomal enzyme, trypanothione reductase, which is essential for the survival of the parasite [123, 124].

Harmine (Figure 1.8, **30**) and Harmaline (Figure 1.8, **32**) are also quinazoline alkaloids that are found in the seeds of *Peganum harmala*. These alkaloids have been shown to exhibit anti-trypanosomal activity against *Trypanosoma cruzi*, the causative agent of Chagas disease. Harmaline and Harmine work by inhibiting the activity of the trypanosomal enzyme, cruzain, which is essential for the survival of the parasite [124, 125].

Vasicinone (Figure 1.8, 33) is a quinazoline alkaloid that is found in the leaves of *Adhatoda vasica*. Vasicinone has been shown to exhibit potent anti-trypanosomal activity against *Trypanosoma brucei*. Vasicinone works by inhibiting the activity of the trypanosomal enzyme, trypanothione reductase [125, 126].

The anti-trypanosomal activity of quinazoline alkaloids makes them potential candidates for the development of new drugs for the treatment of trypanosomiasis. However, the use of these alkaloids as drugs is limited by their low solubility and poor bioavailability. Efforts are being made to improve the solubility and bioavailability of these alkaloids through the development of new formulations and delivery systems [104, 127].

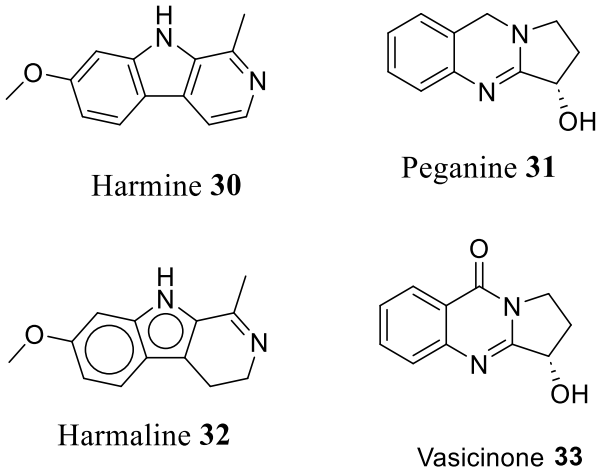

Figure 1.8: Quinazoline alkaloids showing anti-trypanosomal and anti-leishmanial activity

1.8.2.3 Antileishmanial activity of quinazoline alkaloids:

Harmine (figure 1.8, **30**), a quinazoline alkaloid found in *Peganum harmala*, exhibited potent activity against *Leishmania donovani*, the parasite responsible for visceral leishmaniasis. The harmine inhibited the growth of *L. donovani* parasites in vitro and in vivo and was also effective against drug-resistant strains of the parasite [128].

Peganine (figure 1.8, **31**), another quinazoline alkaloid found in *Peganum harmala*, exhibited potent activity against *Leishmania* parasites. Peganine inhibited the

growth of multiple Leishmania species, including *L. donovani*, *L. major*, and *L. infantum*, with IC_{50} values in the low micromolar range. Peganine was also effective against drug-resistant strains of *Leishmania* [123].

The mechanism of action of quinazoline alkaloids against *Leishmania* parasites is not fully understood, but several studies have suggested that they may target multiple pathways involved in parasite growth and survival. Harmine inhibited the activity of the enzyme topoisomerase, which is involved in DNA replication and repair in *Leishmania* parasites. Harmine inhibited the activity of the enzyme farnesyl pyrophosphate synthase, which is involved in protein prenylation and membrane synthesis in *Leishmania* parasites [129].

In addition to their potent anti-leishmanial activity, quinazoline alkaloids have several other advantages as potential drug candidates. They are natural compounds that are readily available from plant sources, and they have relatively low toxicity compared to many synthetic drugs [130].

1.9: Scaffold hopping in drug design:

Scaffold hopping, also known as lead hopping, is a widely used drug design approach to identify novel chemical structures from known biologically active lead compounds with a goal to retain and/or improve the activity as well as optimize pharmacokinetic properties [131]. Validation of topomer similarity as a superior predictor of similar biological activities [132]. The term, “scaffold hopping” was coined by Schneider and colleagues in 1999 as a technique to identify molecular structures with the same biological activity, but significantly different molecular backbones [133]. This approach in-

volves the modification of the core structure or the scaffold of the parent molecule to generate a novel skeleton and maintain and/or optimize the activity and improve the pharmacokinetic properties. Scaffold hopping is classified into four major categories [134]:

1.9.1 Heterocycle replacements

1.9.2 Ring opening or closure

1.9.3 Peptidomimetics

1.9.4 Topology-based hopping

1.9.1 Heterocycle replacements:

The minor modifications such as replacing or swapping carbon and heteroatoms in the core structure, are classified as heterocycle replacements. Replacing the C with heteroatoms N, O, and S can result in novel scaffolds with improved binding affinity if the heterocycle is directly involved in interactions with the target protein. For example, three diaryl heterocyclic cyclooxygenase 2 (COX-2) selective inhibitors Du697 (Figure 1.9, **34**), celecoxib (Figure 1.9, **35**) and rofecoxib ((Figure 1.9, **36**) differ from each other mainly in the backbone heterocyclic rings, their potency against COX-2 is comparable, but show varied pharmacology [135].

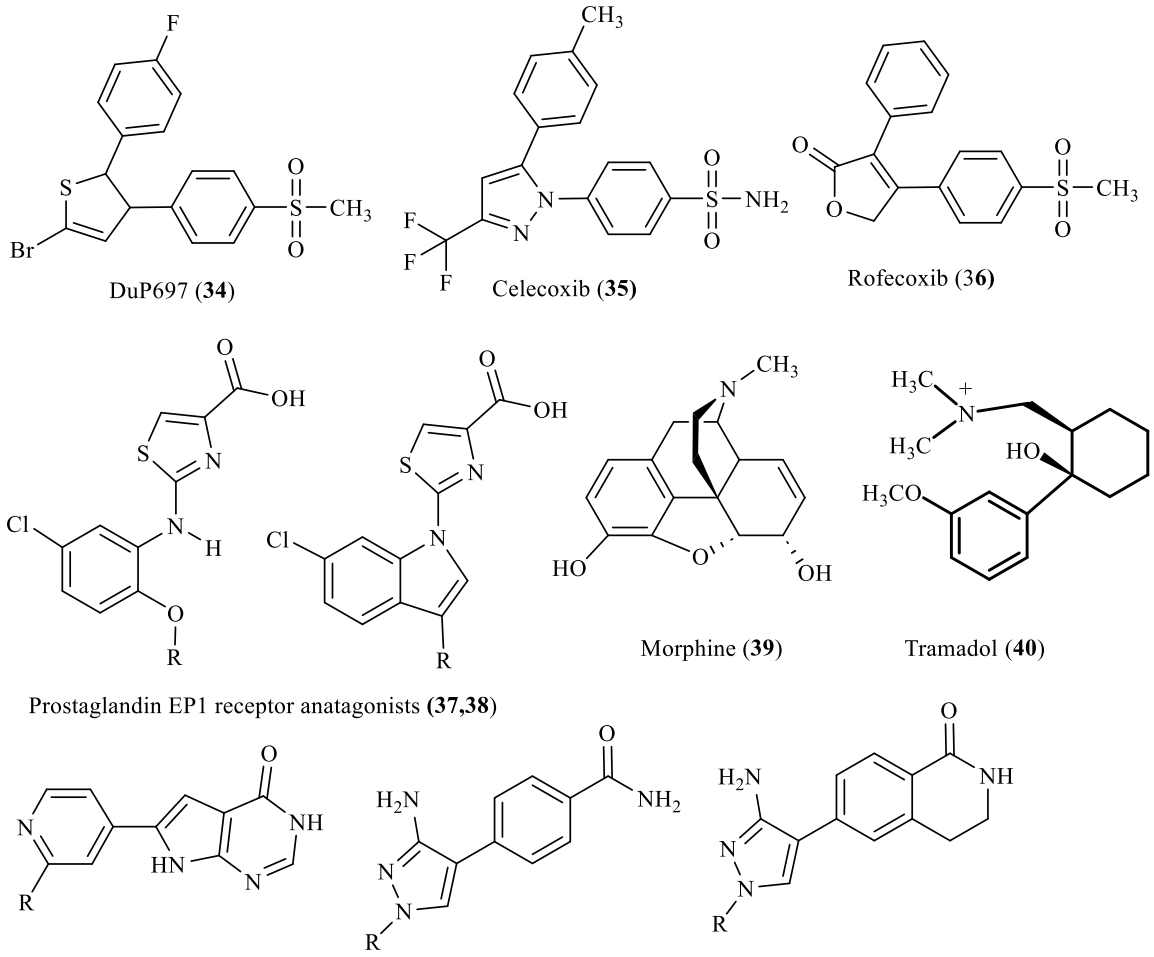

Figure 1.9. Heterocyclic replacements and ring opening/closing stratgies

1.9.2 Ring opening or closure:

Most drug-like molecules contain at least one ring, ring opening and ring closure are two viable strategies to create novel scaffolds. Molecular flexibility greatly enhances the entropy of the binding free energy as well as membrane permeability and absorption [136], hence ring opening, and closure are useful strategies for improving the drug-like properties of molecules. Ring opening and closure alters the flexibility of a molecule by

regulating the total number of free rotatable bonds. For example, the indole containing prostaglandin EP1 receptor antagonists (**37,38**) (Figure 1.9) synthesized by Glaxo SmithKline successfully locked the molecules into a bioactive conformation via ring closure [137]. Conversion of an alkyl chain to cyclohexane, piperazine or piperidine [138], 2-hydroxybenzoyl moiety to quinazoline ring system [139], and arylamine or arylamide to a fused ring system are widely used ring closure approaches [140]. On the contrary, too many rings, especially aromatic rings, in a molecule may reduce the drug likeness of the molecule due to decreased pharmacokinetic properties [141]. To circumvent this, introducing saturated rings in a molecule can decrease its structural flexibility and maintain drug likeness, but may pose some challenges to synthesize the resulting chiral molecules such as spiropiperidine-based stearoyl-CoA desaturase-1 inhibitors: Identification of 1′-{6-[5-(pyridin-3-ylmethyl)-1,3,4-oxadiazol-2-yl]pyridazin-3-yl}[80, 142, 143] -5-(trifluoromethyl)-3,4- dihydrospiro[chromene-2,4′-piperidine].

The structural modification of potent opioid analgesic morphine ((Figure 1.9, **39**) to less potent, but less toxic tramadol ((Figure 1.9, **40**) by ring opening is one of the earliest examples of scaffold hopping [144]. 3D structures of both the opioids, as determined by the Flexible Alignment program in the Molecular Operating Environment (MOE) software [145], conserves the key pharmacophore features, the positively charged tertiary amine, the aromatic ring, and the hydroxyl group attached to phenyl ring. Tramadol undergoes *O*-demethylation by CYP2D6 to form the corresponding hydroxy derivative. Although tramadol is only one-tenth of the potency of morphine, it is almost completely absorbed after oral administration, and the duration of action is enhanced (6 hours).

Concurrent ring opening and ring closure on the same molecule may lead to ring migration [146]. For example, opening of the pyrimidinone ring in the lead MAP (mitogen-activated protein) kinase-activated protein kinase 2 (MK2) inhibitor, pyrrolopyrimidone ((Figure 1.9) , **41**) along with the retention of the amide group, and swapping of 5- and 6-member rings [147]resulted in a compound that was 4-fold less potent than the lead compound. However, appending the amide group back to the phenyl ring reduced the flexibility of the amide which in turn increased the affinity by 25-fold. These modifications led to the highly potent (84 nM) MK2 inhibitor dihydroisoquinolinone **(**(Figure 1.9, **42**) [147].

The generation of a macrocyclic structure (ring-based molecule having nine or more atoms) from a linear molecule is a special ring closure strategy that is used to introduce conformational constrains in a molecule [148].

1.9.3 Peptidomimetics:

The replacement of peptide backbones with non-peptidic moieties (peptidomimetics) is another strategy to create a novel scaffold and improve activity and most importantly the pharmacokinetic properties of the parent peptides. For example, replacement of an amide bond in the second mitochondrial activator of apoptosis, AVPI (ALA-VAL-PRO-ILE) (Figure 1.10) **43** with an oxazole ring **44** (Figure 1.10) resulted in a peptidomimetic with reduced binding affinity with Baculovirus inhibitor of apoptotic protein Repeat 3 (BIR3) domain of XIAP [149]. This is mainly attributed to the loss of key backbone hydrogen bonding interactions with the protein.

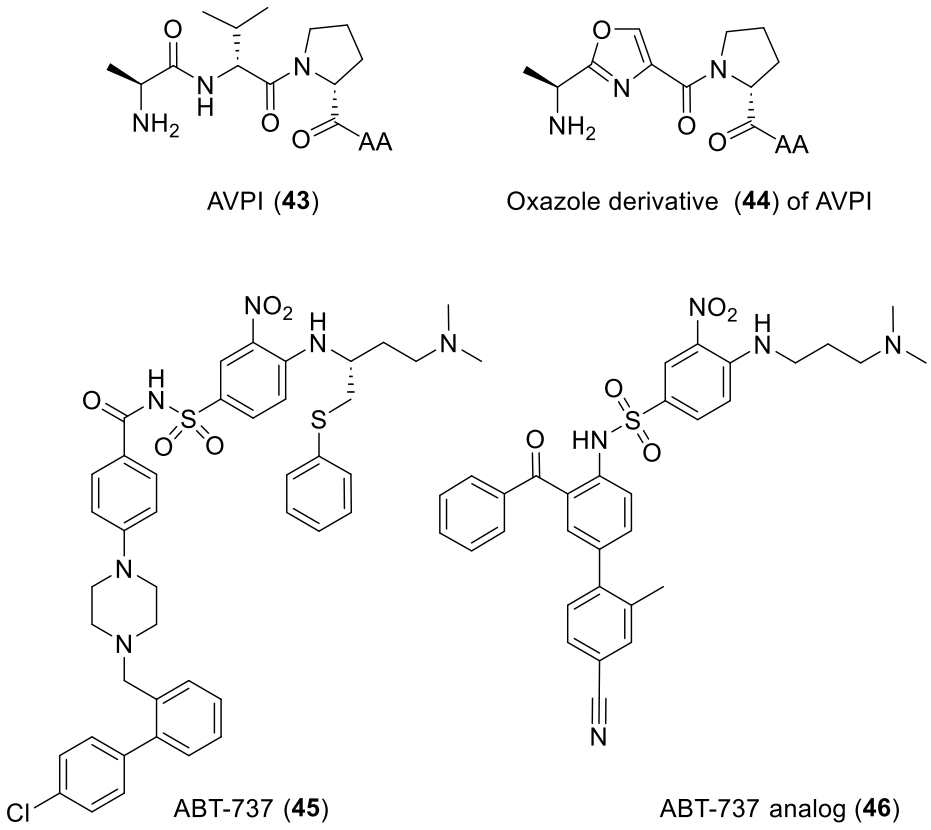

Figure 1.10. Peptidomimetic and topology-based scaffold hopping

1.9.4 Topology-based hopping:

The complete overhauling of the parent core structure to a new structural backbone with the goal of maintaining and/or improving biological activity as well as enhancing the physicochemical and pharmacokinetic properties is referred as topology-based scaffold hopping. Although this approach affords novel structures significantly distinct from the parent molecule, attenuation or complete loss of biological activity and pharmacokinetic properties may reduce the application of topology-based scaffold hopping.

For example, a new series of BCL-xl inhibitors were identified through similarity search using the known inhibitor ABT-737 (**45**) (Figure 1.10) which resulted in a new

series of novel inhibitors, with ((Figure 1.10, **46**) reported to be the most potent, but equi-potent to ABT-737 [150].

1.10 Scaffold hopping in antiparasitic drug discovery:

Various groups have successfully employed scaffold hopping in designing new anti-parasite agents for malaria and the neglected tropical diseases trypanosomiasis (sleeping sickness, and chagas disease), and leishmaniasis.

1.10.1 Scaffold hopping in antimalarial drug discovery:

Scaffold hopping has been used in the development of several anti-malarial drugs, including Artemisinin-Based Combination Therapies (ACTs) and a novel class of antimalarial compounds known as spiro-indolones. Artemisinin (Figure 1.11, **47**), a natural product derived from the plant *Artemisia annua*, is the basis for most ACTs, which are currently the frontline treatment for malaria. Scaffold hopping has been used to modify the artemisinin scaffold to generate new compounds with improved activity against artemisinin-resistant strains [151, 152]. Spiro-indolones, for example cipargamin ((Figure 1.11, **48**) are a new class of anti-malarial compounds that were discovered using scaffold hopping. The compounds were identified through a phenotypic screening campaign of a diverse chemical library. The screening identified a series of compounds with a spiro-indolone scaffold that exhibited potent activity against *P. falciparum* both *in vitro* and *in vivo* [153].

Scaffold hopping has also been used in the development of compounds that target the *Pf*CDPK1 is a validated drug target that plays a critical role in the survival of *P. falciparum*. The use of scaffold hopping has resulted in the identification of several

potent and selective *Pf*CDPK1 inhibitors [154]. Another compound called GNF179 ((Figure 1.11, **49**), has potent antimalarial activity, but showed poor drug-like properties. By modifying the core structure of GNF179, to develop a series of compounds with improved drug-like properties and similar or improved antimalarial activity [155]. Another compound called SJ733 ((Figure 1.11, **50**), has potent antimalarial activity, but poor pharmacokinetic properties. By modifying the core structure of SJ733, to develop a series of compounds with improved pharmacokinetic properties and similar or improved antimalarial activity [156].

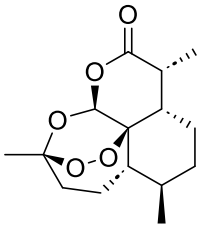

Artemisinin **47**

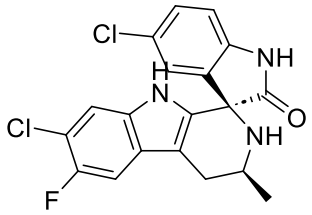

Cipargamin **48**

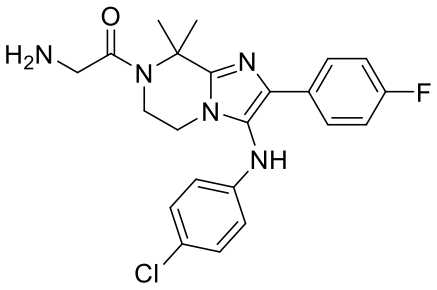

GNF179 **49**

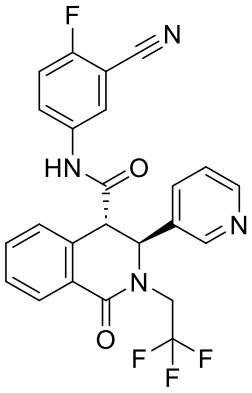

SJ733 **50**

Figure 1.11: Scaffold hopping in anti-malarial drug design

1.10.2 Scaffold hopping in anti-trypanosomal drug design:

Many anti-trypanosomal drugs have been developed using scaffold hopping design approaches. Melarsoprol (Figure 1.12, **51)** is an arsenic-based compound derived from atoxyl that is used to treat late-stage African trypanosomiasis caused by the protozoan parasite *Trypanosoma brucei rhodesiense* [157]. Eflornithine (Figure 1.12, **52**), also known as DFMO (α-difluoromethylornithine), a compound derived from ornithine, inhibits *Trypanosoma brucei* gambiense by blocking ornithine decarboxylase [158]. Treatment for Chagas disease caused by *Trypanosoma cruzi* consists of Nifurtimox (Figure 1.12, **53**) and Benznidazole (Figure 1.12, **54**), which belong to the nitrofuran and nitroimidazole classes, respectively, and were generated by scaffold hopping. The parasites eventually die because of the production of toxic reactive oxygen species and metabolites by these drugs [158, 159]. Scaffold hopping was used to create Fexinidazole (Figure 1.12, **55**), another nitroimidazole compound used to treat African trypanosomiasis. It works by inducing metabolic activation, which generates harmful metabolites leasing to death of the parasite [160].

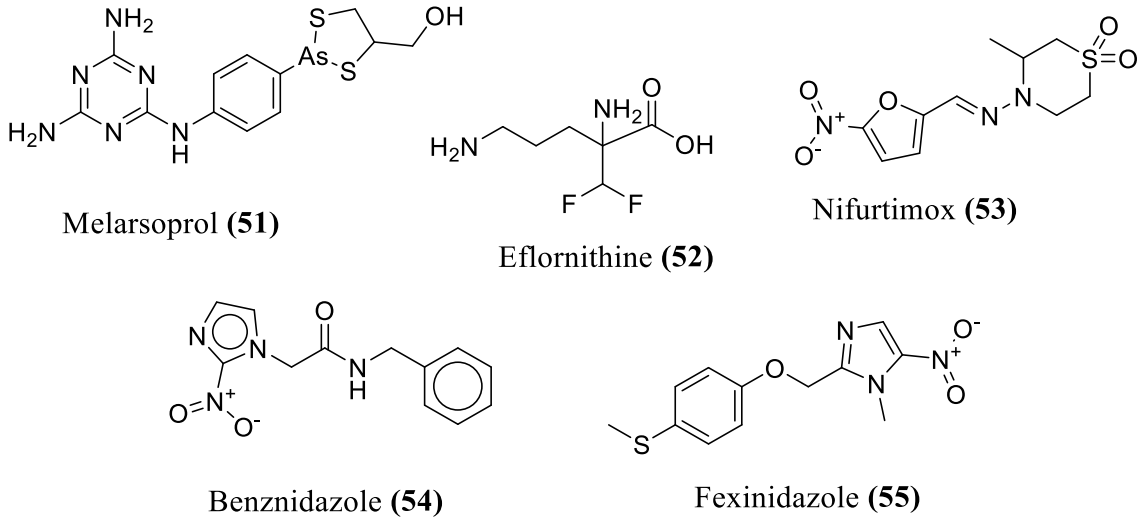

Figure: 1.12: Scaffold hopping in anti-trypanosomal drug design

1.10.3 Scaffold hopping in antileishmanial drug discovery:

The development of antileishmanial drugs has benefited greatly from the application of scaffold hopping design approaches, which have produced new compounds with enhanced efficacy and safety profiles. One notable application of this strategy is the synthesis of liposomal Amphotericin B (Figure 1.13, **56**), or L-AmB.

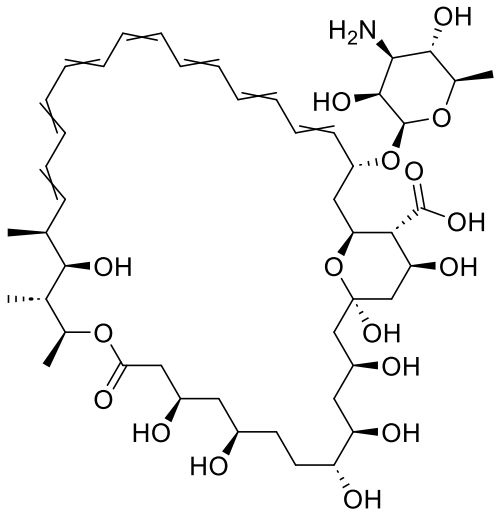

Figure:1.13: Structure of Amphotericin B

Despite having potent antileishmanial activity, amphotericin B's clinical use is restricted due to significant nephrotoxicity. Using the structure of Amphotericin B as a scaffold, scientists created L-AmB, a medication that encapsulates the drug in liposomes to reduce toxicity while maintaining its effectiveness against *Leishmania* parasite. This breakthrough has significantly increased leishmaniasis treatment options, particularly in cases where traditional treatments are toxic and may not be safe [161, 162].

Recently target-based scaffold hopping, and parasitic hopping reported from a previously active antitrypanosomal agent Lapatinib (**58**) (Figure1.14) and related analogs against *Trypanosoma brucei* along with a new series of compounds to develop NEU-1953 (Figure 1.14, **59**) and related analogs against multiple protozoan parasitic species *Trypanosoma cruzi, Leishmania major, Leishmania donovani*, and *Plasmodium falciparum*. This work has resulted in the identification of promising lead molecules having submicromolar activity and improved physicochemical properties against these kinetoplastid diseases and malaria [163].

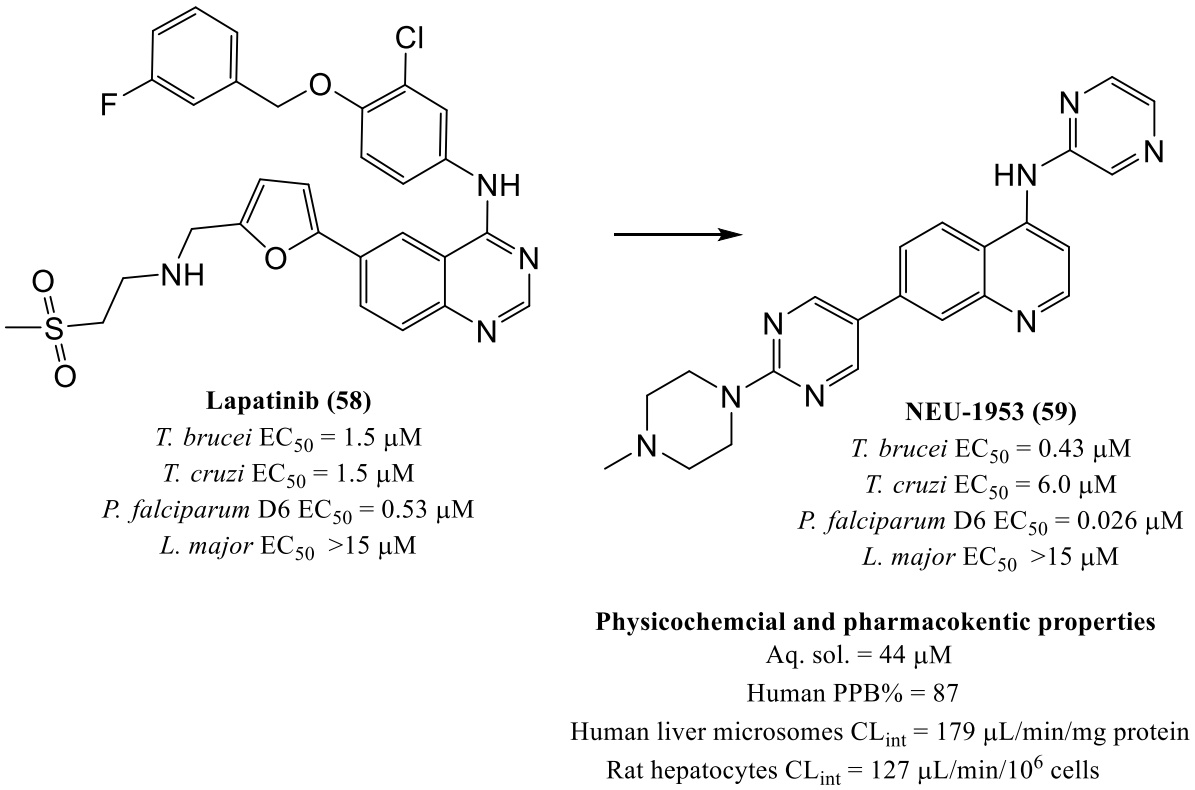

Lapatinib (58)
T. brucei EC_{50} = 1.5 μM
T. cruzi EC_{50} = 1.5 μM
P. falciparum D6 EC_{50} = 0.53 μM
L. major EC_{50} >15 μM

NEU-1953 (59)
T. brucei EC_{50} = 0.43 μM
T. cruzi EC_{50} = 6.0 μM
P. falciparum D6 EC_{50} = 0.026 μM
L. major EC_{50} >15 μM

Physicochemcial and pharmacokentic properties
Aq. sol. = 44 μM
Human PPB% = 87
Human liver microsomes CL_{int} = 179 μL/min/mg protein
Rat hepatocytes CL_{int} = 127 μL/min/10^6 cells

Figure 1.14. Lead optimization of lapatinib (**58**) to more potent analog NEU-1953 (**59**)

Extensive scaffold hopping on 2-phenylimidazo[1,2-a]pyrimidine derivatives has led to the development of an orally efficacious preclinical candidate GSK3494245/DDD01305143 (Figure 1.15, **60**), a proteosome inhibitor [164]. Scaffold hopping on the initial oxazole hit (Figure 1.15, compound **61**) led to a 2-phenylimidazo[1,2-a] pyrimidine core and further optimization of the 6-position to a 6-morpholino substituent increased the potency and metabolic stability. Additionally, the fluorine substitution of the phenyl ring *ortho*- to the bicyclic core increased potency and replacement of the furanyl amide moiety with a pyrrolidinyl urea group improved solubility. This optimization efforts led to an orally efficacious early lead (Figure 1.15, **62)**,

in a mouse model of VL. This also involved a further set of scaffold hops from 2-phenylimidazo[1,2-*a*] pyrimidine.

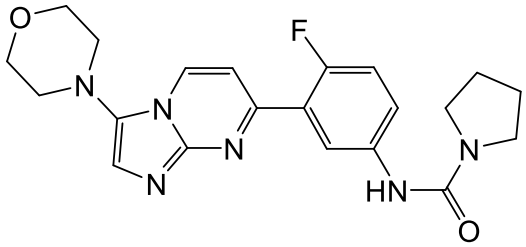

DDD01305143/GSK3494245 (**60**)

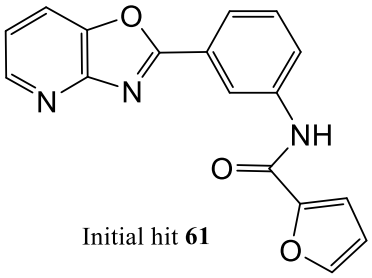

Initial hit **61**

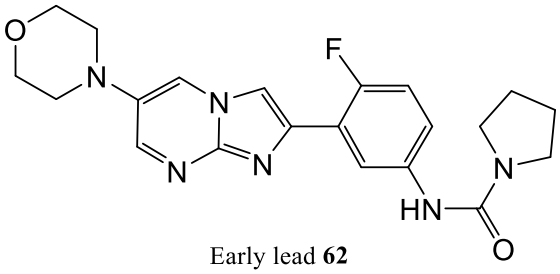

Early lead **62**

Figure 1.15. Structures of DDD01305143/GSK3494245 (**60**), initial hit (**61**), and early lead (**62**).

CHAPTER- 2

DESIGN AND SYNTHESIS OF A NOVEL SCAFFOLD OF PEGANINE

2.1 Introduction:

Leishmaniasis is a major public health concern affecting millions of people in the developing world [165]. The current marketed drugs to treat leishmaniasis are inadequate as they suffer from increasing parasitic resistance, severe nephrotoxicity, high cost, and decreased efficacy of current medications in endemic areas where these aspects are relevant. One of the major drawbacks of the current drugs except miltefosine is their parenteral routes of administration which makes compliance difficult in the endemic area setting of the disease. Miltefosine is the only orally effective drug, however, it has a relatively longer duration of action (4-week treatment) and is also teratogenic. In view of the above limitations of the current drug arsenal for leishmaniasis, newer, safer, cost-effective, and oral drugs with relatively short duration of action are urgently needed to effectively treat this debilitating disease.

We have previously identified a tetra hydro pyrroloquinazoline alkaloid natural product peganine (Figure 2.1, **1**) from *Peganum harmala* that significantly reduces (80%) the parasite burden following oral administration to hamsters infected with visceral leishmaniasis compared to the marketed drug miltefosine [166]. (Figure 2.1) It selectively inhibits the growth of clinically relevant intracellular amastigotes of *Leishmania donovani*, the causative species of the more lethal form visceral leishmaniasis and showed no toxicity to the host macrophages. However, peganine (100mg/kg for 5days) shows efficacy in hamsters at a relatively high dose, therefore, structural modification of the lead molecule is necessary to optimize its antileishmanial activity.

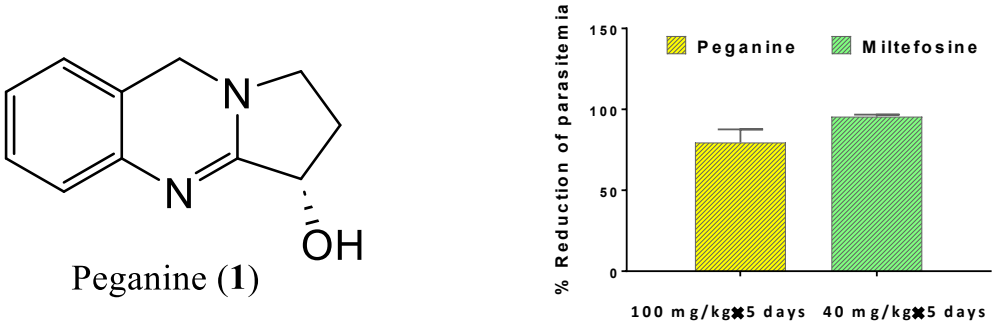

Figure 2.1 Structure of the lead peganine and it's *in vivo* antileishmanial activity.

Peganine showed an IC_{50} 41± 1.53µg/mL with a selectivity of 5 ($CC_{50,}$ 200µg/mL) in intracellular amastigots. The antileishmanial activity of peganine happens to be mediated by a programmed cell death and by inhibition of the topoisomearse 1 of *Leishmania donovani [88]*. Preliminary studies have revealed that peganine has a unique mechanism of action by inhibiting the enzyme alone without the DNA topoisomearse 1 complex, which is different from the known DNA topoisomerase 1 inhibitor, camptothecin. Additional studies are needed to validate the antileishmanial target of peganine.

2.2 Results and discussion:

2.2.1 Design of novel analogs of peganine:

Our laboratory is performing the structural modification of peganine to explore its structure-activity relationships to identify more potent analogs for further development. Preliminary results have shown that peganine inhibits topoisomerase I of *L. donovani* with unique mechanism of action different from the known topoisomerase I inhibitor camptothecin [167]. We are using the classical rational medicinal chemistry drug design (Topliss Operational Scheme) as well as the structure-based drug design approaches to design novel analogs of peganine for evaluation of their antileishmanial activity. Scaffold hopping is a widely used drug design approach to generate novel struc-

tures by modification of the core structure of a lead and maintain and/or improve biological activity and pharmacokinetic properties. The goal of this project is to employ scaffold hopping to design novel analogs of peganine by altering its core scaffold by a heterocyclic replacement of the benzenoid ring and other strategies to optimize the antileishmanial activity of the lead molecule.

Co-crystal structure of camptothecin (Figure 2.2A) bound to human topoisomerase 1 [168] reveals important binding interaction of the inhibitor with the enzyme. This involves an important hydrogen bond between the pyridyl nitrogen of camptothecin and the side chain of arginine (N-H distance = 2.2 Å) of the protein. However, the corresponding co-crystal structure of *Leishmania* topoisomerase is not available with an inhibitor. Topoisomerase 1 of the human and parasite show a high degree of sequence and structural similarity (66-75 % similar, 50 % identical) [169]. Therefore, we used homology modeling to overlay the structure of the parasitic enzyme-DNA-inhibitor complex with co-crystal structures of available human enzyme-DNA-inhibitor complexes (Figure 2.2A). Preliminary modelling studies using the Molecular Operating Environment (MOE) software [170] have shown that the quinazoline nitrogen of peganine similar to the pyridyl nitrogen of camptothecin interacts with the side chain arginine residue of topoisomerase 1 with a strong hydrogen bond (distance = 2.5 Å) as shown in Figure 2.2B.

To further enhance the hydrogen bonding interactions of peganine, we envisioned that an additional hydrogen bond acceptor in the form of a heteroatom (N, O, S) on the adjacent benzenoid ring of the core quinazoline core could lead to more potent interactions with the enzyme and hence more potent antileishmanial activity of the de-

signed analog. Based on this hypothesis, we used the simplest scaffold hopping strategy the heterocyclic replacement initiated where a single ring carbon atom was swapped with a hydrogen bond accepting nitrogen atom (Figure 2.2B). We expect to identify a more potent analog due to its enhanced binding interactions with the arginine residue and hence improved antileishmanial activity.

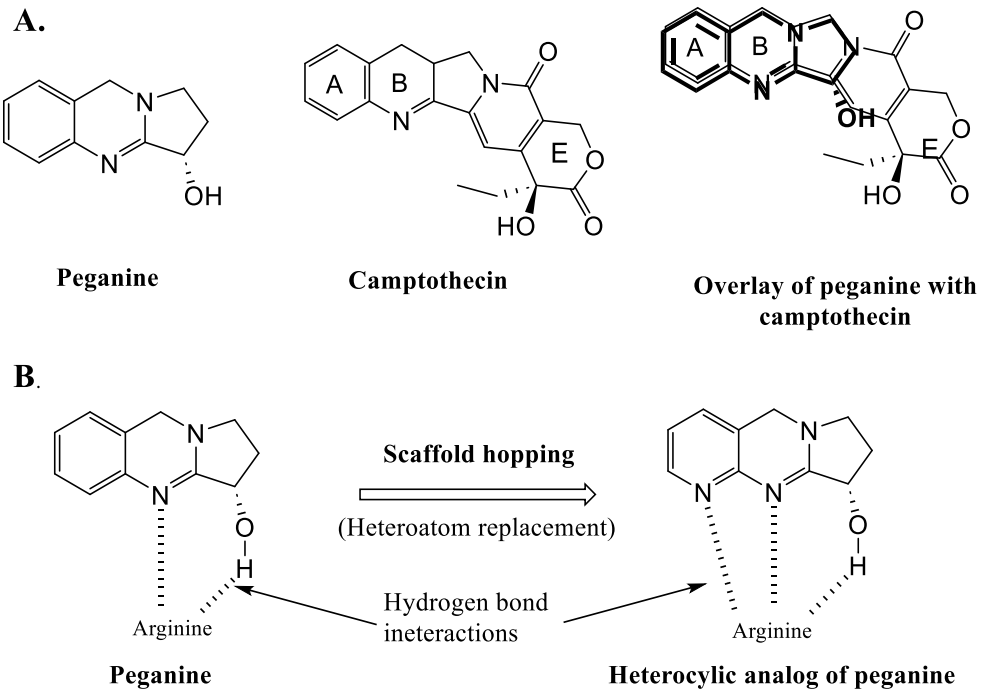

Figure 2.2 (A) Structures of peganine and camptothecin and their superimposition; (B) Heterocylic replacment of peganine to generate a novel scaffold

2.2.2 Retrosynthesis:

The synthesis of peganine is carried out in our laboratory using an established procedure called retrosynthetic analysis [171]. We employed the same synthetic methodology (scheme 2.2) to synthesize this novel scaffold of peganine (figure 2.3). The retrosynthesis analysis of the scaffold was carried out as follows:

Scheme: 2.2: Retrosynthesis of Peganine Scaffold

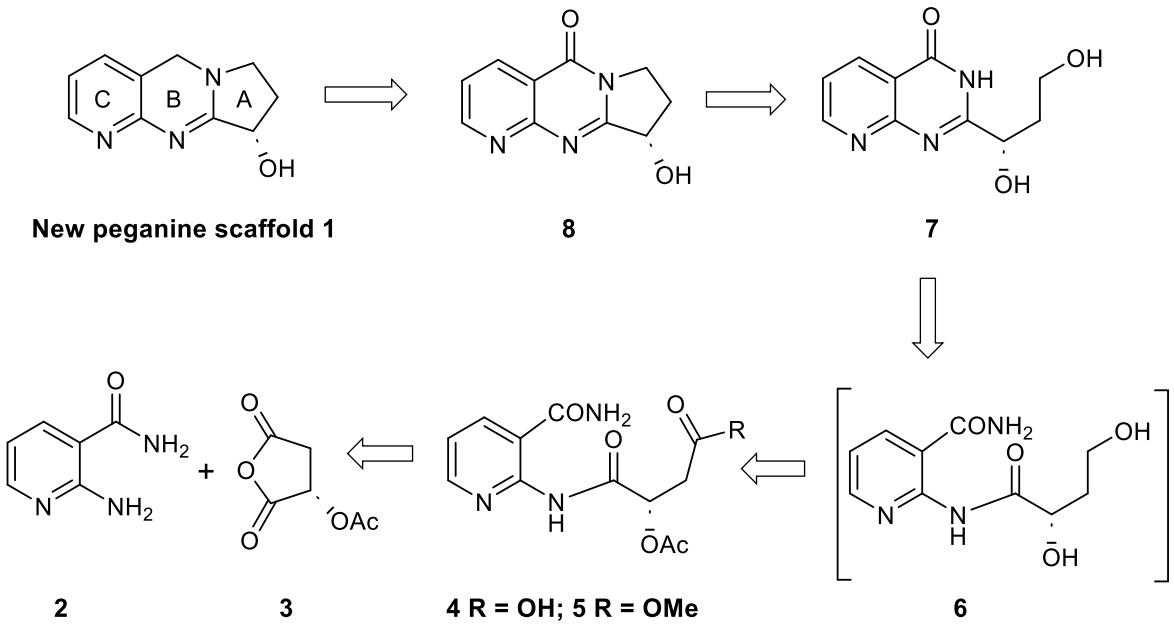

Figure 2.3. Retrosynthesis analysis of the new peganine scaffold

The new scaffold, (S)-5,7,8,9-tetrahydropyrido[2,3-d]pyrrolo[1,2-a]pyrimidin9-ol can be obtained from its quinazoline derivative, which in turn can be obtained from-nthe dihydroxy quinazoline derivative.

2.2.3 Synthesis:

The total synthesis of the novel peganine scaffold (**1**) was carried out by the method of Mhaske and co-workers [172], reported for the synthesis of (-)-vasicinone.

2.2.3.1: Synthesis of (*S*)-2,5-dioxotetrahydrofuran-3yl-acetate (3):

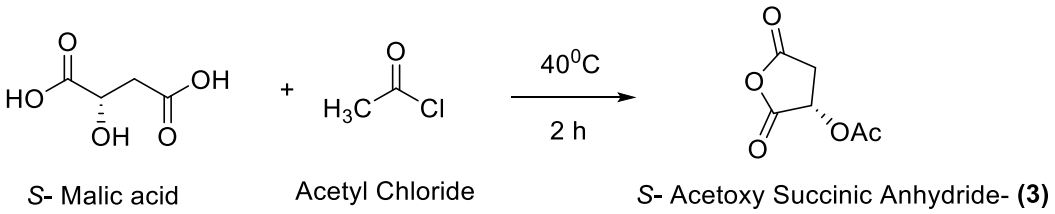

Figure 2.4 Synthesis of (*S)*-2,5-dioxotetrahydrofuran-3yl-acetate **(3)**

The commercially available *S*- malic acid was treated with freshly distilled acetyl chloride to obtain one of the starting materials, (*S*)-2,5-dioxotetrahydrofuran-3yl-acetate [172] (**3**) as represented in figure 2.4. The resulting pure compound was obtained in quantitative yield, characterized by NMR and was used as such for the first reaction with the primary starting material, 2-aminonicotinamide (figure 2.4, **2**).

2.2.3.2: Synthesis of (*S*)-3-acetoxy-4-((3-carbamoyl-pyridine-2yl)-amino)-4-oxobutanoic acid (4):

The reaction of the commercially available primary starting material, 2-amino nicotinamide (**2**), proceeded in a 100% regioselective fashion with (*S*)-2,5-dioxotetrahydrofuran-3yl-acetate (**3**) with a nucleophilic attack of the amino group at the more reactive electron-deficient carbonyl; 2-position of 2-aminonicotinmaide such a regioselectivity with [172] carbon, nitrogen, and oxygen nucleophiles is known. This led to the formation of the ring-opened acid product (**4**) in quantitative yield.

In figure 2.5, the reported reaction was not successful due to insolubility of **2** in 1,4- dioxane, so by replacing 1,4- dioxane with DMF; however, upon optimization of the reactions conditions and the reaction was successful with full conversion of the

starting material (**2**) to yield the acid product (**4**) in quantitative yield as shown in the following scheme (Figure 2.6). The reported method indicated use of dioxane as one of the three solvents for the reaction, however, due to insolubility of the reaction mixture, we used DMF in place of 1,4-dioxane after various solvents were attempted for the reaction. This not only resolved the solubility, but also led to the full conversion of the starting material to the product.

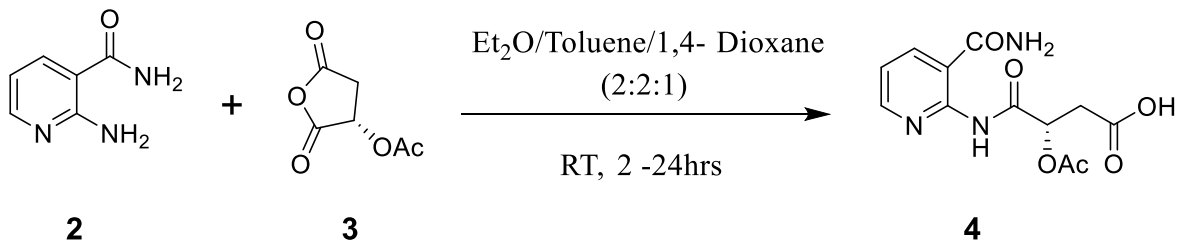

Figure 2.5 Synthesis of (*S*)-3-acetoxy-4-((3-carbamoyl-pyridine-2yl)-amino) -4-oxobutanoic acid **4 (literature report)**

In the following scheme (Figure 2.6), changing the solvent from 1,4-dioxane to DMF, yielded the product in quantitative yield.

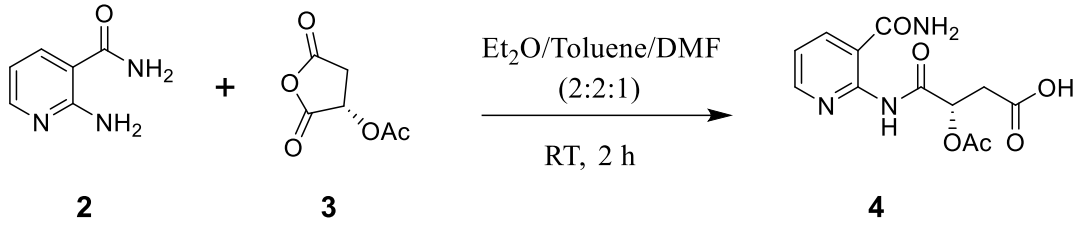

Figure 2.6 Synthesis of (*S*)-3-acetoxy-4-((3-carbamoyl-pyridine-2yl)-amino) -4-oxobutanoic acid **4 (optimized conditions)**

2.2.3.3 Synthesis of methyl (*S*)-3-acetoxy-4-((3-carbamoyl-pyridine-2yl) amino)-4-oxo butanoate 5:

The reaction of (*S*)-3-acetoxy-4-((3-carbamoyl-pyridine-2yl)-amino)-4-oxobutanoic acid (**4)** with EDC, HOBT in DMF at room temperature furnished the corresponding ester intermediate (**5**) in quantitative yield as shown in the following scheme (Figure 2.7).

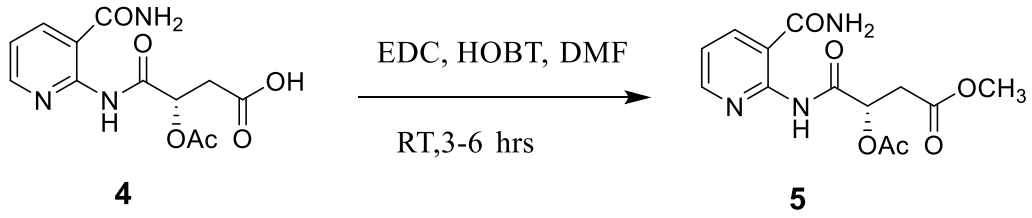

4 **5**

Figure 2.7 Synthesis of methyl*(S)*-3-acetoxy-4-((3-carbamoyl-pyridine -2yl) amino)-4-oxo butanoate (**5)**

Several procedures were unsuccessfully employed to obtain the ester intermediate (**5**). The reaction of compound (**4**) with thionyl chloride, methanol and methylene chloride as solvent was not successful as shown in the following scheme (Figure 2.8). Changing reaction conditions such as extending the reaction did not yield the desired product which was confirmed by the absence of the aromatic peaks of the pyridine ring in the NMR.

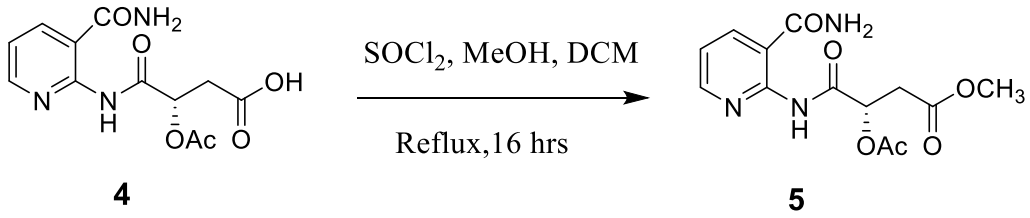

4 **5**

Figure 2.8 Synthesis of methyl(*S*)-3-acetoxy-4-((3-carbamoyl-pyridine-2yl) amino)-4-oxo butanoate**(5)**

Another procedure employing dimethyl maleate (DMM) in presence of potassium bromide (KBr) using DMF as solvent also did not yield the desired product (Figure 2.9). This was also confirmed by the absence of the aromatic peaks of the pyridine ring in the NMR.

4 **5**

Figure 2.9 Synthesis of methyl(*S*)-3-acetoxy-4-((3-carbamoyl-pyridine-2yl) amino)-4-oxo butanoate (**5)**

The reaction of the acid intermediate (**4**) with dimethyl carbonate (DMC) in presence of potassium bicarbonate when refluxed in DMSO for 12 hours also did proceed successfully (Figure 2.10). The absence of the aromatic peaks of the pyridine ring in the NMR indicated the absence of the ester.

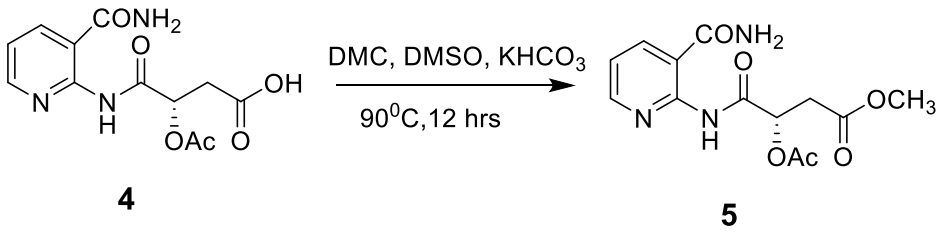

4 **5**

Figure 2.10 Synthesis of methyl(*S*)-3-acetoxy-4-((3-carbamoyl-pyridine-2yl) amino)-4-oxo butanoate (**5)**

The treatment of the acid (**4**) with DMC in K_2CO_3 using chloro tetra butylamine under reflux for 12 hours (Figure 2.11) was also unsuccessful as the formation of the ester product (**5**) was confirmed by NMR which showed the absence of the aromatic peaks of the pyridine ring.

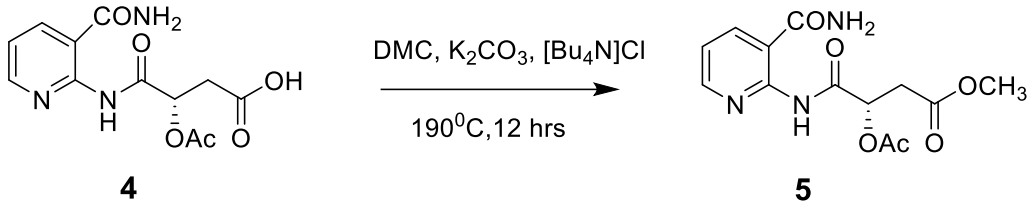

Figure 2.11 Synthesis of methyl*(S)*-3-acetoxy-4-((3-carbamoyl-pyridine-2yl) amino)-4-oxo butanoate **(5)**

The use of dicyclohexylcarbodimide (DCC) in dimethylaminopyridine (DMAP) and DCM led to the desired product (Figure 2.12) as shown by the TLC. However, the product could not be isolated due to the formation of dicyclohexyl urea (DHU) as the by-product which was not easy to remove from the product.

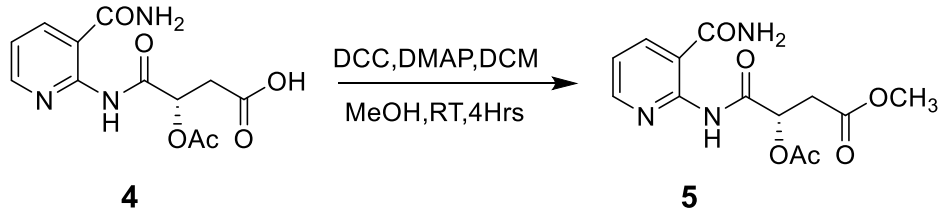

Figure 2.12 Synthesis of methyl(*S*)-3-acetoxy-4-((3-carbamoyl-pyridine-2yl) amino)-4-oxo butanoate **(5)**

The reaction in the following scheme (Figure 2.13) in which DCC was replaced by more reactive EDC did not proceed even after 24 hours. This was confirmed by thin layer chromatography in 5% MeOH in DCM solvent system, compared to the starting material.

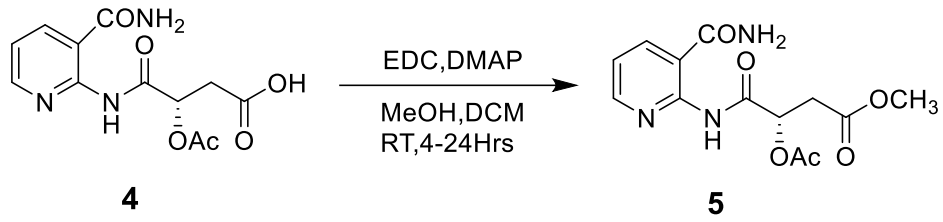

4 **5**

Figure 2.13 Synthesis of methyl(*S*)-3-acetoxy-4-((3-carbamoyl-pyridine-2yl) amino)-4-oxo butanoate (**5)**

Methylation of carboxylic acid and phenols proceeds successfully with methyl iodide (MeI) in potassium carbonate or DBU. However, reaction of the acid (**4**) with MeI in either K_2CO_3 (Figure 2.14) or DBU (Figure 2.15) did not yield the desired product (**5**).

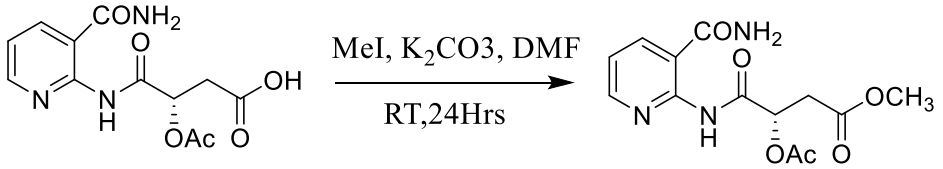

4 **5**

Figure 2.14 Synthesis of methyl(*S*)-3-acetoxy-4-((3-carbamoyl-pyridine-2yl)amino)-4-oxo butanoate (**5)**

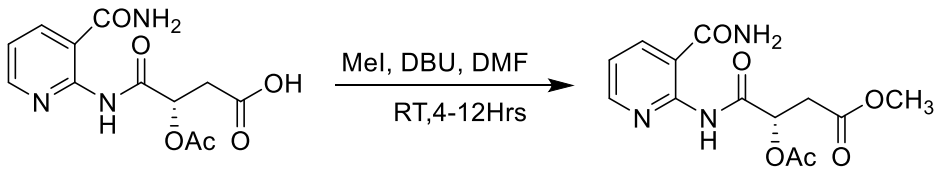

4 **5**

Figure 2.15 Synthesis of methyl(S)-3-acetoxy-4-((3-carbamoyl-pyridine-2yl)amino)-4-oxo butanoate (**5)**

The use of EDC, and HOBT coupling reagents successfully yielded the desired product in a quantitative yield (Figure 2.14) which was confirmed by mass spectrometry, proton NMR, and carbon NMR.

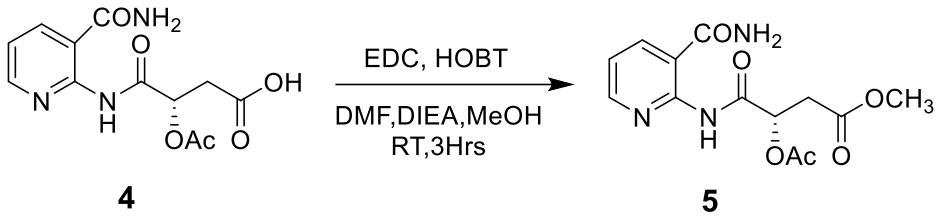

4 **5**

Figure 2.16 Synthesis of methyl(*S*)-3-acetoxy-4-((3-carbamoyl-pyridine-2yl)amino)-4-oxo butanoate (**5)**

2.2.3.4 Synthesis of (*S*)-2-(1,3-dihydroxypropyl)pyrido[2,3-d]pyrimidin-4(3H)-one:

The ester (**5)** was subjected to a chemo-selective reduction with lithium aluminum hydride (LAH) to obtain the reduced intermediate **6**, which undergoes *in situ* LiOH catalyzed [172] dehydrative ring closure to yield the corresponding quinazolinone intermediate (**7)**. Several conditions as shown in the following schemes (Figure 2.17) were employed, but none of the reactions proceeded successfully. This was mainly due to the insolubility of the ester reactant in the commonly used ether solvents for LAH-mediated reduction conditions.

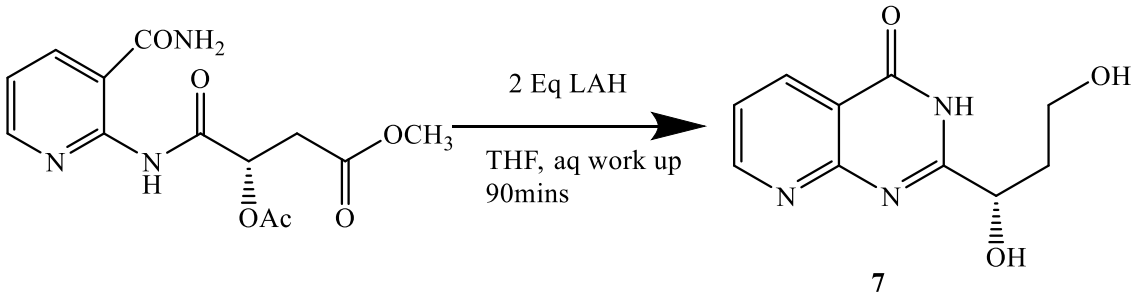

5 **7**

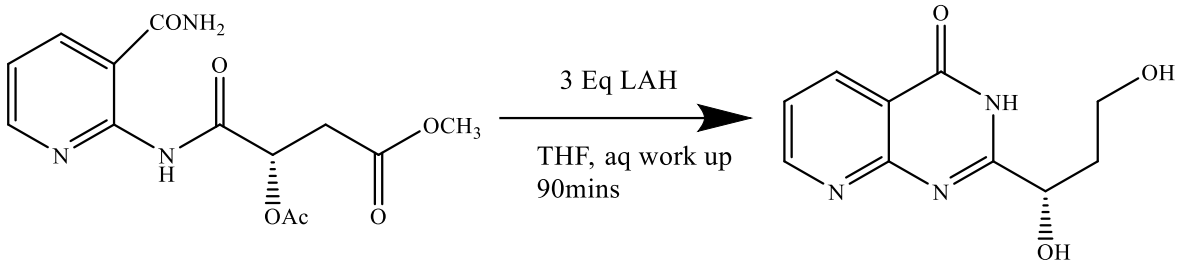
CONH2
O
N
N
H
OCH3
OAc
O
3 Eq LAH
THF, aq work up
90mins
O
NH
OH
N
N
OH

5 **7**

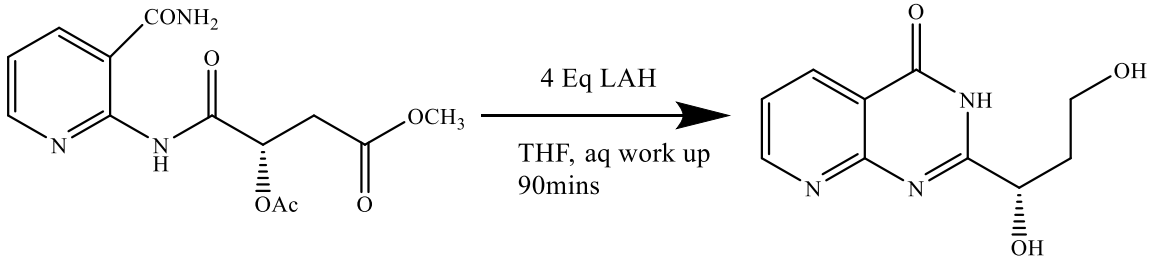
CONH2
O
N
N
H
OCH3
OAc
O
4 Eq LAH
THF, aq work up
90mins
O
NH
OH
N
N
OH

5 **7**

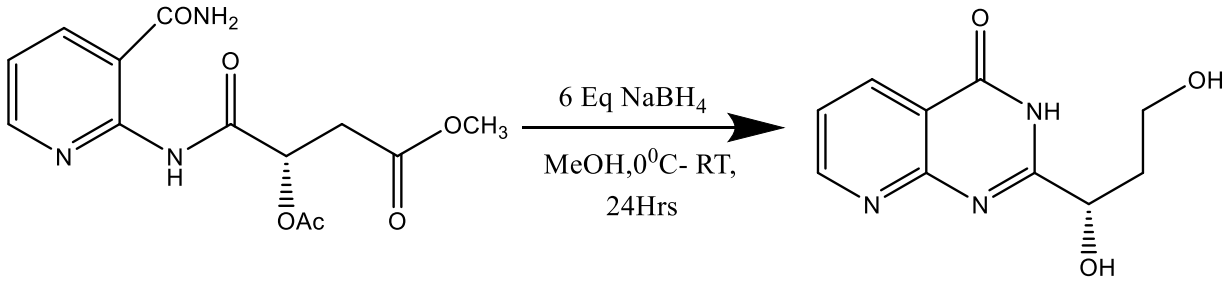
CONH2
O
N
N
H
OCH3
OAc
O
6 Eq NaBH4
MeOH,0⁰C- RT,
24Hrs
O
NH
OH
N
N
OH

5 **7**

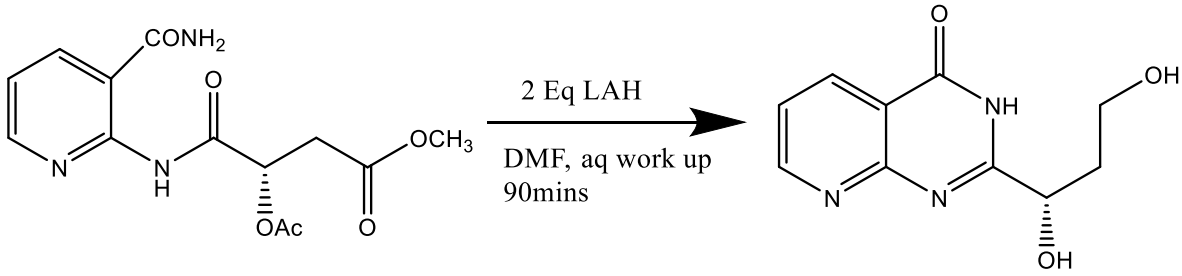
CONH2
O
N
N
H
OCH3
OAc
O
2 Eq LAH
DMF, aq work up
90mins
O
NH
OH
N
N
OH

5 **7**

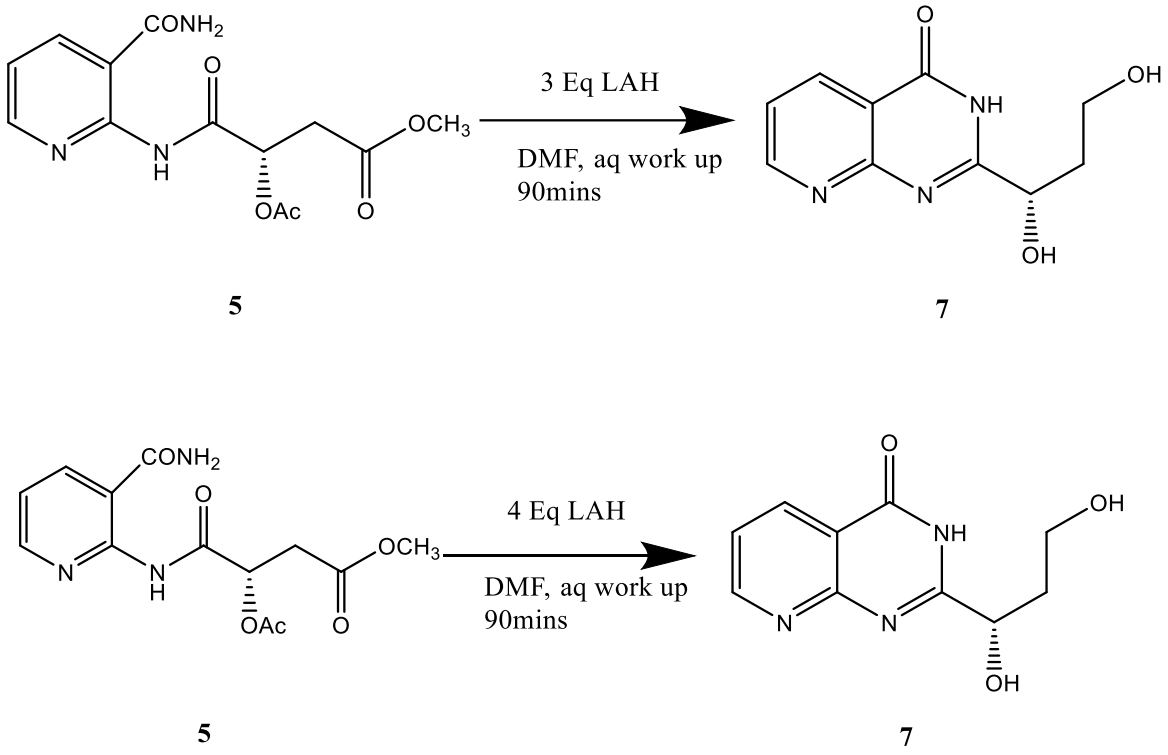

Figure 2.17 Synthesis of 2-(1,3-dihydroxypropyl) pyrido[2,3-d] pyrimidin-4(3H)-one **(7)**

However, use of 2 equivalents of LAH in DME yielded the desired product (**7**) as shown in the following scheme (Figure 2.18). The structural characterization **7** has been performed, but further additional analysis is under progress.

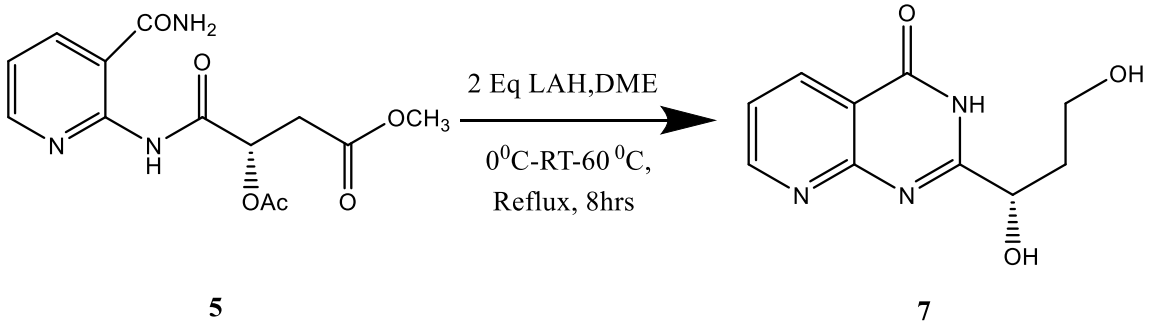

Figure 2.18 Synthesis of 2-(1,3-dihydroxypropyl) pyrido[2,3-d] pyrimidin--4(3H)-one **(7)**

2.2.3.5 Synthesis of (*S*)-9-hydroxy-8,9-dihydropyrido[2,3-d]pyrrolo[1,2-a] pyrimidin-5(7H)one:

The compound **7** on treatment with diisopropylazodicarboxylate (DIAD) and triphenylphosphine (PPh_3) in DCM for 3-9 hours afforded the desired (S)-9-hydroxy-8,9-dihydropyrido[2,3-d]pyrrolo[1,2-a] pyrimidin-5(7H)one **8** as shown in the following scheme (Figure 2.19) by a selective intramolecular Mitsunobu ring-closing reaction with the primary alcohol (C-1) of compound **7**.

Initially tried to proceed the reaction in THF solvent but the reaction was unsuccessful and then tried in DMF solvent which was slightly successful but there is no progress, then changed the solvent to DCM which was successful with moderate yield.

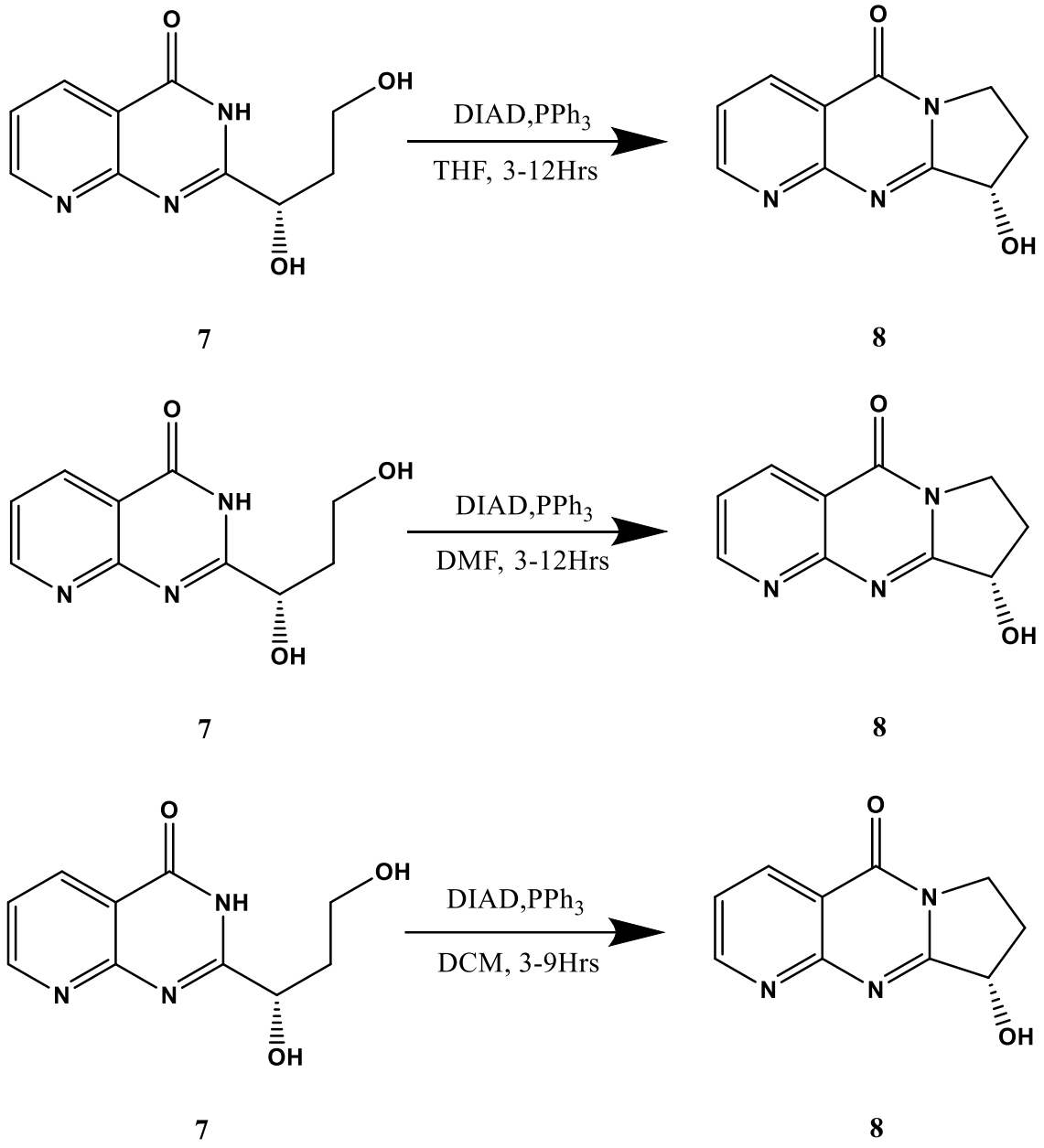

Figure 2.19 Synthesis of *(S)*-9-hydroxy-8,9-dihydropyrido[2,3-d]pyrrolo[1,2-a] pyrimidin-5(7H)one. (**8**)

2.2.3.6 Synthesis of (*S*)-5,7,8,9-tetrahydropyrido[2,3-d]pyrrolo[1,2-a]pyrimidin9-ol:

A solution of BH_3·THF complex (1.0 M) was added in a dropwise manner to (*S*)-9-hydroxy-8,9-dihydropyrido[2,3-d]pyrrolo[1,2-a] pyrimidin-5(7H)one (**8)** under

inert atmosphere. The green reaction mixture was heated at reflux for 1 hr. A solution of 6 N HCl (0.5 mL) was added in a dropwise manner at 0 °C (ice-bath) to hydrolyze the borate complex and excess reagent.

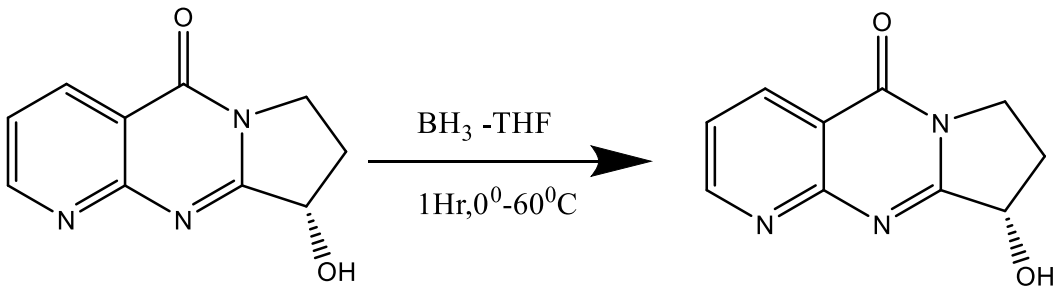

8 **1**

Figure 2.20 Synthesis of *(S)*-5,7,8,9-tetrahydropyrido[2,3-d]pyrrolo [1,2-a]pyrimidin9-ol (**1**)

The compound **8** was treated with TMSCl (1.2 mol equiv) in DCM in an ice-bath for 15 minutes and to the resultant reaction mixture was added a reducing agent, LAH (1.4 mol equiv). The reaction was completed in 3hours. Further analysis and characterization is required to confirm the product.

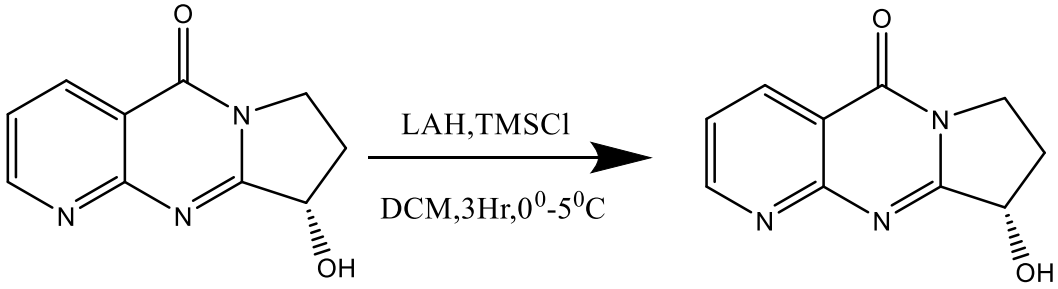

8 **1**

Figure 2.21 Synthesis of *(S)*-5,7,8,9-tetrahydropyrido[2,3-d]pyrrolo [1,2-a]pyrimidin9-ol (1)

2.2.4 Discussion

The current treatments against the protozoan parasitic disease leishmaniasis suffer from parasitic resistance, drug toxicity, teratogenicity, high cost, reduced efficacy in some endemic regions, and routes of administration incompatible to the settings where the disease is prevalent. Moreover, the efforts to treat leishmaniasis are further hindered by the lack of financial resources in the disease prevalent regions and the lack of support from the pharmaceutical partners. Therefore, it is incumbent upon the academic institutions to undertake the drug discovery process to address the growing public health concern in the underdeveloped regions of the world. Newer, safer, orally active, and cost-effective drugs are urgently needed to alleviate the poorer populations affected by this debilitating disease.

Drug discovery efforts against leishmaniasis are growing with several compounds in late preclinical or early clinical stages of development as indicated by the Drugs for Neglected Diseases Initiative (DNDI) [173]. New drug leads have been identified for leishmaniasis through phenotypic screening, repurposing of known drugs such as anticancer, antidepressant, anti-HIV agents and kinase inhibitors [165]. The derivatization of known anti-infective scaffolds has been carried out to rationally design leishmanicidal agents through structural modification of already known compounds exhibiting anti-infective activity. Natural products derived from plants, bacteria, fungi, and marine organisms have become a valuable source to contribute to the drug arsenal pipeline for leishmaniasis. Several natural products with diverse structural complexity have shown potent activity against the two most prevalent forms of the disease such as visceral, and cutaneous leishmaniasis in various *in vitro* and *in vivo* models.

Derivatization of the natural product leads through systematic structure-activity relationships (SARs) have also provided potent compounds against leishmaniasis. Quinazoline alkaloids either as natural products or derivatives have also shown potent antiparasitic activity against three major protozoan parasitic diseases malaria, trypanosomiasis, and leishmaniasis.

Our laboratory is focused on the design and synthesis of novel antiparasitic agents for the protozoan parasitic diseases leishmaniasis and trypanosomiasis. We have previously reported the antileishmanial activity of a pyrroloquinazoline alkaloid peganine isolated from a medicinal plant, *Peganum harmala* [167]. Peganine reduced the parasitic burden significantly following oral administration to hamsters infected with acute visceral leishmaniasis at a relative high dose compared to the marketed oral drug miltefosine. Because the lead molecule kills the *Leishmania* parasite at clinically irrelevant dose, structural modification is imperative to optimize its activity and facilitate its further development. We are exploring the structure-activity relationships (SARs) of peganine using the classical and rational drug design approach Topliss Operational Scheme as well as the structure-based drug design methods to identify novel analogs with improved activity. Preliminary studies have also shown that peganine inhibits the parasite topoisomerase I without binding to DNA with a unique mechanism of action different from known topoisomerase I inhibitor, camptothecin [172]. Molecular modelling also revealed that peganine can be superimposed with camptothecin and the important interactions with the enzyme are conserved. The pyridyl nitrogen of camptothecin and the quinazoline nitrogen of peganine occupy the same position while interacting with the enzyme and form strong hydrogen bond interactions with the arginine residue

of the enzyme. Based on the molecular modeling studies, we employed scaffold hopping design strategy to modify the core structure of peganine by introducing a heterocyclic replacement (N) into the benzenoid ring. This generated a new core structure of peganine called pyrrolopyrimidinol. We expect the new scaffold to increase the hydrogen bonding interactions by hydrogen bond accepting property of nitrogen atom with the same arginine residue and retain and/or have an improved activity and possess favorable pharmacokinetic properties.

We carried out the total synthesis of the pyrrolopyrimidinol scaffold by following a procedure similar to the one [171] used for the synthesis of our lead molecule. The synthesis of this new scaffold was accomplished up to the penultimate intermediate, a pyrrolopyrimidinone derivative which will be subjected to the lactam reduction to furnish the target molecule. All the intermediates were purified by flash chromatography and obtained in excellent yields. The compounds were characterized by mass spectroscopy and nuclear magnetic resonance. We expect to obtain the target molecule and evaluate its antileishmanial activity and based on the results, design and synthesize additional analogs to explore its structure-activity relationships for further development.

2.3: Conclusion:

We have designed a novel analog of promising antileishmanial lead, peganine using scaffold hopping drug design approach. The simplest scaffold hopping strategy, which is heterocyclic replacement in which the core benzenoid ring of pganine was replaced by a pyridine ring was employed to generate a novel scaffold to improve the antileishmanial activity and pharmacokinetic properties of peganine. The total synthesis of the designed analog was accomplished upto the penultimate step in moderate to excel-

lent yields, we expect to complete the final reaction to afford the target and evaluate its antileishmanial activity. In future studies, based on the initial results, additional analogs of the molecule will be designed to synthesize for evaluation of the antileishmanial activity to develop SARs facilitate the further development.

2.4 Experimental Materials and Methods:

2.4.1 General:

All reactions were carried out with anhydrous solvents in oven-dried and argon-charged glassware. All anhydrous solvents were further dried over molecular sieves. All solvents used in workup, extraction procedures and chromatography were used as received from commercial suppliers without prior purification. The starting materials 2-aminonicotinamide and L(-)-malic acid were obtained from Fisher Scientific (Pittsburgh, PA), and all other reagents were purchased from Sigma Aldrich (St. Louis, MO) and are used without further purification.

2.4.2 Chromatography:

Analytical thin layer chromatography (TLC) was performed on precoated Aluminum backed plates (with Silica Gel 60 W F254 with 200μm thickness metric) were purchased from Sigma Aldrich. The components were visualized by ultraviolet light (254 nm) and their Rf determined. Flash column chromatography was conducted on a Teledyne ISCO CombiFlash NextGen 300^{+} chromatography system with Redisef gold and silver columns (Teledyne ISCO, Lincoln NE) with mesh size 60-120 μm.

2.4.3 Nuclear Magnetic Resonance (NMR):

^{1}H NMR spectra were recorded at ambient temperature using a Bruker Avance 600 MHz solutions NMR spectrometer in the solvent indicated. ^{13}C NMR spectra were recorded using Bruker Advance 600 MHz solutions NMR spectrometer (at 100 MHz, or 150 MHz). All the ^{1}H NMR spectra were reported in chemical shift (δ) units as parts per million (ppm) downfield of Tetramethylsilane and were measured relative to the signals for deuterated methanol (3.31 ppm), dimethyl sulfoxide (2.5 ppm), or acetone (2.05 ppm). All ^{13}C NMR spectra were reported in ppm relative to the signals for deuterated methanol (49.1 ppm), deuterated dimethylsulfoxide (39.5 ppm) or deuterated acetone (29.9, 206.7 ppm) with ^{1}H decoupled resonance. Data for ^{1}H NMR are reported as follows: chemical shift (δ ppm), multiplicity (s = singlet, d = doublet, t = triplet, q = quartet, p = pentet, m = multiplet), coupling constant (Hz) and integration whereas ^{13}C NMR were reported as chemical shift values. All the NMR data were analyzed using MestReNova (Mnova Suite Chemist) Software (version 15.0.1).

2.4.4 Mass spectrometry (MS):

Low resolution mass spectra were recorded using an Agilent mass spectrometer in the electrospray ionization (ESI) method as the protonated ions both in the positive and negative ion modes.

2..4.5 General Procedure for the synthesis of intermediates:

2.4.5.1 Synthesis of (*S*)- 2,5-dioxotetrahydrofuran-3yl-acetate (3):

A mixture of (*S*)-malic acid (10.0 g, 74.8 mmol) and freshly distilled acetyl chloride (75 mL) was stirred at 40 °C in an oil bath for 2 hr. The excess of acetyl chloride

and acetic acid or acetic anhydride formed were distilled off *in vacuo*. The obtained solid residue was used for the next step without any further purification. The analytically pure sample was obtained by recrystallization from toluene. 11.62 g (98.5% yield);

2.4.5.2 Synthesis of (*S*)-3-acetoxy-4-((3-carbamoyl-pyridine-2yl)-amino)-4-oxobutanoic acid (4):

To a solution of the (*S*)-2,5-dioxotetrahydrofuran-3yl-acetate **3** (3.46 g, 21.87 mmol) in ether (21.89 mL) was added a solution of 2-amino nicotinamide **2**, (3.00 g, 21.87 mmol) in toluene-dimethylformamide (DMF) mixture (33.08 mL, 2:1) in a dropwise fashion with constant stirring at room temperature. The reaction mixture was further stirred for 2 hr, and the formed precipitate was filtered under vacuum and washed with ethyl acetate (22 mL). The obtained compound **4** was used for the next step without any further purification. Analytically pure **4** was obtained by recrystallization from ethyl acetate. Yield: 6.46g (96.5%);

^{1}H NMR (DMSO-*d*6, 600 MHz) δ 7.85 (s, 1H), 7.73 – 7.70 (m, 2H), 7.08 (s, 1H), 6.96 (s, 2H), 6.39 – 6.34 (m, 1H), 4.97 (d, *J* = 8.0 Hz, 1H), 2.94 (s, 1H), 2.66 (s, 1H), 2.62 (s, 1H), 2.28 (s, 1H), 1.82 (s, 3H).

^{13}C NMR (DMSO, 151 MHz) δ 175.97, 174.81, 174.40, 173.51, 166.17, 162.69, 154.25,141.58, 132.71, 131.99, 129.10, 115.11, 113.24, 72.54, 43.45, 34.44, 24.60,

24.02.

MS (ESI) *m/z* $[M-H]^-$ 294.1

2.4.5.3 Synthesis of methyl(*S*)-3-acetoxy-4-((3-carbamoyl-pyridine-2yl) amino)-4-oxo butanoate 5:

To a solution of the acid **4** (1.00g, 3.39 mmol) in DMF (5 mL) was added DIEA (4.25 ml, 9.7 mmol). The mixture was cooled to 0°C and treated with EDC-HCl (1.2 g, 3.39 mmol), HOBt (879 mg, 3.39 mmol), followed by the addition of and methanol (0.5 mL, 13.56 mmol). The reaction was stirred at RT for 3 hours. After completion, the mixture was diluted with H_2O (50 mL) and extracted with Ethylacetate (50 mL). The organic layer was dried over sodium sulphate (Na_2SO_4) and concentrated in *vacuo*. The resulting material was purified by silica gel column chromatography to provide the product as a semi white crystalline solid. **5**: 0.995g(95.02% yield);

^{1}H NMR (600 MHz, DMSO-*d*6) δ 8.05 (dd, J = 4.8, 1.8 Hz, 1H), 7.99 – 7.91 (m, 2H), 7.30 (s, 1H), 7.17 (s, 2H), 6.54 (dd, J = 7.6, 4.7 Hz, 1H), 3.40 (s, 3H), 2.55 (s, 1H), 2.50 (s, 3H).

^{13}C NMR (151 MHz, DMSO-*d*6) δ 170.68, 170.20, 159.48, 151.84, 151.75, 148.90, 137.45, 111.45, 109.00, 88.24, 60.08, 21.00, 14.40.

MS (ESI) m/z $[M-H]^-$ 308.1.

2.4.5.4 Synthesis of (S)-2-(1,3-dihydroxypropyl)pyrido[2,3-d]pyrimidin-4(3H)-one (7):

To the solution of ester **5** (0.80 g, 2.59 mmol) in DME (10 mL) was added solution of LAH (2.152, 5.18 mmol) in THF a in a dropwise fashion at 0°C over a period of 15 minutes with continuous stirring. The reaction mixture was further stirred at room temperature and then refluxed for 8 hours at 60°C. The reaction was slowly quenched with water (6.8 mL) and further stirred for 1 h at room temperature. Saturated ammoni-

um chloride (NH_4Cl) solution (2.6 mL) was added to the reaction mixture, and then it was completely concentrated under vacuum and dried under the rotavapor. The residue was stirred with THF (20 mL) for 1 h, and the organic layer was filtered through Celite, dried over sodium sulphate Na_2SO_4, and concentrated *in vacuo*. The obtained crude product was purified by silica gel column chromatography using hexane and Ethyl acetate (1:9) to furnish compound **7**: 0.53 g (93.0% yield).

^{1}H NMR (600 MHz, Acetone) δ 8.50 (dd, *J* = 4.7, 1.7 Hz, 1H), 8.06 (dd, *J* = 4.7, 1.8 Hz, 1H), 7.76 – 7.67 (m, 2H), 5.80 (s, 0H), 5.22 (t, *J* = 4.9 Hz, 1H), 4.16 (s, 1H), 3.95 (s, 1H), 3.71 (q, *J* = 7.4 Hz, 2H), 3.62 (s, 1H), 3.63 – 3.57 (m, 1H), 3.18 (d, *J* = 9.4 Hz, 1H), 2.81 (s, 2H).

^{13}C NMR (151 MHz, DMSO) δ 178.42,175.02, 162.92, 153.62, 125.49, 124.07, 107.53, 67.15,67.00, 61.22, 30.01, 23.76.

2.4.5.5 Synthesis of (S)-9-hydroxy-8,9-dihydropyrido[2,3-d]pyrrolo[1,2-a] pyrimidin-5(7H)one:

To the solution of 7 (0.55 g, 2.50 mmol) and TPP (0.85 g, 3.25 mmol) in THF (7 mL) was added a solution of DIAD (0.48 ml, 2.75 mmol) in DCM (5 mL) in a dropwise fashion with continuous stirring at room temperature, and the reaction mixture was further stirred for 12 h. The reaction mixture was concentrated *in vacuo*, and the residue was chromatographed on silica gel using hexane and isopropanol (60:40) to obtain the pure compound **8**: 0.31 g (61% yield).

^{1}H NMR (600 MHz, Acetone) δ 7.84 (dd, *J* = 12.1, 7.4 Hz, 2H), 7.61 – 7.46 (m, 1H), 4.05 – 4.00 (m, 1H), 3.67 (d, *J* = 6.2 Hz, 1H), 3.56 (dd, *J* = 11.8, 5.7 Hz, 2H), 3.52 (d, *J* = 5.4 Hz, 1H), 1.84 – 1.77 (m, 1H), 1.56 (d, *J* = 2.6 Hz, 1H).

^{13}C NMR (151 MHz, Acetone) δ 173.33, 171.78, 164.40, 132.83, 132.22,129.40, 71.93, 62.34, 61.75, 54.91, 29.45, 23.72.

2.2.2.6 Synthesis of (S)-5,7,8,9-tetrahydropyrido[2,3-d]pyrrolo[1,2-a]pyrimidin9-ol:

The compound 8 was treated with TMSCl (1.2 mol equiv) in DCM in an ice bath for 15 min and to the resultant reaction mixture was added a reducing agent, LAH (1.4 mol equiv). The reaction was completed in 3hours. The reaction mixture was quenched with KOH 2M solution and extracted with water and DCM and the DCM extract was concentrated and purified using 5% MeOH and DCM solvent system and the desired product was obtained and further need to be confirmed by proton NMR.

BIBLIOGRAPHY

1. Organization, W.H.O *Leishmaniasis*. 2023 [cited 2023 23rd December]; Available from: https://www.who.int/en/news-room/fact-sheets/detail/leishmaniasis.
2. Steverding, D., *The history of leishmaniasis.* Parasites & Vectors, 2017. **10**(1): p. 82.
3. Organization, P.A.H. 2023 [cited 2023 23rd December]; Leishmaniasis]. Available from: https://www.paho.org/en/topics/leishmaniasis.
4. Costa-da-Silva, A.C., et al., *Immune Responses in Leishmaniasis: An Overview.* Trop Med Infect Dis, 2022. **7**(4).
5. Jamshaid, H., F.u. Din, and G.M. Khan, *Nanotechnology based solutions for anti-leishmanial impediments: a detailed insight.* Journal of Nanobiotechnology, 2021. **19**(1): p. 106.
6. Curtin, J.M. and N.E. Aronson, *Leishmaniasis in the United States: Emerging Issues in a Region of Low Endemicity.* Microorganisms, 2021. **9**(3).
7. Mody, R.M., et al., *Asymptomatic Visceral Leishmania infantum Infection in US Soldiers Deployed to Iraq.* Clinical Infectious Diseases, 2018. **68**(12): p. 2036-2044.
8. Stahlman, S., V.F. Williams, and S.B. Taubman, *Incident diagnoses of leishmaniasis, active and reserve components, U.S. Armed Forces, 2001-2016.* Msmr, 2017. **24**(2): p. 2-7.

9. Boggild, A.K., et al., *Cutaneous and mucocutaneous leishmaniasis in travellers and migrants: a 20-year GeoSentinel Surveillance Network analysis.* J Travel Med, 2019. **26**(8).

10. Irshad, H., *Types and Treatments of Leishmaniasis.* Biomedical Journal of Scientific & Technical Research, 2022. **42**: p. 34037-34042.

11. Pradhan, S., et al., *Treatment options for leishmaniasis.* Clinical and Experimental Dermatology, 2022. **47**(3): p. 516-521.

12. Madusanka, R.K., H. Silva, and N.D. Karunaweera, *Treatment of Cutaneous Leishmaniasis and Insights into Species-Specific Responses: A Narrative Review.* Infect Dis Ther, 2022. **11**(2): p. 695-711.

13. Nagle, A.S., et al., *Recent Developments in Drug Discovery for Leishmaniasis and Human African Trypanosomiasis.* Chemical Reviews, 2014. **114**(22): p. 11305-11347.

14. Casalle, N., et al., *Mucocutaneous Leishmaniasis with Rare Manifestation in the Nasal Mucosa and Cartilage Bone Septal.* Case Reports in Infectious Diseases, 2020. **2020**: p. 8876020.

15. Mümtaz, G., *An Overview of Leishmaniasis: Historic to Future Perspectives*, in *Vectors and Vector-Borne Zoonotic Diseases*, S. Sara, Editor. 2018, IntechOpen: Rijeka. p. Ch. 5.

16. Wamai, R.G., et al., *Visceral leishmaniasis: a global overview.* J Glob Health Sci, 2020. **2**(1).

17. Pacheco-Fernandez, T., et al., *Revival of Leishmanization and Leishmanin.* Frontiers in Cellular and Infection Microbiology, 2021. **11**.

18. Wilhelm, T.J., *[Visceral leishmaniasis].* Chirurg, 2019. **90**(10): p. 833-837.

19. Ruiz-Postigo, J.A., et al., *Global leishmaniasis surveillance: 2019-2020, a baseline for the 2030 roadmap/Surveillance mondiale de la leishmaniose: 2019-2020, une periode de reference pour la feuille de route a l'horizon 2030.* Weekly Epidemiological Record, 2021. **96**: p. 401+.

20. Safavi, M., H. Eshaghi, and Z. Hajihassani, *Visceral Leishmaniasis: Kala-azar.* Diagn Cytopathol, 2021. **49**(3): p. 446-448.

21. Berriatua, E., et al., *Leishmaniases in the European Union and Neighboring Countries.* Emerg Infect Dis, 2021. **27**(6): p. 1723-7.

22. Long, S., et al., *Indole-Containing Pyrazino[2,1-b]quinazoline-3,6-diones Active against Plasmodium and Trypanosomatids.* ACS Medicinal Chemistry Letters, 2022. **13**(2): p. 225-235.

23. Sasidharan, S. and P. Saudagar, *Leishmaniasis: where are we and where are we heading?* Parasitology Research, 2021. **120**(5): p. 1541-1554.

24. Chakravarty, J., et al., *Determinants for progression from asymptomatic infection to symptomatic visceral leishmaniasis: A cohort study.* PLOS Neglected Tropical Diseases, 2019. **13**(3): p. e0007216.

25. Aronson, N., et al., *Diagnosis and Treatment of Leishmaniasis: Clinical Practice Guidelines by the Infectious Diseases Society of America (IDSA) and the American Society of Tropical Medicine and Hygiene (ASTMH).* Clinical Infectious Diseases, 2016. **63**(12): p. e202-e264.

26. Hirve, S., et al., *Transmission Dynamics of Visceral Leishmaniasis in the Indian Subcontinent – A Systematic Literature Review.* PLOS Neglected Tropical Diseases, 2016. **10**(8): p. e0004896.

27. Scarpini, S., et al., *Visceral Leishmaniasis: Epidemiology, Diagnosis, and Treatment Regimens in Different Geographical Areas with a Focus on Pediatrics.* Microorganisms, 2022. **10**(10).

28. Lemma, W., et al., *Preliminary study on investigation of zoonotic visceral leishmaniasis in endemic foci of Ethiopia by detecting Leishmania infections in rodents.* Asian Pac J Trop Med, 2017. **10**(4): p. 418-422.

29. Fiebig, M., S. Kelly, and E. Gluenz, *Comparative Life Cycle Transcriptomics Revises Leishmania mexicana Genome Annotation and Links a Chromosome Duplication with Parasitism of Vertebrates.* PLOS Pathogens, 2015. **11**(10): p. e1005186.

30. Alves, C.R., et al., *Understanding serine proteases implications on Leishmania spp lifecycle.* Experimental Parasitology, 2018. **184**: p. 67-81.

31. Inbar, E., et al., *The Transcriptome of Leishmania major Developmental Stages in Their Natural Sand Fly Vector.* mBio, 2017. **8**(2): p. 10.1128/mbio.00029-17.

32. De Pablos, L.M., T.R. Ferreira, and P.B. Walrad, *Developmental differentiation in Leishmania lifecycle progression: post-transcriptional control conducts the orchestra.* Current Opinion in Microbiology, 2016. **34**: p. 82-89.

33. Kraeva, N., et al., *Leptomonas seymouri: Adaptations to the Dixenous Life Cycle Analyzed by Genome Sequencing, Transcriptome Profiling and Co-infection with Leishmania donovani.* PLOS Pathogens, 2015. **11**(8): p. e1005127.

34. Wheeler, R.J., J.D. Sunter, and K. Gull, *Flagellar pocket restructuring through the Leishmania life cycle involves a discrete flagellum attachment zone.* Journal of Cell Science, 2016. **129**(4): p. 854-867.

35. Cecílio, P., A. Cordeiro-da-Silva, and F. Oliveira, *Sand flies: Basic information on the vectors of leishmaniasis and their interactions with Leishmania parasites.* Communications Biology, 2022. **5**(1): p. 305.

36. Berbert, T.R.N., et al., *Pentavalent Antimonials Combined with Other Therapeutic Alternatives for the Treatment of Cutaneous and Mucocutaneous Leishmaniasis: A Systematic Review.* Dermatology Research and Practice, 2018. **2018**: p. 9014726.

37. An, I., et al., *The effect of pentavalent antimonial compounds used in the treatment of cutaneous leishmaniasis on hemogram and biochemical parameters.* Cutaneous and Ocular Toxicology, 2019. **38**(3): p. 294-297.

38. Brito, N.C., A. Rabello, and G.F. Cota, *Efficacy of pentavalent antimoniate intralesional infiltration therapy for cutaneous leishmaniasis: A systematic review.* PLOS ONE, 2017. **12**(9): p. e0184777.

39. Rodrigues, B.C., et al., *A retrospective cohort study of the effectiveness and adverse events of intralesional pentavalent antimonials in the treatment of cutaneous leishmaniasis.* International Journal for Parasitology: Drugs and Drug Resistance, 2020. **14**: p. 257-263.

40. Vieira-Gonçalves, R., et al., *Clinical and immunological evidence that low doses of pentavalent antimonials are effective in maintaining long-term cure of Leishmania (Viannia) braziliensis cutaneous lesions.* British Journal of Dermatology, 2015. **173**(2): p. 571-573.

41. Sundar, S. and A. Singh, *Recent developments and future prospects in the treatment of visceral leishmaniasis.* Therapeutic Advances in Infectious Disease, 2016. **3**(3-4): p. 98-109.

42. Ibiapina, A.B., Francisca Miriane de Araújo Batista, Bruno Guedes Alcoforado Aguiar, Vagner José Mendonça, Dorcas Lamounier Costa, Carlos Henrique Nery Costa, and Verônica Mendes Abdala., *Evidence Map of Diagnosis, Treatment, Prognosis, Prevention, and Control in Visceral Leishmaniasis.* 2022.

43. Badaro, R., et al., *Treatment of Visceral Leishmaniasis with Pentavalent Antimony and Interferon Gamma.* New England Journal of Medicine, 1990. **322**(1): p. 16-21.

44. Nico, D., L. Conde, and C.B. Palatnik de Sousa, *Classical and Modern Drug Treatments for Leishmaniasis*, in *Antiprotozoal Drug Development and Delivery*, A.B. Vermelho and C.T. Supuran, Editors. 2022, Springer International Publishing: Cham. p. 1-21.

45. Ponte-Sucre, A., et al., *Drug resistance and treatment failure in leishmaniasis: A 21st century challenge.* PLOS Neglected Tropical Diseases, 2017. **11**(12): p. e0006052.

46. Roatt, B.M., et al., *Recent advances and new strategies on leishmaniasis treatment.* Applied Microbiology and Biotechnology, 2020. **104**(21): p. 8965-8977.

47. Dermatol., A.B., *American tegumentary leishmaniasis: severe side effects of pentavalent antimonial in a patient with chronic renal failure.* Tropical/Infectoparasitary Dermatology, May-Jun 2019. **94 (3)**

48. Frézard, F., et al., *New insights into the chemical structure and composition of the pentavalent antimonial drugs, meglumine antimonate and sodium stibogluconate.* Journal of Inorganic Biochemistry, 2008. **102**(4): p. 656-665.

49. Morelle, C., et al., *Well-Tolerated Amphotericin B Derivatives That Effectively Treat Visceral Leishmaniasis.* ACS Infectious Diseases, 2021. **7**(8): p. 2472-2482.

50. Berman, J., *Amphotericin B formulations and other drugs for visceral leishmaniasis.* Am J Trop Med Hyg, 2015. **92**(3): p. 471-473.

51. Kumari, S., et al., *Amphotericin B: A drug of choice for Visceral Leishmaniasis.* Acta Tropica, 2022. **235**: p. 106661.

52. Rodrigo, C., et al., *Amphotericin B for treatment of visceral leishmaniasis: systematic review and meta-analysis of prospective comparative clinical studies including dose-ranging studies.* Clinical Microbiology and Infection, 2018. **24**(6): p. 591-598.

53. Greene, R.E., et al., *Comparative cost-effectiveness of voriconazole and amphotericin B in treatment of invasive pulmonary aspergillosis.* American Journal of Health-System Pharmacy, 2007. **64**(24): p. 2561-2568.

54. Sundar, S. and D. Agarwal, *Visceral Leishmaniasis—Optimum Treatment Options in Children.* The Pediatric Infectious Disease Journal, 2018. **37**(5): p. 492-494.

55. Asad, M., et al., *Therapeutic and immunomodulatory activities of short-course treatment of murine visceral leishmaniasis with KALSOME™10, a new liposomal amphotericin B.* BMC Infectious Diseases, 2015. **15**(1): p. 188.

56. Palić, S., J.H. Beijnen, and T.P.C. Dorlo, *An update on the clinical pharmacology of miltefosine in the treatment of leishmaniasis.* International Journal of Antimicrobial Agents, 2022. **59**(1): p. 106459.

57. Monge-Maillo, B. and R. López-Vélez, *Miltefosine for Visceral and Cutaneous Leishmaniasis: Drug Characteristics and Evidence-Based Treatment Recommendations.* Clinical Infectious Diseases, 2015. **60**(9): p. 1398-1404.

58. Sunyoto, T., J. Potet, and M. Boelaert, *Why miltefosine—a life-saving drug for leishmaniasis—is unavailable to people who need it the most.* BMJ Global Health, 2018. **3**(3): p. e000709.

59. Ware, J.M., et al., *Efficacy and Tolerability of Miltefosine in the Treatment of Cutaneous Leishmaniasis.* Clinical Infectious Diseases, 2020. **73**(7): p. e2457-e2562.

60. van Henten, S., et al., *Miltefosine for the treatment of cutaneous leishmaniasis—A pilot study from Ethiopia.* PLOS Neglected Tropical Diseases, 2021. **15**(5): p. e0009460.

61. dos Santos Nogueira, F., et al., *Use of miltefosine to treat canine visceral leishmaniasis caused by Leishmania infantum in Brazil.* Parasites & Vectors, 2019. **12**(1): p. 79.

62. Sundar, S. and P.L. Olliaro, *Miltefosine in the treatment of leishmaniasis: Clinical evidence for informed clinical risk management.* Ther Clin Risk Manag, 2007. **3**(5): p. 733-40.

63. Melcon-Fernandez, E., et al., *Miltefosine and Nifuratel Combination: A Promising Therapy for the Treatment of Leishmania donovani Visceral Leishmaniasis.* International Journal of Molecular Sciences, 2023. **24**(2): p. 1635.

64. Sundar, S., et al., *Efficacy and Safety of Miltefosine in Treatment of Post-Kala-Azar Dermal Leishmaniasis.* The Scientific World Journal, 2015. **2015**: p. 414378.

65. Pokharel, P., R. Ghimire, and P. Lamichhane, *Efficacy and Safety of Paromomycin for Visceral Leishmaniasis: A Systematic Review.* Journal of Tropical Medicine, 2021. **2021**: p. 8629039.

66. Matos, A.P.S., et al., *A review of current treatments strategies based on paromomycin for leishmaniasis.* Journal of Drug Delivery Science and Technology, 2020. **57**: p. 101664.

67. Sosa, N., et al., *Topical paromomycin for New World cutaneous leishmaniasis.* PLOS Neglected Tropical Diseases, 2019. **13**(5): p. e0007253.

68. Jamil, K.M., et al., *Effectiveness Study of Paromomycin IM Injection (PMIM) for the Treatment of Visceral Leishmaniasis (VL) in Bangladesh.* PLOS Neglected Tropical Diseases, 2015. **9**(10): p. e0004118.

69. Rahman, R., et al., *Safety and efficacy of short course combination regimens with AmBisome, miltefosine and paromomycin for the treatment of visceral leishmaniasis (VL) in Bangladesh.* PLOS Neglected Tropical Diseases, 2017. **11**(5): p. e0005635.

70. Wijnant, G.-J., et al., *Efficacy of Paromomycin-Chloroquine Combination Therapy in Experimental Cutaneous Leishmaniasis.* Antimicrobial Agents and Chemotherapy, 2017. **61**(8): p. 10.1128/aac.00358-17.

71. Moradzadeh, R., et al., *Effectiveness of Paromomycin on Cutaneous Leishmaniasis in Iran: A Systematic Review and Meta-Analysis.* Iran J Med Sci, 2019. **44**(3): p. 185-195.

72. Coser, E.M., et al., *Activity of paromomycin against Leishmania amazonensis: Direct correlation between susceptibility in vitro and the treatment outcome in vivo.* International Journal for Parasitology: Drugs and Drug Resistance, 2020. **14**: p. 91-98.

73. Piccica, M., et al., *Efficacy and safety of pentamidine isethionate for tegumentary and visceral human leishmaniasis: a systematic review.* Journal of Travel Medicine, 2021. **28**(6).

74. Kaur, G. and B. Rajput, *Comparative Analysis of the Omics Technologies Used to Study Antimonial, Amphotericin B, and Pentamidine Resistance in Leishmania.* Journal of Parasitology Research, 2014. **2014**: p. 726328.

75. Emami, S., P. Tavangar, and M. Keighobadi, *An overview of azoles targeting sterol 14α-demethylase for antileishmanial therapy.* European Journal of Medicinal Chemistry, 2017. **135**: p. 241-259.

76. Galvão, E.L., A. Rabello, and G.F. Cota, *Efficacy of azole therapy for tegumentary leishmaniasis: A systematic review and meta-analysis.* PLOS ONE, 2017. **12**(10): p. e0186117.

77. Braga, S.S., *Multi-target drugs active against leishmaniasis: A paradigm of drug repurposing.* European Journal of Medicinal Chemistry, 2019. **183**: p. 111660.

78. Cragg, G.M. and D.J. Newman, *Natural products: a continuing source of novel drug leads.* Biochimica et Biophysica Acta (BBA)-General Subjects, 2013. **1830**(6): p. 3670-3695.

79. Schmidt, T.J., et al., *The potential of secondary metabolites from plants as drugs or leads against protozoan neglected diseases-part II.* 2012.

80. Mishra, B.B., et al., *Fighting against Leishmaniasis: search of alkaloids as future true potential anti-Leishmanial agents.* Mini reviews in medicinal chemistry, 2009. **9**(1): p. 107-123.

81. Polonio, T. and T. Efferth, *Leishmaniasis: drug resistance and natural products.* International journal of molecular medicine, 2008. **22**(3): p. 277-286.

82. Martín-Quintal, Z., et al., *In vitro activity of Tridax procumbens against promastigotes of Leishmania mexicana.* Journal of Ethnopharmacology, 2009. **122**(3): p. 463-467.

83. Tiuman, T.S., et al., *Antileishmanial activity of parthenolide, a sesquiterpene lactone isolated from Tanacetum parthenium.* Antimicrobial agents and chemotherapy, 2005. **49**(1): p. 176-182.

84. Odonne, G., et al., *Antileishmanial sesquiterpene lactones from Pseudelephantopus spicatus, a traditional remedy from the Chayahuita Amerindians (Peru). Part III.* Journal of Ethnopharmacology, 2011. **137**(1): p. 875-879.

85. Honda, P., et al., *Efficacy of components from leaves of Calophyllum brasiliense against Leishmania (Leishmania) amazonensis.* Phytomedicine, 2010. **17**(5): p. 333-338.

86. Inacio, J.D., M.M. Canto-Cavalheiro, and E.E. Almeida-Amaral, *In vitro and in vivo effects of (−)-epigallocatechin 3-O-gallate on Leishmania amazonensis.* Journal of natural products, 2013. **76**(10): p. 1993-1996.

87. Roldos, V., et al., *Activity of a hydroxybibenzyl bryophyte constituent against Leishmania spp. and Trypanosoma cruzi: In silico, in vitro and in vivo activity studies.* European Journal of Medicinal Chemistry, 2008. **43**(9): p. 1797-1807.

88. Khaliq, T., et al., *Peganine hydrochloride dihydrate an orally active antileishmanial agent.* Bioorganic & medicinal chemistry letters, 2009. **19**(9): p. 2585-2586.

89. Kumarihamy, M., et al., *Antiprotozoal and antimicrobial compounds from the plant pathogen Septoria pistaciarum.* Journal of natural products, 2012. **75**(5): p. 883-889.

90. Rahman, A.A., et al., *Antiparasitic and antimicrobial isoflavanquinones from Abrus schimperi.* Natural product communications, 2011. **6**(11): p. 1934578X1100601120.

91. Ankisetty, S., et al., *Aromatic Constituents of Uvaria g randiflora.* Journal of natural products, 2006. **69**(4): p. 692-694.

92. Nkwengoua, E.T., et al., *In vitro inhibitory effects of palmatine from Enantia chlorantha on Trypanosoma cruzi and Leishmania infantum.* Natural product research, 2009. **23**(12): p. 1144-1150.

93. Santos, E.d.A.d., et al., *Synthesis and biological activity of sulfur compounds showing structural analogy with combretastatin A-4.* Quimica nova, 2013. **36**: p. 279-283.

94. Nour, A.M., et al., *The antiprotozoal activity of sixteen asteraceae species native to Sudan and bioactivity-guided isolation of xanthanolides from Xanthium brasilicum.* Planta medica, 2009. **75**(12): p. 1363-1368.

95. Georgopoulou, K., et al., *In vitro activity of 10-deacetylbaccatin III against Leishmania donovani promastigotes and intracellular amastigotes.* Planta medica, 2007. **73**(10): p. 1081-1088.

96. Ishigami, S.-T., et al., *Cristaxenicin A, an antiprotozoal xenicane diterpenoid from the deep sea gorgonian Acanthoprimnoa cristata.* The Journal of Organic Chemistry, 2012. **77**(23): p. 10962-10966.

97. Borges, A., et al., *In vitro leishmanicidal activity of Tityus discrepans scorpion venom.* Parasitology research, 2006. **99**: p. 167-173.

98. Bhattacharya, S., et al., *In vivo and in vitro antileishmanial activity of Bungarus caeruleus snake venom through alteration of immunomodulatory activity.* Experimental parasitology, 2013. **135**(1): p. 126-133.

99. Brenzan, M., et al., *Effects of (−) mammea A/BB isolated from Calophyllum brasiliense leaves and derivatives on mitochondrial membrane of Leishmania amazonensis.* Phytomedicine, 2012. **19**(3-4): p. 223-230.

100. Gul, W., et al., *Modification at the C9 position of the marine natural product isoaaptamine and the impact on HIV-1, mycobacterial, and tumor cell activity.* Bioorganic & medicinal chemistry, 2006. **14**(24): p. 8495-8505.

101. Endeshaw, M., et al., *8, 8-dialkyldihydroberberines with potent antiprotozoal activity.* Journal of natural products, 2013. **76**(3): p. 311-315.

102. Hameed, A., et al., *Quinazoline and quinazolinone as important medicinal scaffolds: a comparative patent review (2011–2016).* Expert Opinion on Therapeutic Patents, 2018. **28**(4): p. 281-297.

103. Karan, R., et al., *Recent Advances on Quinazoline Derivatives: A Potential Bioactive Scaffold in Medicinal Chemistry.* ChemEngineering, 2021. **5**(4): p. 73.

104. Shang, X.F., et al., *Biologically active quinoline and quinazoline alkaloids part I.* Med Res Rev, 2018. **38**(3): p. 775-828.

105. Khan, I., et al., *Quinazolines and quinazolinones as ubiquitous structural fragments in medicinal chemistry: An update on the development of synthetic methods and pharmacological diversification.* Bioorg Med Chem, 2016. **24**(11): p. 2361-81.

106. S. Shobha Rani, R.B., *Review on quinazoline derivatives.* (2015). **6(2)**: p. 2510 – 2527.

107. Upasani, A.S. and A.S. Jagdale, *Quinazoline and its diverse array of therapeutic application: A review.* IJMS, 2021. **5**(2): p. 7.

108. Patel, T.S., et al., *Ionic liquid mediated stereoselective synthesis of alanine linked hybrid quinazoline-4(3H)-one derivatives perturbing the malarial reductase activity in folate pathway.* Bioorg Med Chem, 2017. **25**(24): p. 6635-6646.

109. Alsibaee, A.M., H.M. Al-Yousef, and H.S. Al-Salem, *Quinazolinones, the Winning Horse in Drug Discovery.* Molecules, 2023. **28**(3).

110. Tiwary, B.K., et al., *Implication of quinazoline-4 (3H)-ones in medicinal chemistry: a brief review.* J. Chem. Biol. Ther, 2015. **1**(104): p. 2572-0406.1000104.

111. Tiwary, B., et al., *Implication of Quinazoline-4(3H)-ones in Medicinal Chemistry: A Brief Review.* 2015. **1**.

112. Alam, M., et al., *A review: Recent investigations on quinazoline scaffold.* Int. j. adv. res, 2015. **3**: p. 1656-1664.

113. Maddeshiya, J., et al., *SYNTHESIS, CHARACTERIZATION AND ANTIMICROBIAL ACTIVITY OF SOME NEWER QUINAZOLINE DERIVATIVES.* Indian Journal of Heterocyclic Chemistry, 2012. **22**: p. 121-126.

114. Ravez, S., et al., *Quinazoline derivatives as anticancer drugs: a patent review (2011 – present).* Expert Opinion on Therapeutic Patents, 2015. **25**(7): p. 789-804.

115. Khan, I., et al., *Recent advances in the structural library of functionalized quinazoline and quinazolinone scaffolds: synthetic approaches and multifarious applications.* Eur J Med Chem, 2014. **76**: p. 193-244.

116. Zou, Y., et al., *Discovery of Tryptanthrin and Its Derivatives and Its Activities against NSCLC In Vitro via Both Apoptosis and Autophagy Pathways.* Int J Mol Sci, 2023. **24**(2).

117. Uzor, P.F., *Alkaloids from Plants with Antimalarial Activity: A Review of Recent Studies.* Evidence-Based Complementary and Alternative Medicine, 2020. **2020**: p. 8749083.

118. Shang, X.-F., et al., *Biologically active quinoline and quinazoline alkaloids part II.* Medicinal research reviews, 2018. **38**(5): p. 1614-1660.

119. Patel, T.S., et al., *Novel stereoselective 2,3-disubstituted quinazoline-4(3H)-one derivatives derived from glycine as a potent antimalarial lead.* New Journal of Chemistry, 2015. **39**(11): p. 8638-8649.

120. Auti, P.S., G. George, and A.T. Paul, *Recent advances in the pharmacological diversification of quinazoline/quinazolinone hybrids.* RSC Advances, 2020. **10**(68): p. 41353-41392.

121. Maiden, T.M.M., et al., *A convergent strategy towards febrifugine and related compounds.* Organic & Biomolecular Chemistry, 2018. **16**(22): p. 4159-4169.

122. da Rosa, R., E.P. Schenkel, and L.S. Campos Bernardes, *Semisynthetic and newly designed derivatives based on natural chemical scaffolds: moving beyond natural products to fight Trypanosoma cruzi.* Phytochemistry Reviews, 2020. **19**(1): p. 105-122.

123. Herraiz, T., et al., *Identification, occurrence and activity of quinazoline alkaloids in Peganum harmala.* Food and Chemical Toxicology, 2017. **103**: p. 261-269.

124. Wink, M., *Modes of Action of Herbal Medicines and Plant Secondary Metabolites.* Medicines, 2015. **2**(3): p. 251-286.

125. Gharirvand Eskandari, E., M. Setorki, and M. Doudi, *Medicinal Plants With Antileishmanial Properties: A Review Study.* Pharmaceutical and Biomedical Research, 2020. **6**(1): p. 1-16.

126. Filali, I., A. Jelassi, and H.B. Jannet, *New Bioactive Esters and Phosphonates Semisynthesized From (±)-Vasicinone: An Alkaloid Isolated From Peganum harmala.* Natural Product Communications, 2019. **14**(12): p. 1934578X19893544.

127. Jesumoroti, O.J., R.M. Beteck, and L.J. Legoabe, *In-vitro Anti-trypanosomal and Cytotoxicity Evaluation of 3-methyl-3,4-dihydroquinazolin-2(1H)-one Derivatives.* Drug Res (Stuttg), 2021. **71**(06): p. 335-340.

128. Mamadalieva, N.Z., M.L. Ashour, and N.A. Mamedov, *Peganum harmala: Phytochemistry, Traditional Uses, and Biological Activities*, in *Biodiversity, Conservation and Sustainability in Asia: Volume 2: Prospects and Challenges in South and Middle Asia*, M. Öztürk, et al., Editors. 2022, Springer International Publishing: Cham. p. 721-744.

129. Eser, M. and İ. Çavuş, *In Vitro and In Silico Evaluations of the Antileishmanial Activities of New Benzimidazole-Triazole Derivatives.* Vet Sci, 2023. **10**(11).

130. Torres Suarez, E., et al., *Antileishmanial activity of synthetic analogs of the naturally occurring quinolone alkaloid N-methyl-8-methoxyflindersin.* PLoS One, 2020. **15**(12): p. e0243392.

131. Martin, Y.C. and S. Muchmore, *Beyond QSAR: lead hopping to different structures.* QSAR & Combinatorial Science, 2009. **28**(8): p. 797-801.

132. Cramer, R.D., et al., *"Lead hopping". Validation of topomer similarity as a superior predictor of similar biological activities.* Journal of medicinal chemistry, 2004. **47**(27): p. 6777-6791.

133. Schneider, G., et al., *"Scaffold-hopping" by topological pharmacophore search: a contribution to virtual screening.* Angewandte Chemie International Edition, 1999. **38**(19): p. 2894-2896.

134. Sun, H., G. Tawa, and A. Wallqvist, *Classification of scaffold-hopping approaches.* Drug discovery today, 2012. **17**(7-8): p. 310-324.

135. DeWitt, D.L., *Cox-2-selective inhibitors: the new super aspirins.* Molecular pharmacology, 1999. **55**(4): p. 625-631.

136. Vieth, M., et al., *Characteristic physical properties and structural fragments of marketed oral drugs.* Journal of medicinal chemistry, 2004. **47**(1): p. 224-232.

137. Hall, A., et al., *Discovery of a novel indole series of EP1 receptor antagonists by scaffold hopping.* Bioorganic & medicinal chemistry letters, 2008. **18**(8): p. 2684-2690.

138. Evelyn, C.R., et al., *Design, synthesis and prostate cancer cell-based studies of analogs of the Rho/MKL1 transcriptional pathway inhibitor, CCG-1423.* Bioorganic & medicinal chemistry letters, 2010. **20**(2): p. 665-672.

139. Hodge, C.N. and J. Pierce, *A diazine heterocycle replaces a six-membered hydrogen-bonded array in the active site of scytalone dehydratase.* Bioorganic & Medicinal Chemistry Letters, 1993. **3**(8): p. 1605-1608.

140. Eastwood, P., et al., *Discovery of potent and selective bicyclic A2B adenosine receptor antagonists via bioisosteric amide replacement.* Bioorganic & Medicinal Chemistry Letters, 2010. **20**(5): p. 1634-1637.

141. Lovering, F., J. Bikker, and C. Humblet, *Escape from flatland: increasing saturation as an approach to improving clinical success.* Journal of medicinal chemistry, 2009. **52**(21): p. 6752-6756.

142. Sen, R. and M. Chatterjee, *Plant derived therapeutics for the treatment of Leishmaniasis.* Phytomedicine, 2011. **18**(12): p. 1056-1069.

143. Schmidt, T., et al., *DE NC; STEINDEL, M.* TEMPONE, AG The potencial of secundar metabolites from plants as drug or leads against protozoan neglected diseases–Part I. Currente Medicinal Chemistry, 2012. **19**: p. 2128-2175.

144. Sneader, W., *Drug prototypes and their exploitation.* European Journal of Medicinal Chemistry, 1997. **1**(32): p. 91.

145. Labute, P., et al., *Flexible alignment of small molecules.* Journal of medicinal chemistry, 2001. **44**(10): p. 1483-1490.

146. Tasler, S., et al., *N-substituted 2'-(aminoaryl) benzothiazoles as kinase inhibitors: Hit identification and scaffold hopping.* Bioorganic & Medicinal Chemistry Letters, 2009. **19**(5): p. 1349-1356.

147. Velcicky, J., et al., *Novel 3-aminopyrazole inhibitors of MK-2 discovered by scaffold hopping strategy.* Bioorganic & medicinal chemistry letters, 2010. **20**(3): p. 1293-1297.

148. Reid, R.C., et al., *Countering cooperative effects in protease inhibitors using constrained β-strand-mimicking templates in focused combinatorial libraries.* Journal of medicinal chemistry, 2004. **47**(7): p. 1641-1651.

149. Wist, A.D., et al., *Structure–activity based study of the Smac-binding pocket within the BIR3 domain of XIAP.* Bioorganic & medicinal chemistry, 2007. **15**(8): p. 2935-2943.

150. Lee, E., et al., *Crystal structure of ABT-737 complexed with Bcl-xL: implications for selectivity of antagonists of the Bcl-2 family.* Cell Death & Differentiation, 2007. **14**(9): p. 1711-1713.

151. Banek, K., et al., *Adherence to artemisinin-based combination therapy for the treatment of malaria: a systematic review of the evidence.* Malaria Journal, 2014. **13**(1): p. 7.

152. Duffy, S. and V.M. Avery, *Routine In Vitro Culture of Plasmodium falciparum: Experimental Consequences?* Trends in Parasitology, 2018. **34**(7): p. 564-575.

153. White, N.J., et al., *Spiroindolone KAE609 for Falciparum and Vivax Malaria.* New England Journal of Medicine, 2014. **371**(5): p. 403-410.

154. Adelusi, T.I., et al., *Targeting Plasmodium falciparum calcium dependent protein kinase-1: Computational modelling approach towards the discovery of antimalarial drug from medicinal herbs and clinically approved anti-malarial drugs pharmacophores.* bioRxiv, 2022: p. 2022.08.22.504824.

155. LaMonte, G.M., et al., *Pan-active imidazolopiperazine antimalarials target the Plasmodium falciparum intracellular secretory pathway.* Nature Communications, 2020. **11**(1): p. 1780.

156. SheelaNair, A., et al., *Similarly efficacious anti-malarial drugs SJ733 and pyronaridine differ in their ability to remove circulating parasites in mice.* Malaria Journal, 2022. **21**(1): p. 49.

157. Field, M.C., et al., *Anti-trypanosomatid drug discovery: an ongoing challenge and a continuing need.* Nature Reviews Microbiology, 2017. **15**(4): p. 217-231.

158. Fino, R., et al., *Computer-Aided Design and Synthesis of a New Class of PEX14 Inhibitors: Substituted 2,3,4,5-Tetrahydrobenzo[F][1,4]oxazepines as Potential New Trypanocidal Agents.* Journal of Chemical Information and Modeling, 2021. **61**(10): p. 5256-5268.

159. Brand, S., et al., *Discovery and Optimization of 5-Amino-1,2,3-triazole-4-carboxamide Series against Trypanosoma cruzi.* Journal of Medicinal Chemistry, 2017. **60**(17): p. 7284-7299.

160. Gupta, R., et al., *Functionalized Nitroimidazole Scaffold Construction and Their Pharmaceutical Applications: A 1950–2021 Comprehensive Overview.* Pharmaceuticals, 2022. **15**(5): p. 561.

161. Khanra, S., et al., *In vitro screening of known drugs identified by scaffold hopping techniques shows promising leishmanicidal activity for suramin and netilmicin.* BMC Research Notes, 2018. **11**(1): p. 319.

162. Zhao, L., et al., *Improving the metabolic stability of antifungal compounds based on a scaffold hopping strategy: Design, synthesis, and structure-activity*

relationship studies of dihydrooxazole derivatives. European Journal of Medicinal Chemistry, 2021. **224**: p. 113715.

163. Singh, B., et al., *Scaffold and parasite hopping: discovery of new protozoal proliferation inhibitors.* ACS Medicinal Chemistry Letters, 2020. **11**(3): p. 249-257.

164. Thomas, M., et al., *Scaffold-hopping strategy on a series of proteasome inhibitors led to a preclinical candidate for the treatment of visceral leishmaniasis.* Journal of Medicinal Chemistry, 2021. **64**(9): p. 5905-5930.

165. Nagle, A.S., et al., *Recent developments in drug discovery for leishmaniasis and human African trypanosomiasis.* Chemical reviews, 2014. **114**(22): p. 11305-11347.

166. Tanvir Khaliq, T.K., et al., *Peganine hydrochloride dihydrate an orally active antileishmanial agent.* 2009.

167. Misra, P., et al., *Antileishmanial activity mediated by apoptosis and structure-based target study of peganine hydrochloride dihydrate: an approach for rational drug design.* Journal of antimicrobial chemotherapy, 2008. **62**(5): p. 998-1002.

168. Staker, B.L., et al., *Structures of three classes of anticancer agents bound to the human topoisomerase I− DNA covalent complex.* Journal of medicinal chemistry, 2005. **48**(7): p. 2336-2345.

169. Stewart, L., et al., *A model for the mechanism of human topoisomerase I.* Science, 1998. **279**(5356): p. 1534-1541.

170. Inc, C., *Molecular operating environment (MOE), Chemical Computing Group Inc. 1010 Sherbooke St.* West, Suite, 2016. **910**.

171. Mhaske, S.B. and N.P. Argade, *Concise and Efficient Synthesis of Bioactive Natural Products Pegamine, Deoxyvasicinone, and (−)-Vasicinone.* The Journal of Organic Chemistry, 2001. **66**(26): p. 9038-9040.

172. Mhaske, S.B. and N.P. Argade, *Concise and efficient synthesis of bioactive natural products pegamine, deoxyvasicinone, and (−)-Vasicinone.* The Journal of Organic Chemistry, 2001. **26**(66): p. 9038-9040.

APPENDIX

^{1}H NMR of (S)-2,5-dioxotetrahydrofuran-3yl-acetate **3** :

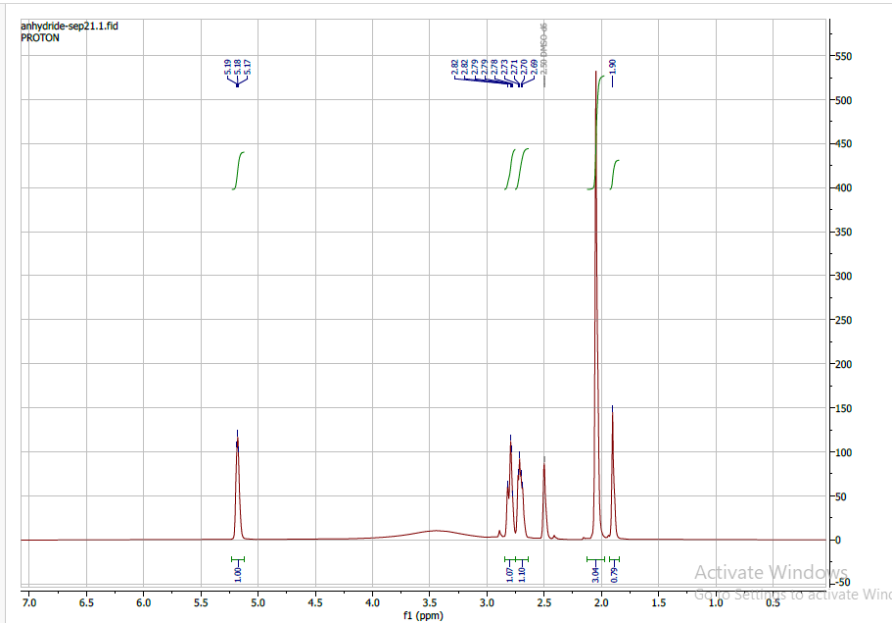

The residual peaks of acetic acid were shown at 1.90 in ^{1}H NMR and 21.11, 172.11 in the ^{13}C NMR

^{13}C NMR of (S)-2,5-dioxotetrahydrofuran-3yl-acetate **3**:

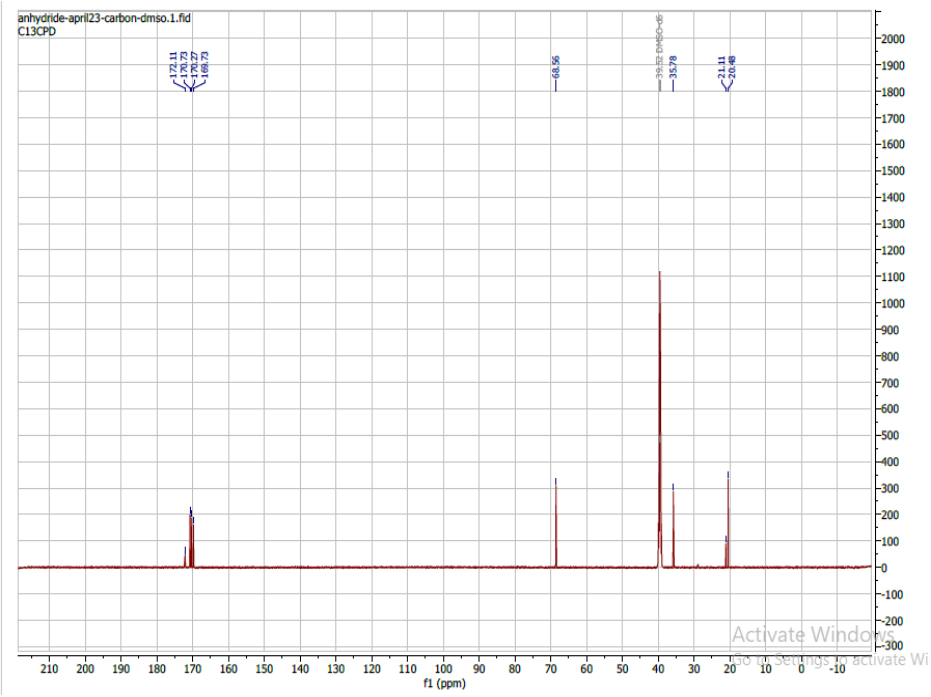

^{1}H NMR of (*S*)-3-acetoxy-4-((3-carbamoyl-pyridine-2yl)-amino)-4-oxobutanoic acid **4**:

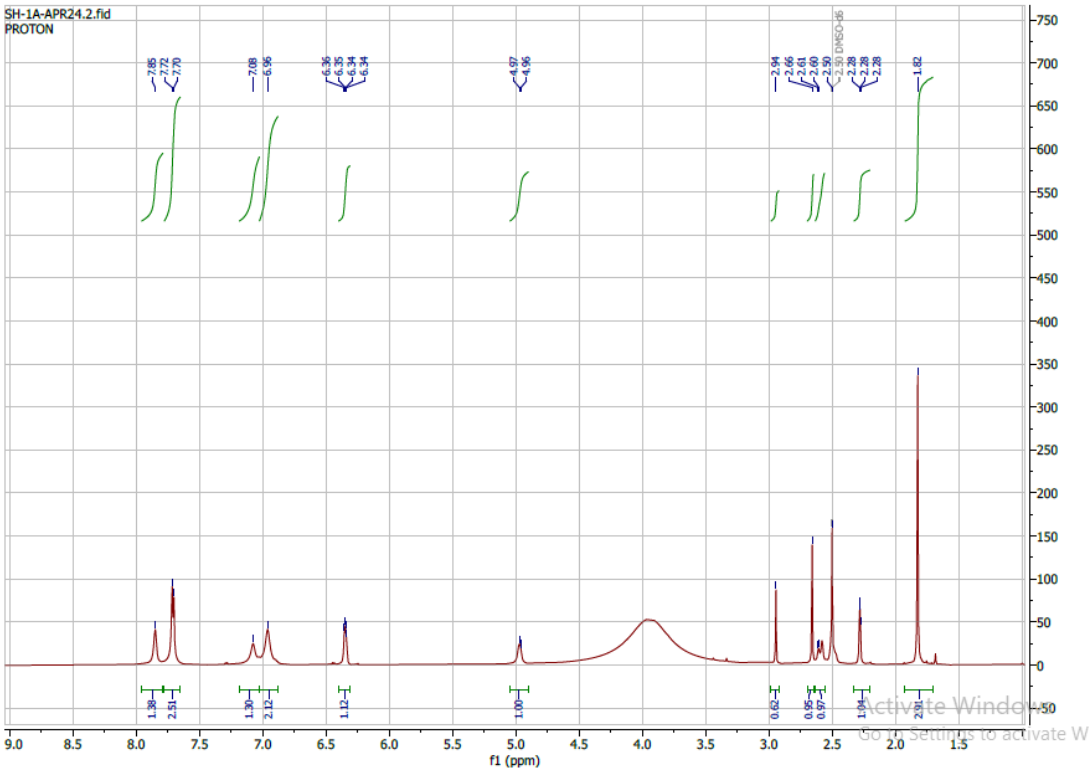

The residual DMF peaks were seen at 7.85, 2.94, 2.66 ppm.

^{13}C NMR of (*S*)-3-acetoxy-4-((3-carbamoyl-pyridine-2yl)-amino)-4-oxobutanoic acid **4**:

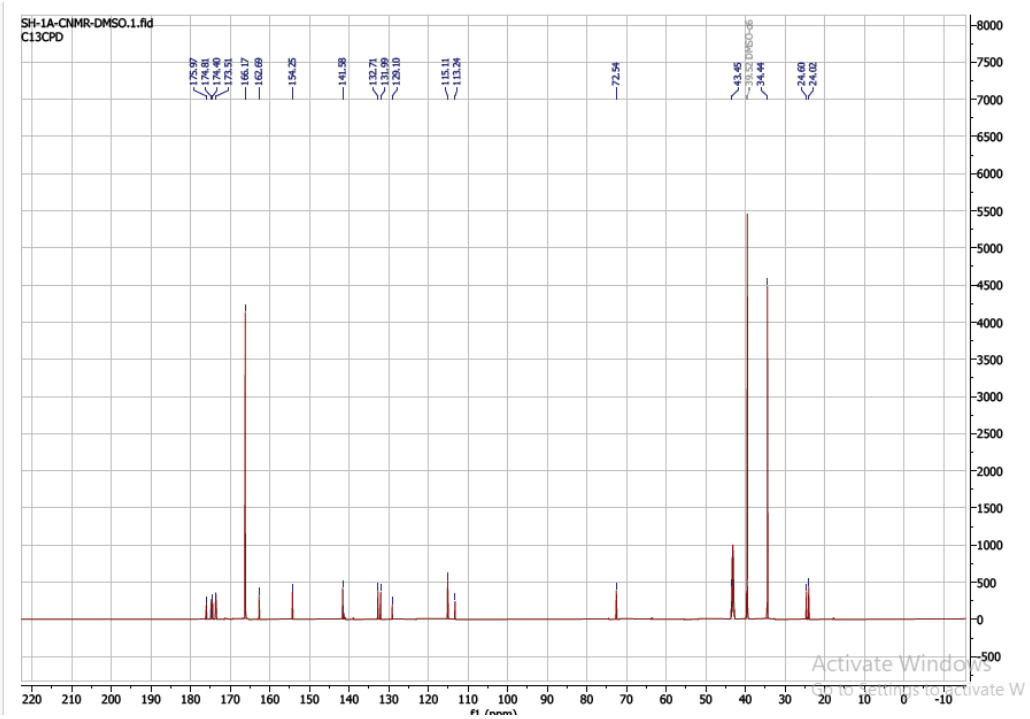

Mass spectrometry of (*S*)-3-acetoxy-4-((3-carbamoyl-pyridine-2yl)-amino)-4-oxobutanoic acid **4**:

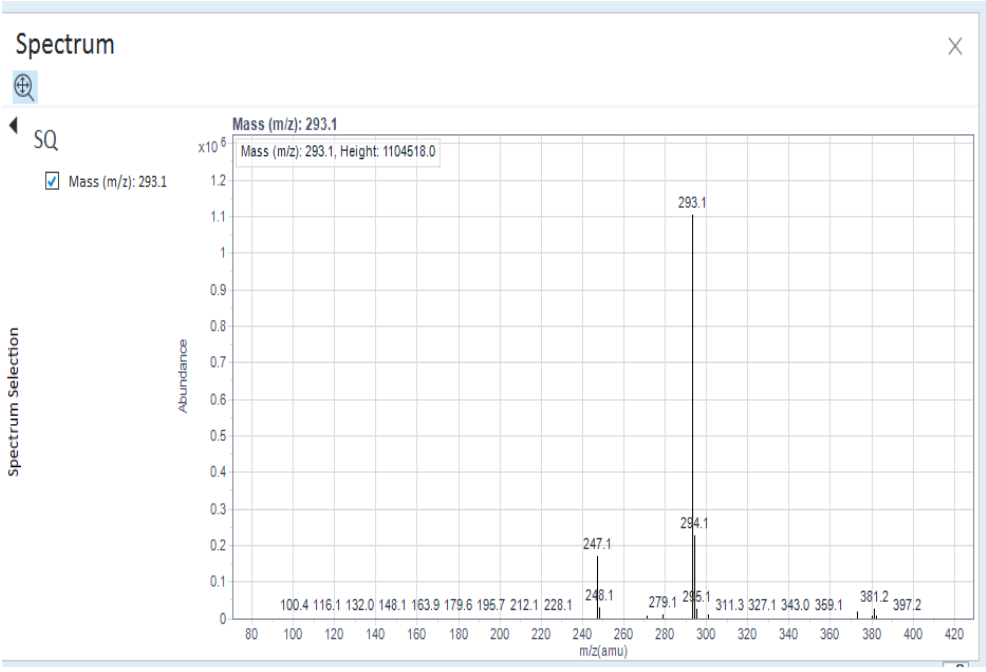

^{1}H NMR of methyl (*S*)-3-acetoxy-4-((3-carbamoyl-pyridine-2yl)

amino)-4-oxo butanoate **5**:

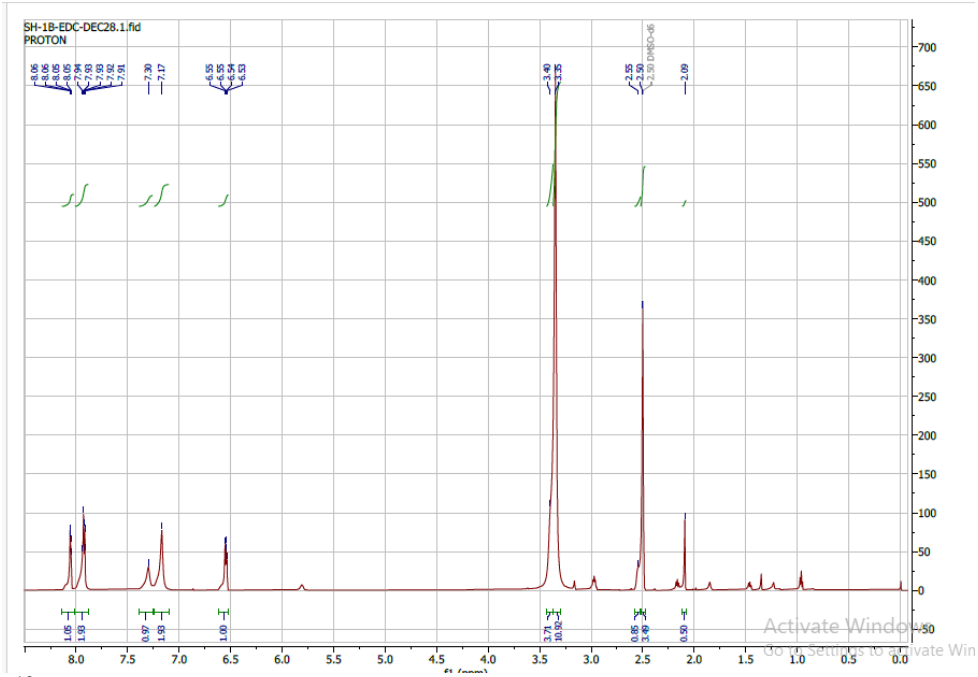

^{13}C NMR of methyl (*S*)-3-acetoxy-4-((3-carbamoyl-pyridine-2yl)

amino)-4-oxo butanoate **5**:

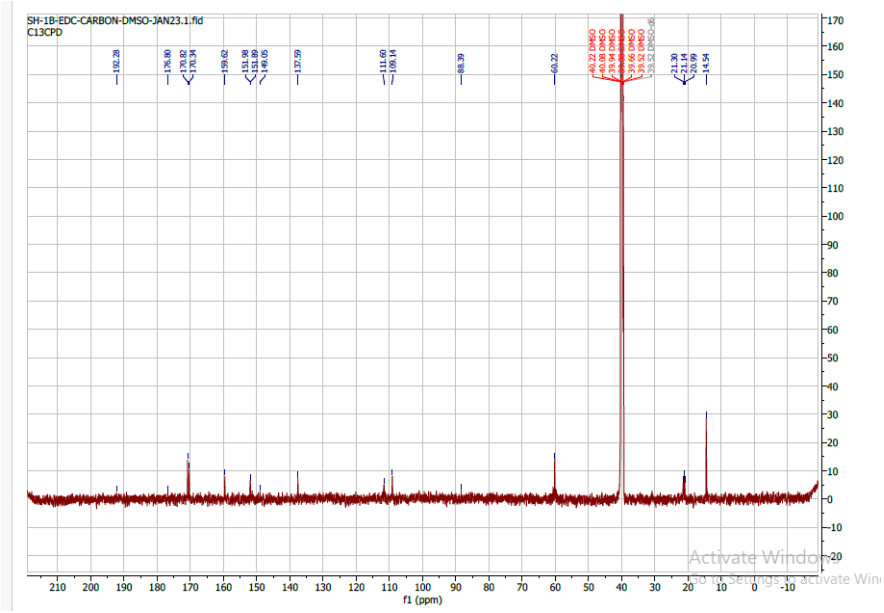

Mass spectrometry of methyl (*S*)-3-acetoxy-4-((3-carbamoyl-pyridine-2yl) amino)-4-oxo butanoate **5**:

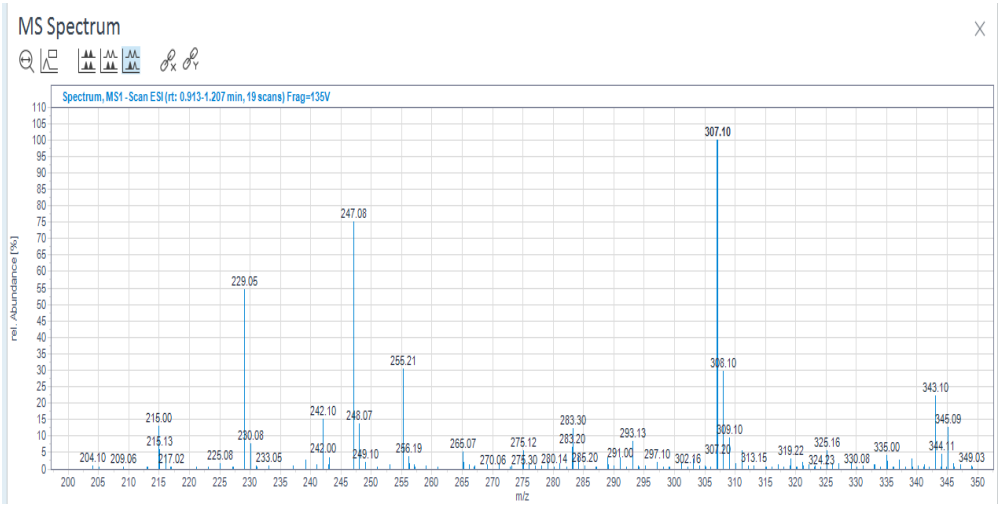

Purification of compound **5** using CombiFlash CombiFlash NextGen 300^{+} chromatography system:

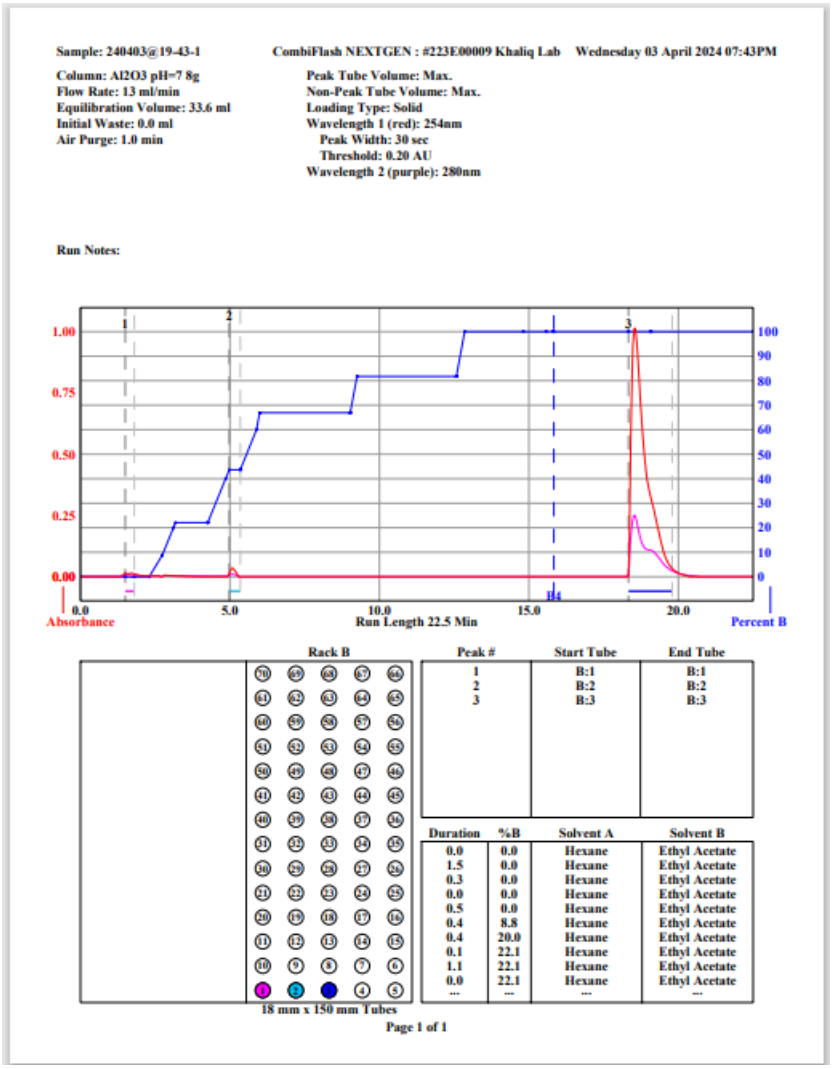

Sample: 240403@19-43-1
CombiFlash NEXTGEN : #223E00009 Khaliq Lab
Wednesday 03 April 2024 07:43PM

Column: Al2O3 pH=7 8g
Flow Rate: 13 ml/min
Equilibration Volume: 33.6 ml
Initial Waste: 0.0 ml
Air Purge: 1.0 min

Peak Tube Volume: Max.
Non-Peak Tube Volume: Max.
Loading Type: Solid
Wavelength 1 (red): 254nm
Peak Width: 30 sec
Threshold: 0.20 AU
Wavelength 2 (purple): 280nm

Run Notes:

Rack B

18 mm x 150 mm Tubes

Peak #	Start Tube	End Tube
1	B:1	B:1
2	B:2	B:2
3	B:3	B:3

Duration	%B	Solvent A	Solvent B
0.0	0.0	Hexane	Ethyl Acetate
1.5	0.0	Hexane	Ethyl Acetate
0.3	0.0	Hexane	Ethyl Acetate
0.0	0.0	Hexane	Ethyl Acetate
0.5	0.0	Hexane	Ethyl Acetate
0.4	8.8	Hexane	Ethyl Acetate
0.4	20.0	Hexane	Ethyl Acetate
0.1	22.1	Hexane	Ethyl Acetate
1.1	22.1	Hexane	Ethyl Acetate
0.0	22.1	Hexane	Ethyl Acetate
---	---	---	---

Page 1 of 1

^{1}H NMR of (*S*)-2-(1,3-dihydroxypropyl)pyrido[2,3-d]

pyrimidin-4(3H)-one:

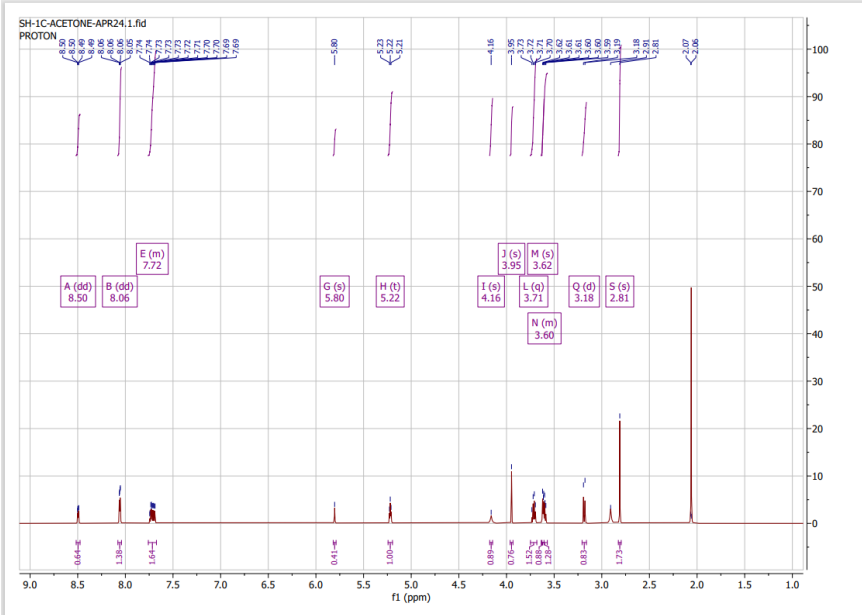

Residual THF solvent peaks were seen at 3.62 in proton NMR and 29.44, 66.70 ppm in carbon NMR.

^{13}C NMR of (*S*)-2-(1,3-dihydroxypropyl)pyrido[2,3-d]

pyrimidin-4(3H)-one:

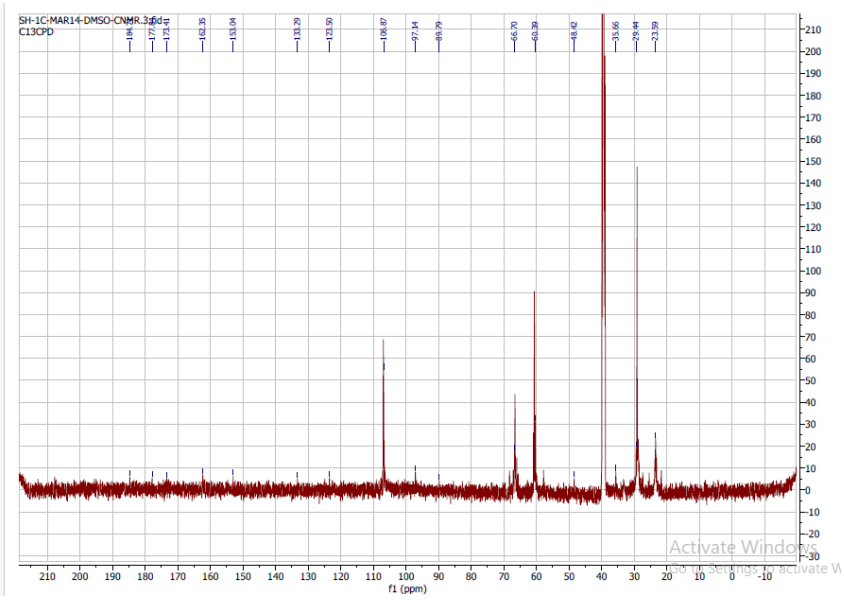

Purification of compound **7** using CombiFlash CombiFlash NextGen 300^{+} chromatography system:

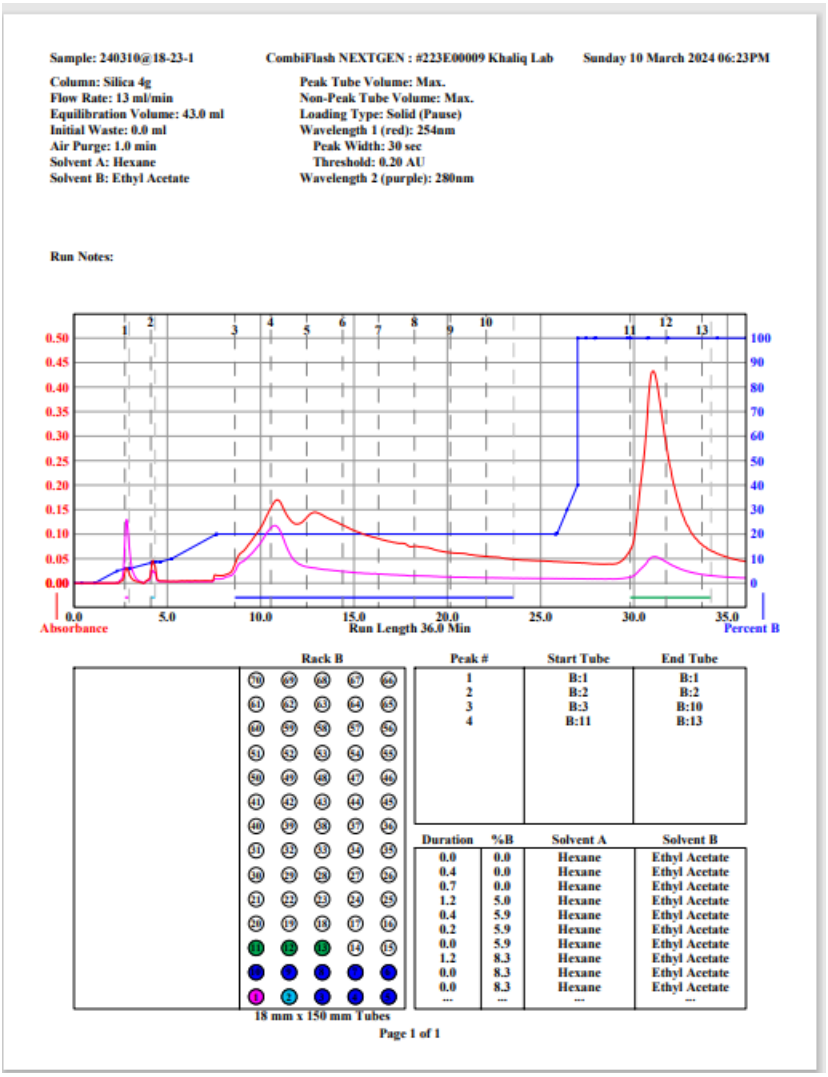

Sample: 240310@18-23-1 CombiFlash NEXTGEN : #223E00009 Khaliq Lab Sunday 10 March 2024 06:23PM

Column: Silica 4g
Flow Rate: 13 ml/min
Equilibration Volume: 43.0 ml
Initial Waste: 0.0 ml
Air Purge: 1.0 min
Solvent A: Hexane
Solvent B: Ethyl Acetate

Peak Tube Volume: Max.
Non-Peak Tube Volume: Max.
Loading Type: Solid (Pause)
Wavelength 1 (red): 254nm
Peak Width: 30 sec
Threshold: 0.20 AU
Wavelength 2 (purple): 280nm

Run Notes:

Rack B

18 mm x 150 mm Tubes

Peak #	Start Tube	End Tube
1	B:1	B:1
2	B:2	B:2
3	B:3	B:10
4	B:11	B:13

Duration	%B	Solvent A	Solvent B
0.0	0.0	Hexane	Ethyl Acetate
0.4	0.0	Hexane	Ethyl Acetate
0.7	0.0	Hexane	Ethyl Acetate
1.2	5.0	Hexane	Ethyl Acetate
0.4	5.9	Hexane	Ethyl Acetate
0.2	5.9	Hexane	Ethyl Acetate
0.0	5.9	Hexane	Ethyl Acetate
1.2	8.3	Hexane	Ethyl Acetate
0.0	8.3	Hexane	Ethyl Acetate
0.0	8.3	Hexane	Ethyl Acetate
---	---	---	---

Page 1 of 1

^{1}H NMR of (*S*)-9-hydroxy-8,9-dihydropyrido[2,3-d]pyrrolo

[1,2-a] pyrimidin-5(7H)one:

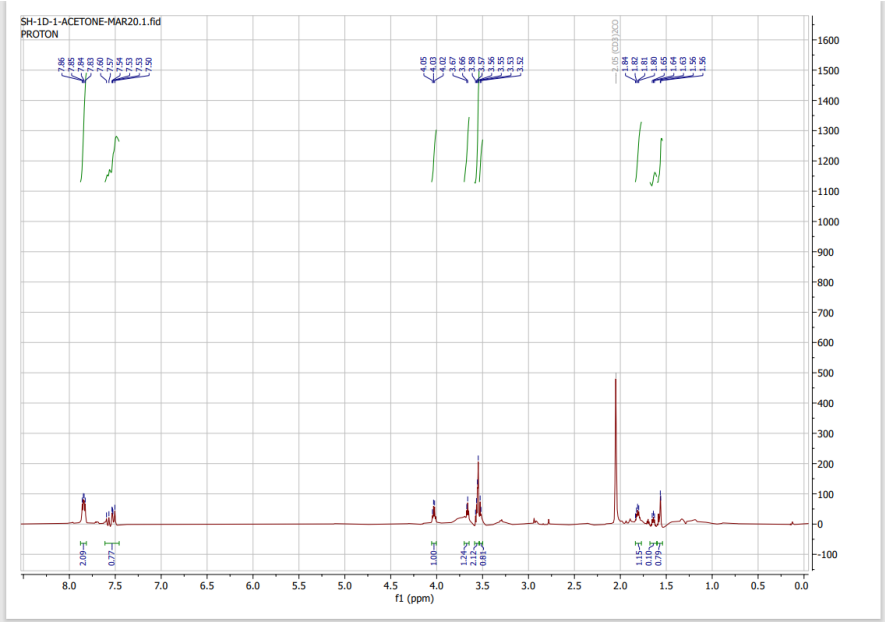

Residual THF peaks were seen at 3.53 ppm in proton NMR and 62.34 ppm in carbon NMR.

^{13}C NMR of (*S*)-9-hydroxy-8,9-dihydropyrido[2,3-d]pyrrolo

[1,2-a]pyrimidin-5(7H)one:

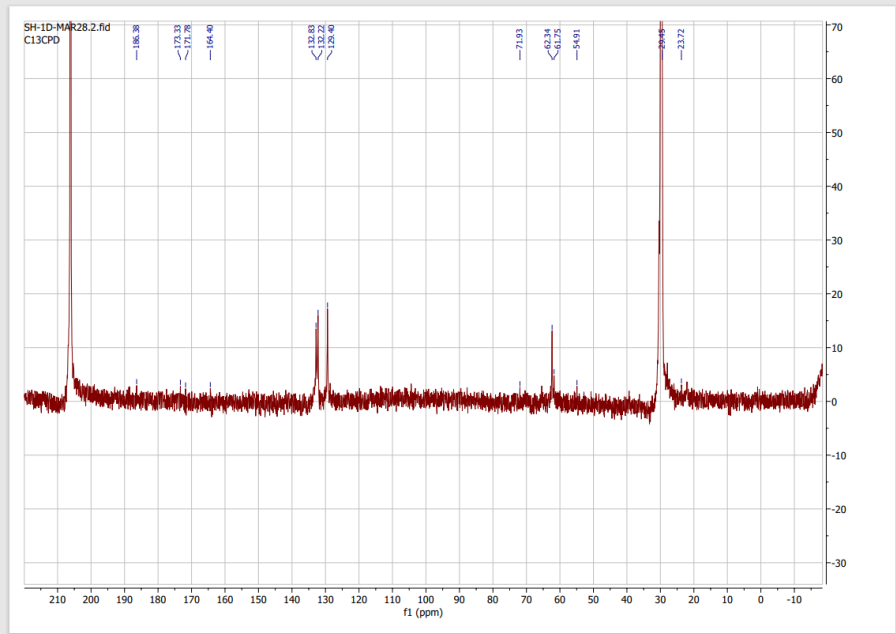

Purification of compound **8** using CombiFlash CombiFlash NextGen 300^{+} chromatography system:

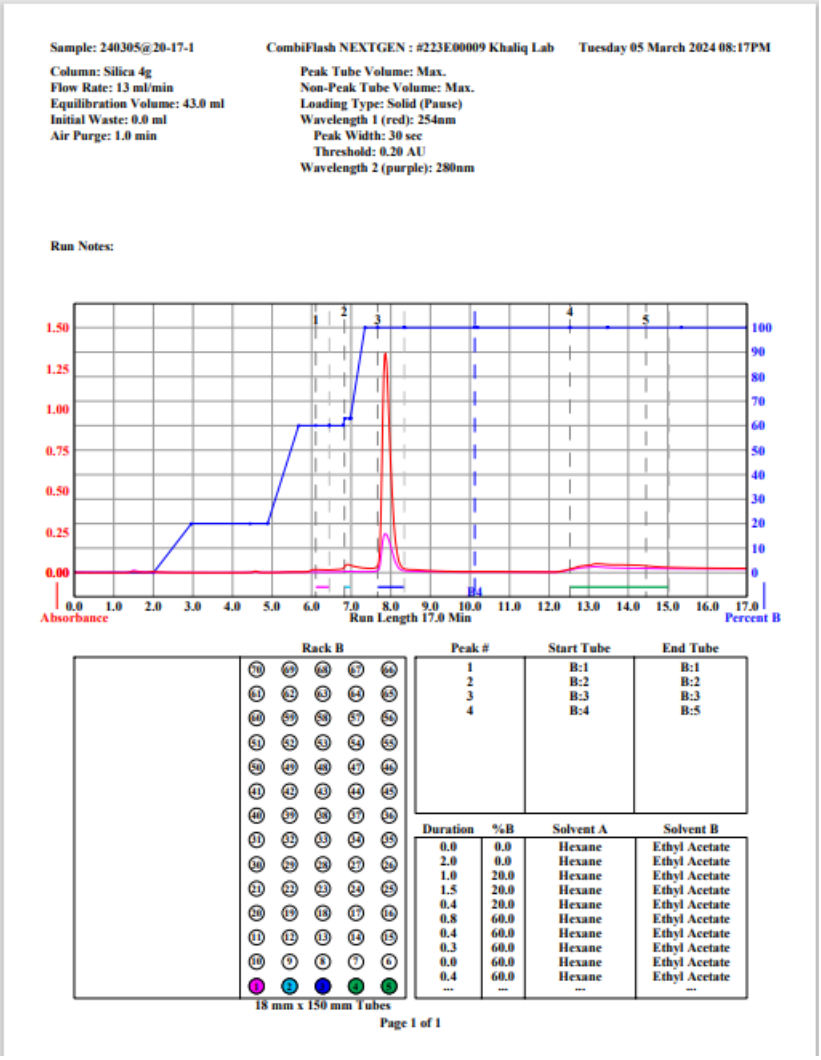

Sample: 240305@20-17-1
CombiFlash NEXTGEN : #223E00009 Khaliq Lab
Tuesday 05 March 2024 08:17PM

Column: Silica 4g
Flow Rate: 13 ml/min
Equilibration Volume: 43.0 ml
Initial Waste: 0.0 ml
Air Purge: 1.0 min

Peak Tube Volume: Max.
Non-Peak Tube Volume: Max.
Loading Type: Solid (Pause)
Wavelength 1 (red): 254nm
Peak Width: 30 sec
Threshold: 0.20 AU
Wavelength 2 (purple): 280nm

Run Notes:

Absorbance
Run Length 17.0 Min
Percent B

Rack B

18 mm x 150 mm Tubes

Peak #	Start Tube	End Tube
1	B:1	B:1
2	B:2	B:2
3	B:3	B:3
4	B:4	B:5

Duration	%B	Solvent A	Solvent B
0.0	0.0	Hexane	Ethyl Acetate
2.0	0.0	Hexane	Ethyl Acetate
1.0	20.0	Hexane	Ethyl Acetate
1.5	20.0	Hexane	Ethyl Acetate
0.4	20.0	Hexane	Ethyl Acetate
0.8	60.0	Hexane	Ethyl Acetate
0.4	60.0	Hexane	Ethyl Acetate
0.3	60.0	Hexane	Ethyl Acetate
0.0	60.0	Hexane	Ethyl Acetate
0.4	60.0	Hexane	Ethyl Acetate
---	---	---	---

Page 1 of 1